

Distributed PID Control for Consensus and Synchronization of Multi-agent Networks



Ph.D Thesis

Daniel Alberto Burbano Lombana

Tutor

Ch.mo prof. Mario di Bernardo

University of Naples Federico II
Department of Electric Engineering and Information Technology
Naples, Italy
2015

*To my family,
Marlene and Natalia*

*and the memory of
Maria Isabel Cordoba*

*“Mathematics knows no races or geographic boundaries;
for mathematics, the cultural world is one country”.*
David Hilbert

“Birds born in a cage think flying is an illness”.
Alejandro Jodorowsky

Contents

| | |
|--|-----------|
| 1. Introduction | 1 |
| 1.1. Thesis Outline | 3 |
| 1.2. List of Main Contributions | 4 |
| 2. Preliminaries and Background | 5 |
| 2.1. Complex networks: generalities | 5 |
| 2.2. The structure of complex networks: algebraic graph theory | 7 |
| 2.3. Multiplex networks | 9 |
| 2.4. Mathematical notation and preliminaries | 10 |
| 2.5. Consensus in multi-agent systems | 12 |
| 2.6. Synchronization in complex networks | 16 |
| 2.6.1. Master stability function | 17 |
| 3. PID Consensus in Heterogeneous Linear Multi-Agent Networks | 22 |
| 3.1. Distributed PI control | 23 |
| 3.1.1. Consensus equilibrium | 24 |
| 3.1.2. Block decomposition of \mathcal{L} | 24 |
| 3.1.3. Error dynamics | 26 |
| 3.2. Distributed PID control | 32 |
| 3.2.1. Properties of $\tilde{\mathcal{L}}$ | 33 |
| 3.2.2. Closed-loop network | 35 |
| 3.2.3. Homogeneous node dynamics | 39 |
| 3.2.4. Heterogeneous node dynamics | 44 |
| 4. Multiplex PI Control for Networks of Heterogeneous Agents | 48 |
| 4.1. Consensus equilibrium | 50 |
| 4.2. Error dynamics | 51 |

| | |
|--|------------|
| 4.3. Convergence theorem | 55 |
| 4.4. Control algorithm | 58 |
| 5. Distributed PID Control for Synchronization in Networks of Nonlinear Units | 61 |
| 5.1. Local stability analysis | 62 |
| 5.1.1. MSF for distributed PD | 62 |
| 5.1.2. MSF for distributed PI | 64 |
| 5.2. Global stability analysis | 69 |
| 5.2.1. Distributed PD control | 69 |
| 5.2.2. Distributed PI control | 74 |
| 5.3. Performance assessment | 77 |
| 5.3.1. Heterogeneity between nodes | 77 |
| 5.3.2. Constant disturbances | 79 |
| 6. Applications | 82 |
| 6.1. Synchronization of power generators | 82 |
| 6.1.1. Distributed controller | 82 |
| 6.1.2. Simulation | 84 |
| 6.2. Electrical Circuits | 86 |
| 6.2.1. Chua's Circuit | 88 |
| 6.2.2. Synchronization in networks of Chua's Circuit | 88 |
| 6.2.2.1. Local admissible synchronization of Chua's Circuit | 89 |
| 6.2.2.2. Global admissible synchronization of Chua's Circuit | 89 |
| 6.2.2.3. Heterogeneity between nodes | 93 |
| 7. Conclusions | 95 |
| 7.1. Future Work | 96 |
| A. Matrix Calculations | 97 |
| A.1. Computation of Ψ matrix | 97 |
| A.2. Derivation of Ψ for generic node dynamics | 99 |
| B. Lyapunov Exponents | 101 |
| B.1. Estimating the Lyapunov exponents | 102 |
| Bibliography | 103 |

List of Figures

| | |
|---|----|
| 2-1. General diagram of a network | 5 |
| 2-2. Wiring diagrams of some complex networks. (a) Electrical power grid of northern Italy, each node represents a power generator or consumer while the links represent buses [51] (b) Brain network, here the nodes ans links represent neurons and the interactions between them respectively [71], (c) a visualization of the network structure of the Internet at the level of autonomous systems-local groups of computers each representing hundreds or thousands of machines [53]. | 6 |
| 2-3. Example of: (a) an Internet network, (b) a Hollywood actor network, (c) a protein-protein interaction network. All of these networks are represented by the same graph (d). Images taken from [5]. | 8 |
| 2-4. (a) Network of cities interconnected by rail and plane. (b) Multiplex representation of the network, with just two independent layers (no interconnections between layers, i.e., \mathcal{D} is an empty set) sharing the same set of vertexes. | 10 |
| 2-5. Time response of three different networks of simple integrators (2-9) controlled by (2-11). All link weights are unitary. The blue dashed-line represents the average consensus value x_∞ | 15 |
| 2-6. Three possible cases for the MSF $\Psi(\tilde{\alpha})$: Type P_o : $\Psi(\tilde{\alpha})$ is a monotonically increasing function. Type P_1 : $\Psi(\tilde{\alpha})$ is a monotonically decreasing function, Type P_2 : $\Psi(\tilde{\alpha})$ is a V-shaped function admitting negative values in some region. | 18 |
| 2-7. (a) Chaotic attractor, (b) Lyapunov exponents μ_p . k denotes time step of the algorithm. | 19 |
| 2-8. Master Stability Function for chaotic Lorenz system under different output matrices: (a) $\Gamma = \text{diag}\{1, 1, 1\}$, (b) $\Gamma = \text{diag}\{1, 0, 0\}$, (c) $\Gamma = \text{diag}\{0, 1, 0\}$, and (d) $\Gamma = \text{diag}\{0, 0, 1\}$ | 20 |
| 2-9. Time response of a network of 10 chaotic Lorenz for (a) $\alpha = 3$ and (b) $\alpha = 4$. | 21 |

| | |
|---|----|
| 3-1. Time response of the PI controlled multi-agent system for: (a),(b) three, (c),(d) star network topologies. The dashed-lines represent the equilibrium value. | 29 |
| 3-2. Time response of the PI controlled multi-agent system for: (a),(b) star, (c),(d) all-to-all network topologies. The dashed-lines represent the equilibrium value. | 30 |
| 3-3. Heterogeneous ring network controlled by distributed PI strategy. | 32 |
| 3-4. Time response of the closed-loop heterogeneous network of Fig. 3-3 controlled by distributed PI strategy with $\alpha = \beta = 1$. The dashed-lines represent the equilibrium value. | 33 |
| 3-5. Time response of the PD controlled multi-agent system for different network topologies with $\alpha = 4$ and $\gamma = 1$ | 43 |
| 3-6. Time response of the closed-loop heterogeneous network of Fig. 3-3 controlled by distributed PID strategy with $\alpha = 4$, and $\gamma = \beta = 1$. The dashed-lines represent the equilibrium constant value | 47 |
| 4-1. (a): The network to be controlled is represented by black links and the blue and yellow connections represent the additional proportional and integral links that are used for control. (b) Multiplex representation of a network controlled by proportional and integral distributed controllers. | 49 |
| 4-2. Time response of the closed-loop multiplex network for $\alpha = 13.5$ and $\beta = 7$ where the proportional and integral networks have both ring topologies with all its weights equal to 3 and 1 respectively. | 59 |
| 4-3. Networks with unitary weights representing different architectures for the graph in the integral control layer: (a) all-to-all, (b) star, (c) ring, and (d) Tree. (e) time response of the consensus index d_x when the topology of the integral network is varied | 60 |
| 5-1. Two dimensional representation of the master stability function for Chaotic Lorenz. For each point in the plane corresponds the value of the MSF evaluated at that point, which is represented with different colors. The red-scale colors denote positive values of the MSF, while negative values are represented by the blue-scale. (a)-(b) $\Psi(\tilde{\alpha}, \tilde{\gamma})$ function computed for distributed PD control, (c)-(d) $\Psi(\tilde{\alpha}, \tilde{\beta})$ function computed for PI control. | 66 |
| 5-2. Time response of a network of ten chaotic Lorenz. (a) $\alpha = \beta = 8.58$ (b) $\alpha = 8.58$ and $\gamma = 34.3348$ | 67 |

| | |
|--|----|
| 5-3. Time response of a network of ten chaotic Lorenz. (a) $\alpha = 1.5$ and $\beta = 8$ (b) $\alpha = 1.5$ and $\beta = 0.5$ | 68 |
| 5-4. Estimated regions of global synchronization of networks controlled by distributed PD, using (5-36) with $\lambda_2 = 1$ and (a) $\mu = 4$, (b) $\mu = 8$. The blue color, denotes the region where (5-36) is satisfied and red color otherwise. | 73 |
| 5-5. Estimated regions of global synchronization of networks controlled by distributed PI, using (5-44) with $\mu = 4$, for two different network structures and (a) $\lambda_2 = 0.5188$ and $\lambda_N = 5.7105$, (b) $\lambda_2 = 0.382$ and $\lambda_N = 4$. The blue color, denotes the region where (5-44) is satisfied and red color otherwise. | 77 |
| 5-6. Heterogeneous network of Lorenz systems. | 78 |
| 5-7. Time response of the closed-loop heterogeneous network of heterogeneous Chaotic Lorenz systems with $\Gamma = \mathbf{I}_n$, controlled by distributed P control with $\alpha = 2$ | 78 |
| 5-8. Time response of the closed-loop heterogeneous network of heterogeneous Chaotic Lorenz systems with $\Gamma = \mathbf{I}_n$, controlled by distributed P control with $\alpha = \gamma = 2$ | 79 |
| 5-9. Time response of a ring network of six homogeneous Lorenz oscillators with $a = 2$ under constant perturbations acting on nodes 1, 3 and 4. The network is controlled by just distributed proportional control with $\alpha = 3$ | 80 |
| 5-10. (a) Time response of a ring network of six Lorenz oscillators with $a = 2$ and affected by constant perturbations acting in nodes 1, 3 and 4 controlled by distributed proportional and integral actions with $\alpha = 3$ and $\beta = 1$. (b) Evolution of the disagreement dynamics. | 80 |
| 6-1. (a) Power network represented by the integral layer, (b) Architecture of the network in the proportional layer. | 85 |
| 6-2. Time response of the controlled power network. The blue dash-dot line represent the convergence value ω_∞ | 85 |
| 6-3. (a) Schematic of the nonlinear circuit [24], (b) Different examples of nonlinear circuits. | 86 |
| 6-4. Distributed PID (RLC) network for synchronization in networks of nonlinear circuits. | 87 |
| 6-5. Schematic diagram of Chua's circuit. | 88 |
| 6-6. Chaotic Lorenz attractors with their respective Lyapunov exponents μ_p . k represents the step-number of the L.E. algorithm | 89 |

| | |
|---|-----|
| 6-7. Two dimensional representation of the master stability function for Chaotic Chua. For each point in the plane corresponds the value of the MSF evaluated at that point, which is represented with different colors. The red-scale colors denote positive values of the MSF, while negative values are represented by the blue-scale. (a)-(b) $\Psi(\tilde{\alpha}, \tilde{\gamma})$ function computed for distributed PD control, (c)-(d) $\Psi(\tilde{\alpha}, \tilde{\beta})$ function computed for PI control. | 90 |
| 6-8. Time response of a network of ten chaotic Chua's circuit controlled by distributed PD control with $\alpha = 12.8755$ and (a) $\gamma = 0.6438$ (b) $\gamma = 1.9313$. . . | 91 |
| 6-9. Estimated regions of global synchronization of a network of Chua's circuits controlled by distributed (a) PD and (PI). The blue color, denotes the region where (5-36) is satisfied and red color otherwise. | 92 |
| 6-10. Time response of the closed-loop heterogeneous network of Chua's circuits controlled by distributed P with $\Gamma = \mathbf{I}_n$ | 93 |
| 6-11. Time response of the closed-loop heterogeneous network of Chua's circuits controlled by distributed PD with $\Gamma = \mathbf{I}_n$ | 93 |
| B-1. Divergence of two solutions for nearby initial conditions | 101 |

Abstract

We investigate the use of distributed PID actions to achieve consensus and synchronization in networks of homogeneous and heterogeneous agents. We first analyze the case of distributed PID control on networks with heterogeneous nodes described by first-order linear systems. Convergence of the strategy is proved using appropriate state transformations and Lyapunov functions.

Then, we propose a multiplex proportional-integral approach, for solving consensus problems in networks of heterogeneous n -dimensional node dynamics affected by constant disturbances. The proportional and integral actions are deployed on two different layers across the network, each with its own topology. Furthermore, the contribution of the network topology and node dynamics have been systematically separated giving some sufficient conditions guaranteeing convergence.

Finally, an extension to networks of identical nonlinear node dynamics is presented. We provide local and global stability analysis together with a detailed performance assessment where heterogeneity among nodes and disturbances are considered.

The effectiveness of the theoretical results is illustrated via its application to a representative power grid model recently presented in the literature and also for synchronization in networks of chaotic circuits.

CHAPTER 1

Introduction

Some years ago we could even imagine that disparate diseases like diabetes and Parkinson’s were correlated. Now, these connections are being uncovered using network theory [19, 43]. Networks are inherently part of our universe, and daily life. In simple terms, a network is a collection of units interacting between them through some interconnection links. We can find them in our brain where neurons are connected by electro-chemical channels, cellular and metabolic network, flocks of birds, etc. Moreover man-made networks like world-wide-web, or power distribution systems where generators and consumers are connected to the electrical power grid, represents a good example to illustrate that network theory pervades nature, science and technology.

Networks of dynamical units (or agents) have been used to model everything from earthquakes to ecosystems, neurons to neutrinos [72]. Congestion in communication networks, robot coordination, consensus and synchronization [9], are just some of the problems widely studied in network theory. Hence, finding ways to predict and tame the collective behaviour of a network of dynamical agents towards a desired common target state is a fundamental problem in network control [18, 20, 45]. Centralized or distributed strategies can be used to solve this problem. Unlike centralized control where a central “station” is required for controlling the whole network, distributed control just requires local interactions among agents. Therefore, a distributed control strategy is more apt in all those situations where several constraints are present and cannot be avoided such as limited resources and energy, short wireless communication ranges, narrow bandwidths, etc [15].

One particular problem in distributed control of complex networks is consensus and synchronization, where the goal is for the states of all agents in the network to asymptotically converge towards each other [54, 47]. A large number of notable applications have made this

problem of paramount importance. For instance, distributed formation control in robotics [32, 55], platooning of vehicles in intelligent transportation systems [25, 52], formation and attitude alignment in networks of spacecraft units [61], cooperative fire monitoring [63], frequency synchronization in power networks [27, 35, 70], etc. (For a more comprehensive list of applications see [3, 54] and references therein)

Consensus and synchronization share the same objective; however, in the literature there is just a conceptual difference between them. In consensus problems, the emphasis is on the communication constraints rather than the individual system dynamics (Commonly, the individual systems are modeled as simple integrators and the dynamic evolution of the group is entirely determined by the exchange of information modeled by some communication graph.), while in the synchronization literature, the focus is primarily on the individual dynamics [78].

The existing literature on consensus and synchronization is vast and many extensions and sophisticated techniques have been proposed, e.g. [63, 60]. Typically, it is assumed that the agent dynamics is either trivial or identical across the network. Thus, many of the available strategies only apply to networks of homogeneous systems in the absence of disturbances and noise.

Moreover, results are often obtained in the case where the nodes are either (simple or higher order) integrators [62, 65] or possess scalar linear dynamics [12]. Only a handful of results are available for networks whose nodes are generic n -dimensional LTI systems, see for example [59, 40, 76, 81, 82].

As research on consensus has matured, more complicated and realistic scenarios must be considered and analysed to address real-world application. Often, the agents in a network do not necessarily have the same intrinsic dynamics and also may be affected by noise and disturbances; besides, they may also communicate with different protocols and strategies. Take for instance a network of power generators, as those considered in [27, 74]. Different power sources and transmission lines, multiple load variations, and even communication failures between generators make the network highly heterogeneous.

Then, a pressing open problem is that of guaranteeing convergence of all agents towards the same solution in the presence of heterogeneity among their dynamics, disturbances and noise. In this case, diffusive linear coupling is in general only able to guarantee bounded steady-state error as the coupling gain is increased. See for example [41] where the consensus

problem is studied for networks of heterogeneous first order time-varying systems affected by disturbances.

Some recent work addresses the problem of achieving consensus in networks with some degree of heterogeneity. For instance, in [33], the problem studied is of driving all the linear nodes in a homogeneous network towards a common reference trajectory (leader-follower networks) in the presence of time-varying, yet bounded, disturbances. The case of heterogeneous networks has been studied in the absence of disturbances or noise both for linear [78, 40, 59, 76] and nonlinear node dynamics [81, 82].

The aim of this thesis is to study distributed strategies based on PID control strategy, to solve consensus and synchronization problems as a simple yet effective alternative to diffusive linear coupling (corresponding to a simpler P protocol). PID controllers are well known in classical control as able to provide a certain degree of robustness against constant disturbances and noise together with many other desirable properties [4]. We will show that most of their beneficial effects are preserved when a PID strategy is deployed in a distributed manner over a network of interest.

Related independent work on the use of PI coupling for consensus can be found in the literature. For instance, the use of PI coupling is proposed in [17, 16] to achieve clock synchronization in networks of discrete-time integrators. Also, distributed PI actions are used in [2] to achieve consensus in networks of simple and double integrators affected by constant disturbances. The work presented in this thesis extends these approaches by considering a distributed PID (rather than PI) strategy encompassing the case of networks characterized by linear heterogeneous and non-linear homogeneous node dynamics.

1.1. Thesis Outline

In Chapter 2 we introduce the concept of complex network together with its mathematical representation using graph theory. We also briefly explain the consensus problem in networks of simple integrators, and the master stability function approach is introduced for studying synchronization in diffusive coupled networks with nonlinear node dynamics.

In Chapter 3, distributed PID actions are studied for networks of heterogeneous first-order linear dynamics affected by constant disturbances. Then, in Chapter 4, we extend the distributed PI controller to the case where the nodes have n -dimensional heterogeneous linear systems and are affected by constant disturbances, and most importantly, the proportional

and integral actions can be deployed independently from each other. This provides an extra degree of freedom that can be exploited to enhance the network's performance. In Chapters 3 and 4, full proofs of convergence are given and examples are included to validate the theoretical results.

Then, in Chapter 5 we propose the use of distributed PID controller for synchronizing networks of non-linear units. Here, the master stability function approach and Lyapunov theory are used to derive sufficient conditions to guarantee convergence of all nodes in the closed loop network. We show that the basic properties of the classical PID control are preserved even if the controller is deployed in a distributed fashion. Finally, some applications of the techniques developed in the thesis are given in Chapter 6 where synchronization in networks of power generators and electrical circuits are presented together with numerical validations. Conclusions are drawn in Chapter 7.

1.2. List of Main Contributions

The main contributions of this thesis are fourfold.

- First, we propose the use of a distributed PID control for reaching consensus in networks of heterogeneous first-order linear systems under constant perturbations. Here, the existence of a unique consensus equilibrium representing the collective dynamics of the network, is characterized as a function of the node dynamics. A complete proof of global asymptotic stability, together with numerical validations are presented.
- Secondly, a multilayer approach for reaching consensus in networks of heterogeneous n -dimensional linear dynamics is proposed. The proportional and integral actions are deployed on two different layers across the network, each with its own topology. Explicit expressions for the consensus values are obtained together with sufficient conditions guaranteeing convergence.
- Third, we extend the PID strategy to the case where the nodes are nonlinear and identical across the network. We derive local and global synchronization conditions where extensive simulations routines were performed to validate the theoretical results, together with a detailed performance assessment analysis.
- Finally, The proposed PID techniques are used in applications specifically to the problem of achieving synchronization of power generators and chaotic circuits.

The main results were presented in a number of publications [11, 12, 13, 14]

CHAPTER 2

Preliminaries and Background

2.1. Complex networks: generalities

As we point out in the Introduction, network theory is an emerging and prominent scientific area used to model, describe and analyse ensembles of agents or units interacting with each other. A network has three principal ingredients *Nodes*: denote the function of each agent, *Links*: describe the interaction between agents, and the *Network structure*: representing the architecture of the interconnections among nodes.

In general, networks present some particular properties that make them difficult to predict and control [72], for example

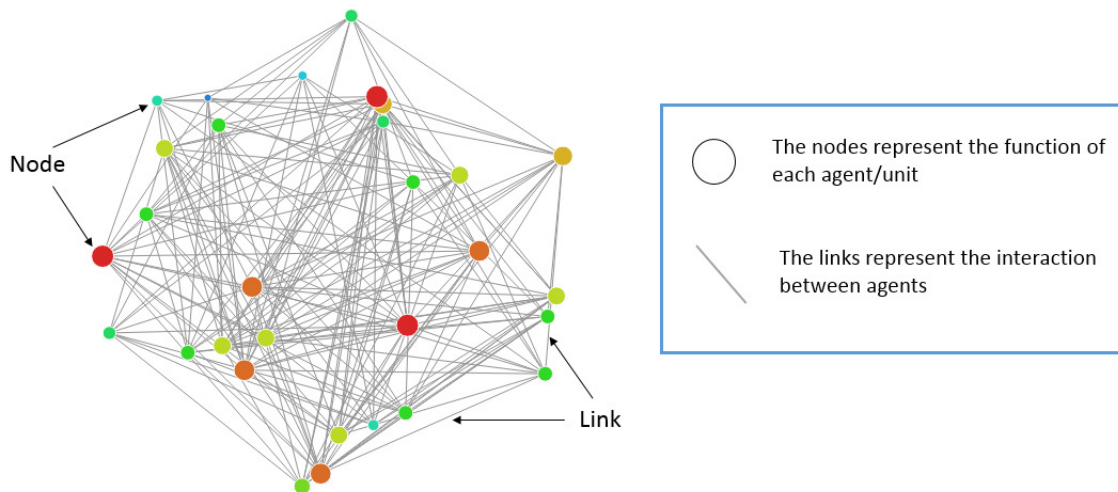


Figure 2-1.: General diagram of a network

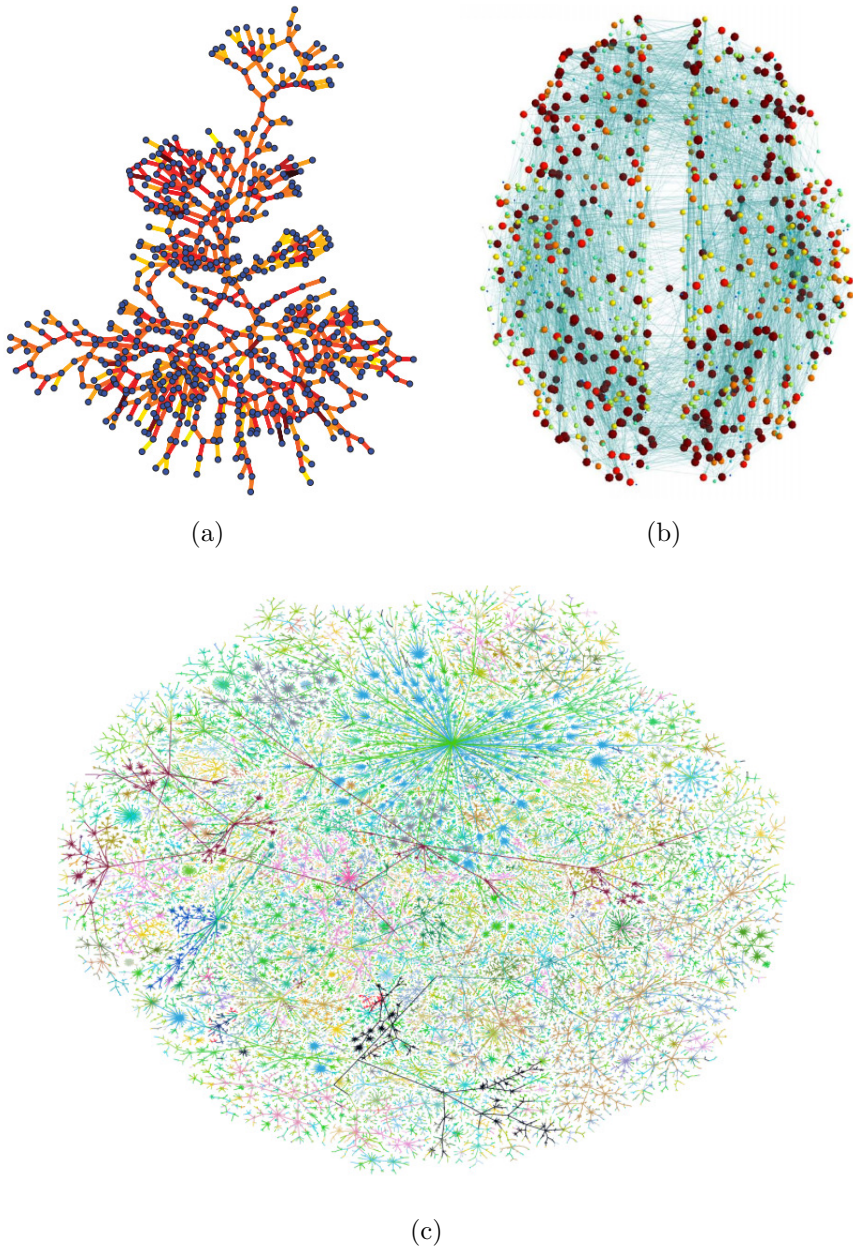


Figure 2-2: Wiring diagrams of some complex networks. (a) Electrical power grid of northern Italy, each node represents a power generator or consumer while the links represent buses [51] (b) Brain network, here the nodes and links represent neurons and the interactions between them respectively [71], (c) a visualization of the network structure of the Internet at the level of autonomous systems-local groups of computers each representing hundreds or thousands of machines [53].

- (i) **Structural complexity:** the architecture of the network could be an intricate tangle. For instance in Fig. 2.2(c) is depicted the complex wiring diagram of Internet.
- (ii) **Evolution of the network topology:** The links in the network may be time-varying. On the World-Wide Web, pages and links are created and lost every minute [53].
- (iii) **Connection diversity:** the links between nodes could have different functions, and weights. Synapses in the nervous system can be strong or weak, inhibitory or excitatory.
- (iv) **Dynamical complexity:** the nodes could be nonlinear dynamical systems. In a gene network or a Josephson junction array, the state of each node can vary in time in complicated ways.
- (v) **Node diversity:** there could be many different kinds of nodes. In an electrical power grid (see Fig. 2.2(a)) the nodes represent consumers and different types of power generators; hydroelectric, eolic, solar, etc.
- (vi) **Meta-complication:** the various features listed above can influence each other. For example, the present layout of a power grid depends on how it has grown over the years a case where network evolution (ii) affects topology (i). When coupled neurons fire together repeatedly, the connection between them is strengthened; this is the basis of memory and learning. Here nodal dynamics (iv) affect connection weights (iii).

Notwithstanding the complexity of networks, there is a significantly large number of problems studied in natural and man-made networks, for instance, congestion in communication networks [49], cascading failures and epidemic spreading [36, 50], brain networks [46], robot coordination and consensus [32, 55], frequency synchronization in power networks [27, 35, 70], etc (For further details about applications see [72, 9] and references there in). These, complex systems share the same mathematical formulation for describing their architectures which is based on graph theory and dynamical systems as we will see below.

2.2. The structure of complex networks: algebraic graph theory

Generally speaking, a network is a collection of nodes and links, each with an associate function or dynamics. One of the most important aspects in a network is its architecture (or structure), which commonly is represented by a *graph*. For instance in Fig. 2-3 three

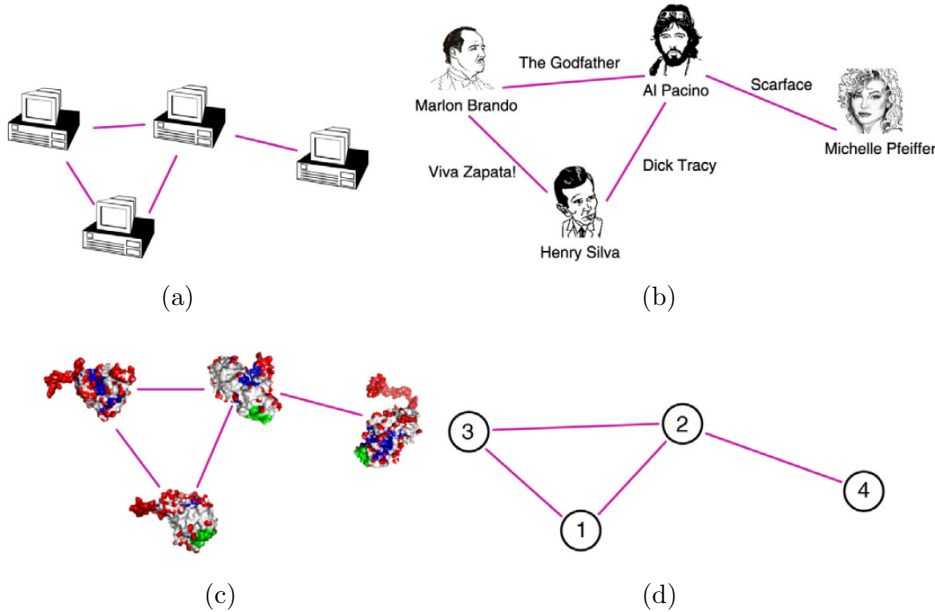


Figure 2-3: Example of: (a) an Internet network, (b) a Hollywood actor network, (c) a protein-protein interaction network. All of these networks are represented by the same graph (d). Images taken from [5].

different networks are depicted (a)-(c), sharing the same structure and are represented by the graph shown in Fig. 2.3(d).

A graph is composed by *vertexes* and *edges*, each one of them representing nodes and links in a network of interest. The links of a network can be directed or undirected. For instance; phone calls, where one person calls the other represents a *directed link*, while the transmission lines on the power grid, on which the electric current can flow in both directions represent *undirected links*.

Definition 2.2.1. (*undirected graph*) An undirected graph \mathcal{G} is a pair defined by $\mathcal{G} = (\mathcal{N}, \mathcal{E})$ where $\mathcal{N} = \{1, 2, \dots, N\}$ is the finite set of N node indices; $\mathcal{E} \subset \mathcal{N} \times \mathcal{N}$ is the set containing the P edges among nodes. Furthermore, we assume each edge has an associated weight denoted by $w_{ij} \in \mathbb{R}^+$ for all $i, j \in \mathcal{N}$.

In general, the topology of a network can be represented using the adjacency matrix [9].

Definition 2.2.2. The weighed adjacency matrix $\mathbf{A}(\mathcal{G}) \in \mathbb{R}^{N \times N}$ with A_{ij} entries, is defined as $A_{ij}(\mathcal{G}) = w_{ij}$ if there is an edge from node i to node j and zero otherwise.

Definition 2.2.3. The degree matrix $\mathbf{D}(\mathcal{G}) \in \mathbb{R}^{N \times N}$ with D_{ij} entries, is defined as $D_{ij} = \sum_{j=1}^n w_{ij}$ for $i=j$ and $D_{ij} = 0$ otherwise.

Definition 2.2.4. The Laplacian matrix $\mathcal{L}(\mathcal{G}) \in \mathbb{R}^{N \times N}$ is defined as the matrix whose elements $\mathcal{L}_{ij}(\mathcal{G}) = \sum_{j=1, j \neq i}^N w_{ij}$ if $i = j$ and $-w_{ij}$ otherwise.

Note that, the Laplacian matrix can be obtained as $\mathcal{L}(\mathcal{G}) = \mathcal{D}(\mathcal{G}) - \mathcal{A}(\mathcal{G})$ [54].

Example 1. Consider the graph depicted in Fig. 2.3(d). Then using definitions 2.2.2, 2.2.3 and 2.2.4 we compute the adjacency, degree and Laplacian matrices which are given by

$$\mathcal{A} = \begin{bmatrix} 0 & 1 & 1 & 0 \\ 1 & 0 & 1 & 1 \\ 1 & 1 & 0 & 0 \\ 0 & 1 & 0 & 0 \end{bmatrix}, \quad \mathcal{D} = \begin{bmatrix} 2 & 0 & 0 & 0 \\ 0 & 3 & 0 & 0 \\ 0 & 0 & 2 & 0 \\ 0 & 0 & 0 & 1 \end{bmatrix}, \quad \mathcal{L} = \begin{bmatrix} 2 & -1 & -1 & 0 \\ -1 & 3 & -1 & -1 \\ -1 & -1 & 2 & 0 \\ 0 & -1 & 0 & 1 \end{bmatrix}$$

Definition 2.2.5. [48] We say that an $N \times N$ matrix $\mathcal{S} = [\mathcal{S}_{ij}], \forall i, j \in \mathcal{N}$ belongs to the set Ω if it verifies the following properties:

1. $\mathcal{S}_{ij} \leq 0, i \neq j$, and $\mathcal{S}_{ii} = -\sum_{j=1, j \neq i}^N \mathcal{S}_{ij}$,
2. its eigenvalues in ascending order are such that $\lambda_1(\mathcal{S}) = 0$ while all the others, $\lambda_k(\mathcal{S}), k \in \{2, \dots, N\}$, are real and positive.

It is important to highlight that the Laplacian matrix \mathcal{L} belongs to the set Ω if its associated graph \mathcal{G} is connected [54].

Lemma 2.2.1. [64] Let \mathcal{G} be a connected undirected graph. Then, its corresponding Laplacian matrix $\mathcal{L} \in \Omega$ can be eigen-decomposed as $\mathcal{L} = \mathbf{U}\Lambda\mathbf{U}^T$ where $\mathbf{U} \in \mathbb{R}^{N \times N}$ is an orthonormal matrix given by $\mathbf{U} := [\mathbf{u}_1, \dots, \mathbf{u}_N]$ where $\mathbf{u}_i \in \mathbb{R}^{N \times 1}$ are the eigenvectors of \mathcal{L} , and $\Lambda := \text{diag}\{0, \lambda_2, \dots, \lambda_N\}$ with non-negative diagonal entries being the eigenvalues of \mathcal{L} , which can be ordered as $0 = \lambda_1 < \lambda_2 \leq \dots \leq \lambda_N$. Moreover, the smallest nonzero eigenvalue satisfies

$$\lambda_2 = \min_{\mathbf{x}^T \mathbf{1}_N = 0, \mathbf{x} \neq 0} \frac{\mathbf{x}^T \mathcal{L} \mathbf{x}}{\mathbf{x}^T \mathbf{x}} \tag{2-1}$$

2.3. Multiplex networks

Multiplex (or multilayer) networks are a collection of networks called layers which may interact with each other, and have been proposed as an effective modelling approach for representing and investigating several problems in many real and man-made networks [42]. They are characterized by the presence of different types of links and interconnections among nodes.

A classical example are transportation networks where two nodes (e.g cities) can be connected by rail and/or road and/or plane, as can be seen in Fig. 2-4 (see [21, 8] for further examples and an extensive review of available results to date).

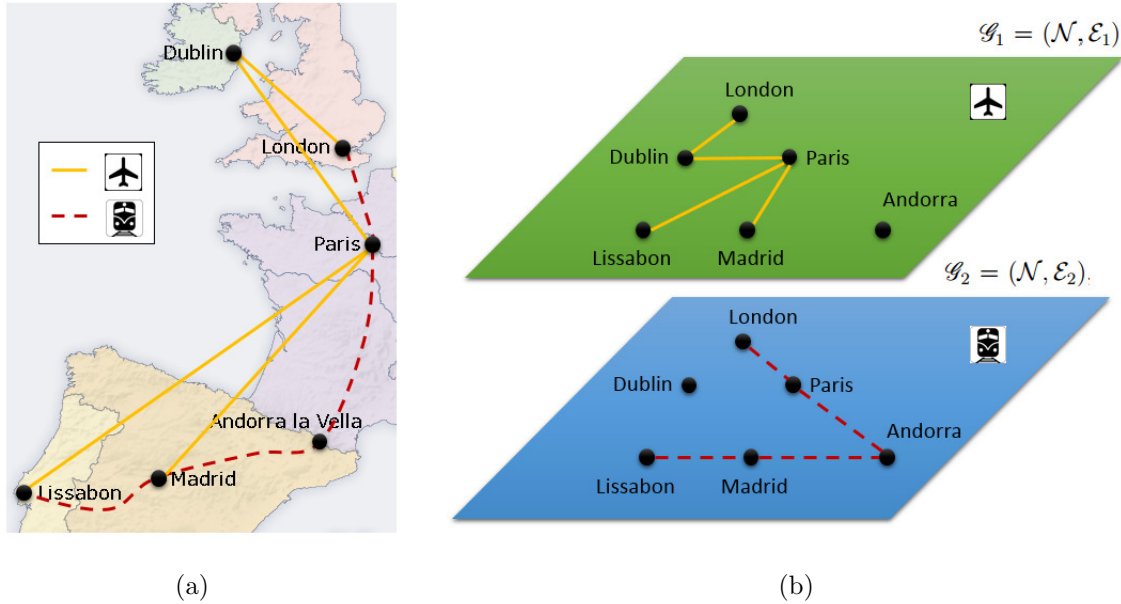


Figure 2-4: (a) Network of cities interconnected by rail and plane. (b) Multiplex representation of the network, with just two independent layers (no interconnections between layers, i.e., \mathcal{D} is an empty set) sharing the same set of vertexes.

To represent multiplex networks we introduce the concept of a multiplex graph which is a collection of graphs together with links between nodes of different graphs [8].

Definition 2.3.1. *A multiplex graph, is a pair $\mathcal{M} = (\mathcal{G}, \mathcal{D})$ where \mathcal{G} is the set of M graphs $\mathcal{G} := \{\mathcal{G}_1, \dots, \mathcal{G}_M\}$ called layers of \mathcal{M} , and \mathcal{D} is the set of edges representing interconnections between nodes of different layers.*

Definition 2.3.2. *Given two graphs sharing the same set of nodes $\mathcal{G}_1 = (\mathcal{N}, \mathcal{E}_1)$ and $\mathcal{G}_2 = (\mathcal{N}, \mathcal{E}_2)$, we define the projection graph as the graph $\text{proj}(\mathcal{G}_1, \mathcal{G}_2) := (\mathcal{N}, \mathcal{E}_p)$ with associated adjacency matrix $\mathbf{A}_p := \mathbf{A}(\mathcal{G}_1) + \mathbf{A}(\mathcal{G}_2)$.*

2.4. Mathematical notation and preliminaries

We denote by \mathbf{I}_N the identity matrix of dimension $N \times N$; by $\mathbf{0}_{M \times N}$ a matrix of zeros of dimension $M \times N$, and by $\mathbf{1}_N$ a $N \times 1$ vector with unitary elements. The Frobenius norm is denoted by $\|\cdot\|$ while the spectral norm by $\|\cdot\|$. A diagonal matrix, say \mathbf{D} , with

diagonal elements d_1, \dots, d_N is indicated by $\mathbf{D} = \text{diag}\{d_1, \dots, d_N\}$. The determinant of a matrix is denoted by $\det(\cdot)$, $\lambda_k(\mathbf{A})$ denotes the k -th eigenvalue of a squared matrix \mathbf{A} , and $\mathbf{A}' = \mathbf{A} + \mathbf{A}^T$ denotes the symmetric part of a matrix, while $\mathbf{A} \succ 0$ indicates that \mathbf{A} is a positive definite matrix.

Proposition 2.4.1. *Given two vectors $\zeta_1 \in \mathbb{R}^{n \times 1}$, $\zeta_2 \in \mathbb{R}^{m \times 1}$ and two matrices $\mathbf{Q}_1 \in \mathbb{R}^{m \times n}$, $\mathbf{Q}_2 \in \mathbb{R}^{m \times m}$, some algebraic manipulations yield [38]*

$$2\zeta_1^T \mathbf{Q}_1^T \mathbf{Q}_2 \zeta_2 \leq \varepsilon \zeta_1^T \mathbf{Q}_1^T \mathbf{Q}_1 \zeta_1 + \frac{1}{\varepsilon} \zeta_2^T \mathbf{Q}_2^T \mathbf{Q}_2 \zeta_2, \forall \varepsilon > 0 \quad (2-2)$$

Proof. Consider the vector $a\mathbf{Q}_1\zeta_1 \pm b\mathbf{Q}_2\zeta_2$ with $a, b \in \mathbb{R}^+$. Hence, from its quadratic form one has

$$(a\mathbf{Q}_1\zeta_1 \pm b\mathbf{Q}_2\zeta_2)^T (a\mathbf{Q}_1\zeta_1 \pm b\mathbf{Q}_2\zeta_2) \geq 0$$

then

$$a^2 \zeta_1^T \mathbf{Q}_1^T \mathbf{Q}_1 \zeta_1 \pm 2ab \zeta_1^T \mathbf{Q}_1^T \mathbf{Q}_2 \zeta_2 + b^2 \zeta_2^T \mathbf{Q}_2^T \mathbf{Q}_2 \zeta_2 \geq 0$$

and regrouping terms we have

$$2\zeta_1^T \mathbf{Q}_1^T \mathbf{Q}_2 \zeta_2 \leq \frac{a}{b} \zeta_1^T \mathbf{Q}_1^T \mathbf{Q}_1 \zeta_1 + \frac{a}{b} \zeta_2^T \mathbf{Q}_2^T \mathbf{Q}_2 \zeta_2$$

Finally, setting $\varepsilon = a/b$ we obtain (2-2). \square

Lemma 2.4.1. *Given a symmetric matrix $\mathbf{A} \in \mathbb{R}^{n \times n}$, denoting by $\lambda_{\min}(\mathbf{A})$ and $\lambda_{\max}(\mathbf{A})$ the smallest and largest eigenvalues of \mathbf{A} , the following statements are true [67]*

$$\lambda_{\min}(\mathbf{A}) \zeta^T \zeta \leq \zeta^T \mathbf{A} \zeta \leq \lambda_{\max}(\mathbf{A}) \zeta^T \zeta, \forall \zeta \in \mathbb{R}^{n \times 1} \quad (2-3)$$

$$\|\mathbf{A}\| = \max_k \{ |\lambda_k(\mathbf{A})| \} \leq \|\mathbf{A}\| \quad (2-4)$$

$$\lambda_{\min}(\mathbf{A}) \leq \lambda_{\min}(\mathbf{A}_o) \leq \lambda_{\max}(\mathbf{A}_o) \leq \lambda_{\max}(\mathbf{A}) \quad (2-5)$$

where $\mathbf{A}_o \in \mathbb{R}^{k \times k}$ is a principal sub-matrix of \mathbf{A} [6].

Example 2. Consider the symmetric matrix

$$\mathbf{A} = \begin{bmatrix} 2 & -1 & -1 \\ -1 & 1 & 0 \\ -1 & 0 & 1 \end{bmatrix}$$

with eigenvalues $\lambda_1 = 0$, $\lambda_2 = 1$ and $\lambda_3 = 3$. Then without loss of generality we select as a principal sub-matrix

$$\mathbf{A}_o = \begin{bmatrix} 2 & -1 \\ -1 & 1 \end{bmatrix}$$

with eigenvalues $\lambda_{o1} = 0.382$ and $\lambda_{o2} = 2.618$. Note that $\lambda_{\max}(\mathbf{A}) = 3$, while $\lambda_{\max}(\mathbf{A}_o) = 2.618$; therefore, we have that expression (2-5) is satisfied.

Lemma 2.4.2. [6] Given the matrices \mathbf{A} , \mathbf{B} , \mathbf{C} and \mathbf{D} of appropriate dimensions, the Kronecker product satisfies the following properties

$$(\mathbf{A} \otimes \mathbf{B}) + (\mathbf{A} \otimes \mathbf{C}) = \mathbf{A} \otimes (\mathbf{B} + \mathbf{C}) \quad (2-6)$$

$$(\mathbf{A} \otimes \mathbf{B})(\mathbf{A} \otimes \mathbf{D}) = \mathbf{AB} \otimes \mathbf{BD} \quad (2-7)$$

$$\|(\mathbf{A} \otimes \mathbf{B})\| = \|\mathbf{A}\| \|\mathbf{B}\| \quad (2-8)$$

Proposition 2.4.2. (Schur complement [10]) Let \mathbf{Q} be a block matrix defined by

$$\mathbf{Q} = \begin{bmatrix} \mathbf{Q}_1 & \mathbf{Q}_2 \\ \mathbf{Q}_2^T & \mathbf{Q}_3 \end{bmatrix}$$

where $\mathbf{Q}_1 = \mathbf{Q}_1^T$ and $\mathbf{Q}_3 = \mathbf{Q}_3^T$. Thus $\mathbf{Q} \succ 0$ if one of the following conditions is fulfilled

$$i) \quad \mathbf{Q}_1 \succ 0, \quad \mathbf{Q}_3 - \mathbf{Q}_2^T \mathbf{Q}_1^{-1} \mathbf{Q}_2 \succ 0$$

$$ii) \quad \mathbf{Q}_3 \succ 0, \quad \mathbf{Q}_1 - \mathbf{Q}_2^T \mathbf{Q}_3^{-1} \mathbf{Q}_2 \succ 0$$

2.5. Consensus in multi-agent systems

One particular problem in distributed control is consensus, where the goal is for all agent states in the network to asymptotically converge towards each other [54].

From the early work reported in [68], achieving consensus in multi-agent systems and networks has become a fundamental problem in Control.

The classical paradigm involves networks of simple or higher-order integrators communicating via linear diffusive coupling on an undirected network. Specifically, consider a multi-agent system of N simple integrators describing the dynamics of each agent

$$\dot{x}_i(t) = u_i(t), \quad i \in \mathcal{N} \quad (2-9)$$

where $x_i(t) \in \mathbb{R}$ represents the state of the i -th agent and $u_i(t) \in \mathbb{R}$ is the distributed control input through which agent i communicates with its neighboring agents.

Hence, the problem is to find a communication algorithm or a distributed controller $u_i(t)$, such that all states $x_i(t)$ converge asymptotically towards each other, i.e. consensus.

Definition 2.5.1. Let \mathfrak{C} be the consensus manifold

$$\mathfrak{C} := \{\mathbf{x} \in \mathbb{R}^N \mid |x_j(t) - x_i(t)| = 0, \forall i, j \in \mathcal{N}, i \neq j\}$$

then, the group of N agents described by (2-9) is said to reach consensus if, for any set of initial conditions $x_i(0) = x_{i0}$,

$$\lim_{t \rightarrow \infty} \mathbf{x}(t) \in \mathfrak{C}, \quad \forall t \geq 0, i \in \mathcal{N}$$

In [68], a distributed algorithm was proposed based on the sum of a proportional error between the i -th node and its neighbors

$$u_i(t) = \sum_{j=1}^N w_{ij}(x_j(t) - x_i(t)) \quad (2-10)$$

where w_{ij} denotes the weight of the link between nodes i and j . This controller can be represented by a graph $\mathcal{G} = (\mathcal{N}, \mathcal{E})$; therefore, using the Laplacian matrix of \mathcal{G} , we can write

$$u_i(t) = - \sum_{j=1}^N \mathcal{L}_{ij} x_j(t) \quad (2-11)$$

In what follows we denote this type of coupling as as distributed proportional control. It is well known that the distributed controller (2-11), is in fact able to solve the consensus problem for the group of agents (2-9).

Theorem 2.5.1. *Under the distributed proportional control dynamics (2-11), a group of N agents described by (2-9) achieves consensus if the undirected graph \mathcal{G} is connected. Moreover all the states asymptotically converge to a constant value x_∞ given by*

$$x_\infty = \frac{1}{N} \sum_{j=1}^N x(0) \quad (2-12)$$

Proof. Let $\mathbf{x}(t) := [x_1(t), \dots, x_N(t)]$ be the stack vector of the states of all agents; then the overall dynamics of the closed-loop network can be written as

$$\dot{\mathbf{x}}(t) = -\mathcal{L}\mathbf{x}(t) \quad (2-13)$$

and its general solution is given by $\mathbf{x}(t) = e^{-\mathcal{L}t}\mathbf{x}(0)$. It follows from Lemma 2.2.1 that $\mathcal{L} = \mathbf{U}\Lambda\mathbf{U}^T$. Hence, one has that

$$\begin{aligned} \mathbf{x}(t) &= e^{-\mathbf{U}\Lambda\mathbf{U}^T} \mathbf{x}(0) \\ &= \mathbf{U} e^{-\Lambda} \mathbf{U}^T \mathbf{x}(0) \\ &= \left[\mathbf{u}_1, \dots, \mathbf{u}_N \right] \begin{bmatrix} 1 & \mathbb{0}_{1 \times (N-1)} \\ \mathbb{0}_{(N-1) \times 1} & e^{-\bar{\Lambda}t} \end{bmatrix} \begin{bmatrix} \mathbf{u}_1^T \\ \vdots \\ \mathbf{u}_N^T \end{bmatrix} \mathbf{x}(0) \end{aligned}$$

where $\bar{\Lambda} := \text{diag}\{\lambda_2, \dots, \lambda_N\}$ is the matrix containing the nonzero eigenvalues of the laplacian matrix. Therefore, asymptotically we have that

$$\begin{aligned} \lim_{t \rightarrow \infty} x(t) &= [\mathbf{u}_1, \dots, \mathbf{u}_N] \begin{bmatrix} 1 & \mathbb{0}_{1 \times (N-1)} \\ \mathbb{0}_{(N-1) \times 1} & \mathbb{0}_{(N-1) \times (N-1)} \end{bmatrix} \begin{bmatrix} \mathbf{u}_1^T \\ \vdots \\ \mathbf{u}_N^T \end{bmatrix} \mathbf{x}(0) \\ &= [\mathbf{u}_1, \dots, \mathbf{u}_N] \begin{bmatrix} \mathbf{u}_1^T \\ \mathbb{0}_{(N-1) \times (N-1)} \end{bmatrix} \mathbf{x}(0) \end{aligned} \quad (2-14)$$

Note that \mathbf{u}_1 is the eigenvector associated with the null eigenvalue and it is given by $\mathbf{u}_1 := [1/\sqrt{N}, \dots, 1/\sqrt{N}]$. Therefore, (2-14) can be recast as

$$\begin{aligned} \lim_{t \rightarrow \infty} x(t) &= \begin{bmatrix} 1/N & \cdots & 1/N \\ \vdots & \ddots & \vdots \\ 1/N & \cdots & 1/N \end{bmatrix} \mathbf{x}(0) \\ &= \frac{1}{N} \left(\sum_{i=1}^N x_i(0) \right) \mathbb{1}_N \end{aligned}$$

and the proof is complete. \square

Example 3. In Fig. 2-5 are shown three different networks of simple integrators (2-9) controlled by the distributed proportional strategy (2-11). Without loss of generality, we assume that all link weights are unitary. This is $w_{ij} = 1$ if there is an associate edge between nodes i and j and $w_{ij} = 0$ otherwise.

In the literature, this proportional algorithm is often called average consensus [32, 55] and only applies for the case where the nodes share trivial dynamics.

As we said in the Introduction, there are several extensions of consensus algorithms, and it is often assumed that the agent dynamics is either trivial or identical across the network. Thus, many of the available strategies only apply to networks of homogeneous systems in the absence of disturbances and noise. Unfortunately, this is not a realistic scenario since heterogeneity is a principal ingredient in real and man-made networks. In the next Chapter we will address the problem of achieving consensus in heterogeneous networks under the presence of constant disturbances acting on each node, by extending the distributed proportional controller (2-11) to the case where integral and derivative actions are also present.

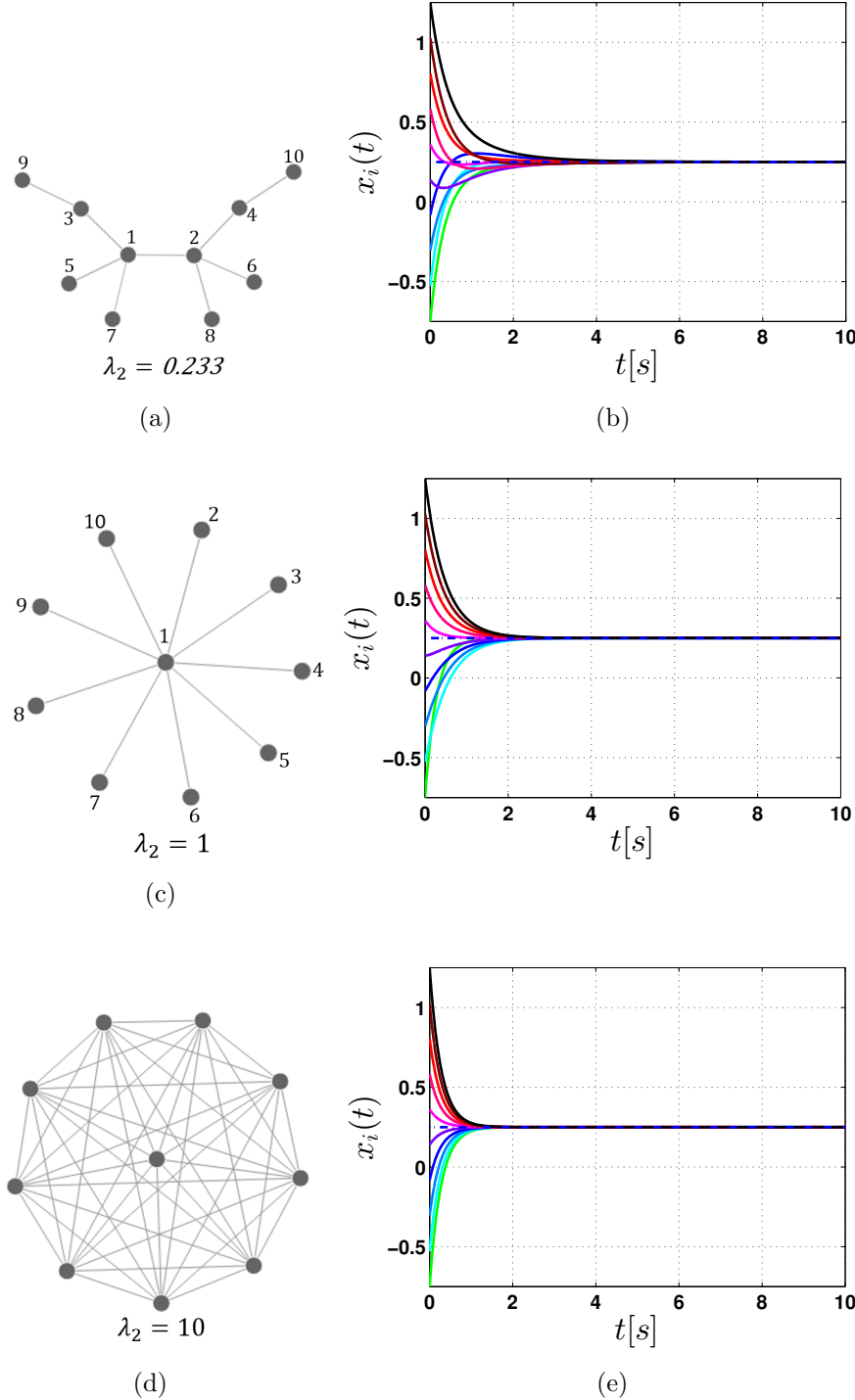


Figure 2-5.: Time response of three different networks of simple integrators (2-9) controlled by (2-11). All link weights are unitary. The blue dashed-line represents the average consensus value x_∞

2.6. Synchronization in complex networks

Synchronization can be traced back in the seventeenth century, to the observation on couple clocks made by the Dutch scientist Christiaan Huygens. He built an experiment consisting of two pendulum clocks hanging from a common support, realizing that after some time, their oscillations coincided perfectly, i.e synchronization. This observation, made a great impact on the scientific community at that time and increased the accuracy of time measurements enormously [58]. Nowadays, synchronization is an active research field due to its potential application in biology and technology [29, 75, 26]. In particular, consider a diffusive coupled network of N nodes given by

$$\dot{\mathbf{x}}_i(t) = \mathbf{f}(\mathbf{x}_i) - \alpha \sum_{j=1}^N \mathcal{L}_{ij} \mathbf{x}_j(t), \forall i \in \mathcal{N} \quad (2-15)$$

where $\mathbf{x}_i \in \mathbb{R}^n$, $\mathbf{f}(\mathbf{x}, t) : \mathbb{R}^n \times \mathbb{R}^+ \cup \{0\} \mapsto \mathbb{R}^n$ is a nonlinear vector field modelling the dynamics of each agent in the network. $\mathbf{\Gamma} \in \mathbb{R}^{n \times n}$ is the inner coupling matrix representing the exchange of information between agents, α is the coupling strength and the architecture of the network is represented by an undirected graph \mathcal{G} where \mathcal{L} is its associated Laplacian matrix. Note that the diffusive term in (2-15) is the generalization for high-order node dynamics of the distributed proportional control in (2-10).

Definition 2.6.1. Let \mathfrak{C} be the synchronization manifold

$$\mathfrak{C} := \left\{ \mathbf{x} \in \mathbb{R}^{nN} \mid \|\mathbf{x}_j(t) - \mathbf{x}_i(t)\| = 0, \forall i, j \in \mathcal{N}, i \neq j \right\}$$

then, network (2-15) is said to reach local admissible synchronization if, for any set of initial conditions $\mathbf{x}_i(0) = \mathbf{x}_{i0}$,

$$\lim_{t \rightarrow \infty} \mathbf{x}(t) \in \mathfrak{C}, \quad \forall t \geq 0, \quad i \in \mathcal{N} \quad (2-16)$$

If in addition (2-16) is satisfied for any initial condition, we said that the network reaches global admissible synchronization.

Synchronization in diffusive coupled networks has been extensively studied in literature, where different approaches and conditions are presented for its achievement. For instance in [47, 44] both local and global techniques are proposed for studying synchronization in networks, while in [22, 23] extensions have been made to the case where the connections weights evolve according to some adaptive law. Usually, global techniques are based on Lyapunov stability and passivity theory; however, there is also an interesting and relative simple strategy to study local synchronization as we shall see below.

2.6.1. Master stability function

The master stability function (MSF) is a local approach for studying synchronization in networks and was originally proposed in [57]. The main advantage of MSF is that allows to reduce the computational complexity required to assess if synchronization is possible, since instead of studying the stability of the whole network, it is just required to study the stability of one node (master node), which represents all the others in the web. Hence, this technique represents a powerful tool for investigating synchronization in generic networks of identical oscillators (some extensions to nearly identical oscillators are available in [73]). Note that when all nodes are synchronized, i.e., $\mathbf{x}_1 = \dots = \mathbf{x}_N = \mathbf{s}(t)$, the equation describing the synchronous motion is given by

$$\dot{\mathbf{s}}(t) = \mathbf{f}(\mathbf{s}) \quad (2-17)$$

Roughly speaking, the master stability function approach, studies the stability of the synchronous solution $\mathbf{s}(t)$, in the presence of small perturbations $\delta\mathbf{x}(t)$. For the sake of clarity, we have split the MSF approach in four steps

1. First, we start by assuming that the network is already in a synchronous state, and also that this state is a solution of an isolated node (2-17), so that $\mathbf{x}_1 = \dots = \mathbf{x}_N = \mathbf{s}(t)$,
2. Next, we perturb the synchronous state of each node by considering $\mathbf{s}(t) = \mathbf{x}_i(t) - \delta\mathbf{x}_i(t)$. Hence, the the perturbation dynamics reads

$$\dot{\delta\mathbf{x}}_i(t) = \mathbf{f}(\delta\mathbf{x}_i + \mathbf{s}) - \alpha \sum_{j=1}^N \mathcal{L}_{ij} \boldsymbol{\Gamma} \delta\mathbf{x}_j(t) - \mathbf{f}(\mathbf{s}), \forall i \in \mathcal{N} \quad (2-18)$$

It follows from Taylor series expansion that

$$\mathbf{f}(\delta\mathbf{x}_i + \mathbf{s}) = \mathbf{f}(\mathbf{s}) + D\mathbf{f}(\mathbf{s})\delta\mathbf{x}_i(t), \forall i \in \mathcal{N}$$

where $D\mathbf{f}(\mathbf{s})$ denotes the Jacobian matrix of $\mathbf{f}(\cdot)$ evaluated along the synchronous solution $\mathbf{s}(t)$. Therefore, (2-18) can be rewritten as

$$\dot{\delta\mathbf{x}}_i(t) = D\mathbf{f}(\mathbf{s})\delta\mathbf{x}_i(t) - \alpha \sum_{j=1}^N \mathcal{L}_{ij} \boldsymbol{\Gamma} \delta\mathbf{x}_j(t), \forall i \in \mathcal{N} \quad (2-19)$$

and therefore, the disagreement dynamics of the whole network are given by

$$\dot{\Delta}(t) = ((\mathbf{I}_N \otimes D\mathbf{f}(\mathbf{s})) - \alpha(\boldsymbol{\mathcal{L}} \otimes \boldsymbol{\Gamma})) \Delta(t) \quad (2-20)$$

where $\Delta(t) := [\delta\mathbf{x}_1^T(t), \dots, \delta\mathbf{x}_N^T(t)]^T$

3. Then, a state transformation is implemented in order to decouple the perturbation dynamics of any single node from the others. So, from the fact that the Laplacian matrix \mathcal{L} is symmetric positive semi-definite matrix, we have from Lemma 2.2.1 that $\mathcal{L} = \mathbf{U}^{-1}\Lambda\mathbf{U}$. Thus, letting $\zeta(t) = (\mathbf{U}^{-1} \otimes I_n) \Delta(t)$, we can recast (2-20) in the new coordinates as

$$\dot{\zeta}(t) = ((\mathbf{I}_N \otimes D\mathbf{f}(\mathbf{s})) - \alpha(\Lambda \otimes \Gamma)) \zeta(t) \quad (2-21)$$

note that (2-21) is in triangular form with blocks $\dot{\zeta}_i(t) = (D\mathbf{f}(\mathbf{s}) - \alpha\lambda_i\Gamma) \zeta_i(t), \forall i \in \mathcal{N}$, where λ_i are the eigenvalues of the Laplacian matrix. Then, letting $\tilde{\alpha} = \alpha\lambda_i$, we have that all the N blocks can be represented by the generic dynamics (master node) $\zeta_s(t)$ given by

$$\dot{\zeta}_s(t) = (D\mathbf{f}(\mathbf{s}) - \tilde{\alpha}\Gamma) \zeta_s(t) \quad (2-22)$$

4. Therefore, the local stability of the synchronous solution $\mathbf{s}(t)$ can be addressed computing the Maximum Lyapunov Exponent (see Appendix B) of the variational equation (2-22). Note that if the synchronous solution $\mathbf{s}(t)$ represent an equilibrium point; then, the stability problem becomes equivalent to study the dominant eigenvalue of (2-22). Throughout the thesis we denote the maximum lyapunov exponent of (2-22) as $\Psi(\tilde{\alpha})$, which is also known as Master Stability Function (MSF) [9].

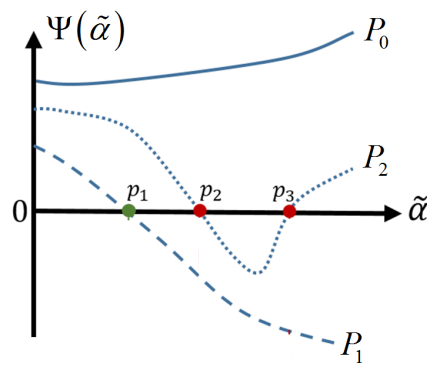


Figure 2-6.: Three possible cases for the MSF $\Psi(\tilde{\alpha})$: Type P_0 : $\Psi(\tilde{\alpha})$ is a monotonically increasing function. Type P_1 : $\Psi(\tilde{\alpha})$ is a monotonically decreasing function, Type P_2 : $\Psi(\tilde{\alpha})$ is a V-shaped function admitting negative values in some region.

Positive values of $\Psi(\tilde{\alpha})$ represent unstable modes, i.e. the network does not exhibit synchronized motion. Moreover, negative values of $\Psi(\tilde{\alpha})$ indicates that the network exhibits *local*

synchronization (the synchronization manifold is locally transversely stable). Note in (2-22), that for $\lambda_1 = 0$ we have that $\tilde{\alpha} = 0$ and the variational equation reads $\dot{\zeta}_s(t) = D\mathbf{f}(\mathbf{s})\zeta_s(t)$ where its Lyapunov exponents are equal to those of the single uncoupled system $\dot{\mathbf{s}}(t) = \mathbf{f}(\mathbf{s})$. Three possible cases of the MSF are shown in Fig. 2-6. Thus we say that the variational equation (2-22) possesses a MSF of type

- P_o : if there is not any intersection point with the zero axis; therefore, synchronization cannot be achieved, no matter the coupling strength,
 - P_1 : if there is just one intersection point p_1 with the zero axis, so for admitting local synchronization it suffices $\alpha > p_1/\lambda_2$,
 - P_2 : if there are two intersection points p_2 and p_3 . Hence, synchronization is guaranteed if $p_2/\lambda_2 < \alpha < p_3/\lambda_N$.

A more general case where the MSF presents multiple intersections can be found in [47].

Example 4. Consider the closed-loop network (2-15), where the non-linear vector-field modelling the intrinsic dynamics of each node is described by the well known Lorenz equation given by

$$\mathbf{f}_1(\mathbf{x}) = \begin{bmatrix} -10x_1 + 10x_2 \\ 28x_1 - x_2 - x_1x_3 \\ -ax_3 + x_1x_3 \end{bmatrix}, D\mathbf{f}_1(\mathbf{x}) = \begin{bmatrix} -10 & 10 & 0 \\ 28 - x_3 & -1 & -x_1 \\ x_2 & x_1 & -a \end{bmatrix} \quad (2-23)$$

This system exhibits chaotic oscillations for $a = 2$ as can be seen in Fig. 2-7, where the

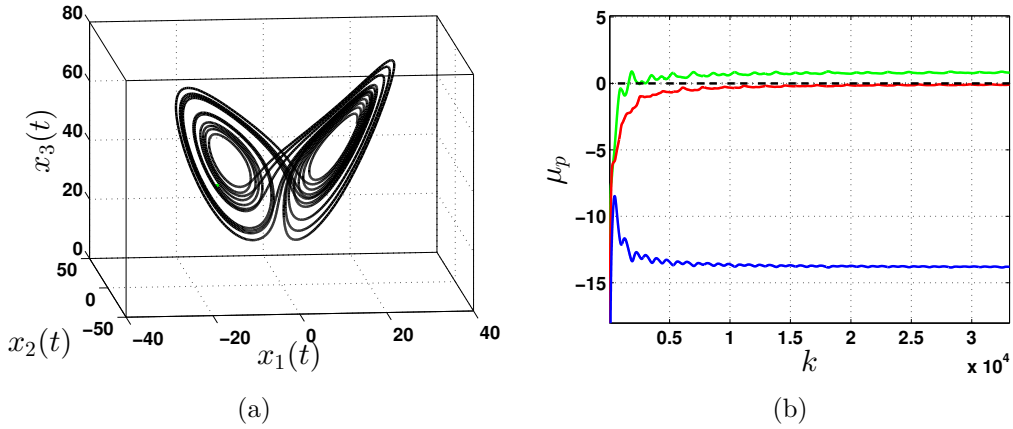


Figure 2-7.: (a) Chaotic attractor, (b) Lyapunov exponents μ_p . k denotes time step of the algorithm.

Lyapunov exponents μ_p for $p = \{1, 2, 3\}$ have been also computed using a standard numerical method with a time step $T = 0.001$ (see Appendix B). For this particular system we have that $\mu_1 \approx 0.849$, $\mu_2 \approx 0$ and $\mu_3 \approx -13.82$. Next, we compute the MSF for the Lorenz equation. So we first integrate system (2-17) for 10^4 steps so that we can reach the chaotic attractor, to then compute for 20×10^4 steps the Lyapunov exponents of the variational equation (2-22). We then repeat this computation for different values of the parameter $\tilde{\alpha}$. The results are depicted in Fig. 2-8 where the MSF $\Psi(\tilde{\alpha})$ has been calculated for different Γ matrices. Note

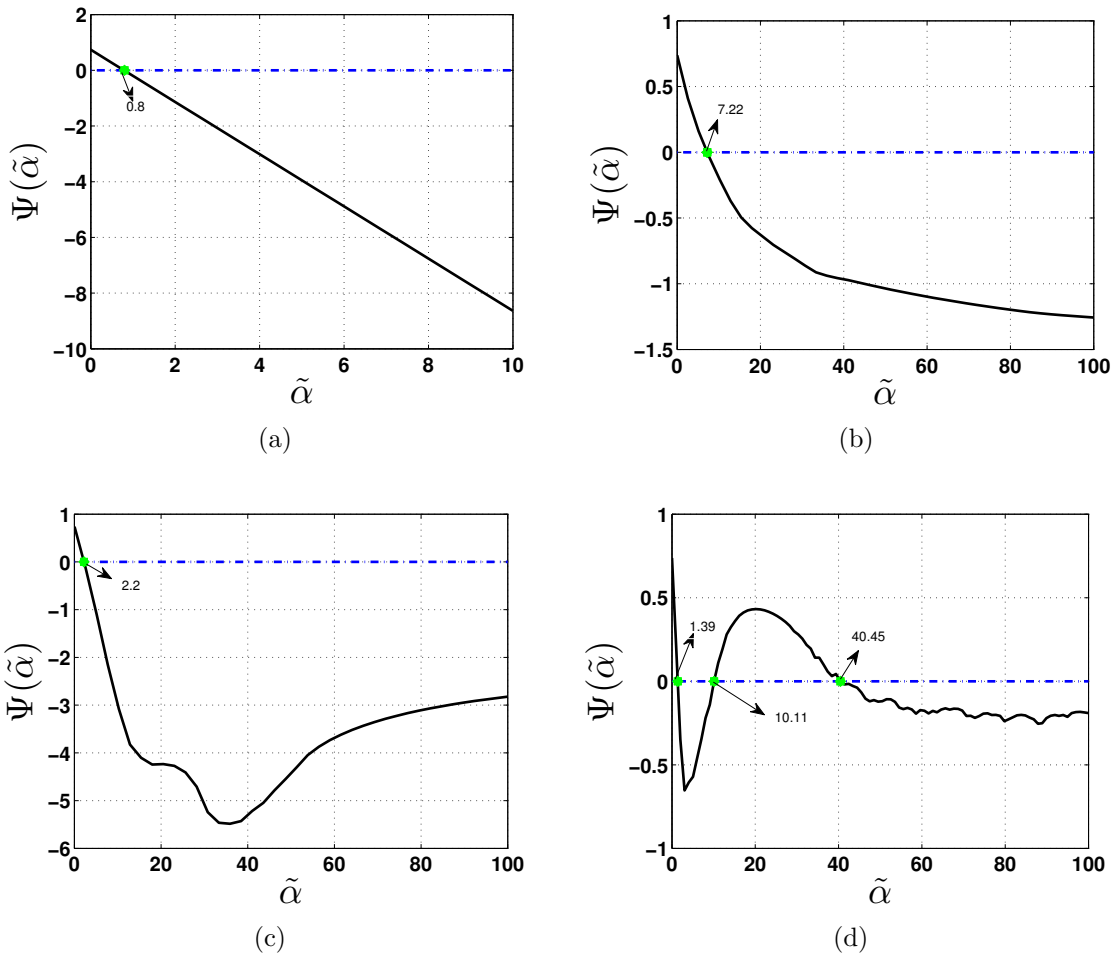


Figure 2-8.: Master Stability Function for chaotic Lorenz system under different output matrices: (a) $\Gamma = \text{diag}\{1, 1, 1\}$, (b) $\Gamma = \text{diag}\{1, 0, 0\}$, (c) $\Gamma = \text{diag}\{0, 1, 0\}$, and (d) $\Gamma = \text{diag}\{0, 0, 1\}$.

that the MSF of Figure 2.8(a), 2.8(b), and 2.8(c) are Type P_1 ; then, local synchronization is expected if $\alpha > 0.8/\lambda_2$, $\alpha > 7.22/\lambda_2$, and $\alpha > 2.2/\lambda_2$ respectively. Specifically, consider a network of three nodes as the one depicted in Fig. 2.5(a) with $\Gamma = \text{diag}\{1, 1, 1\}$. Thus

following previous derivations we have that the network reaches local synchronization if $\alpha > 0.8/0.233 = 3.4335$. The time response of the network is depicted in Fig. 2-9 for two different values of the coupling parameter α .

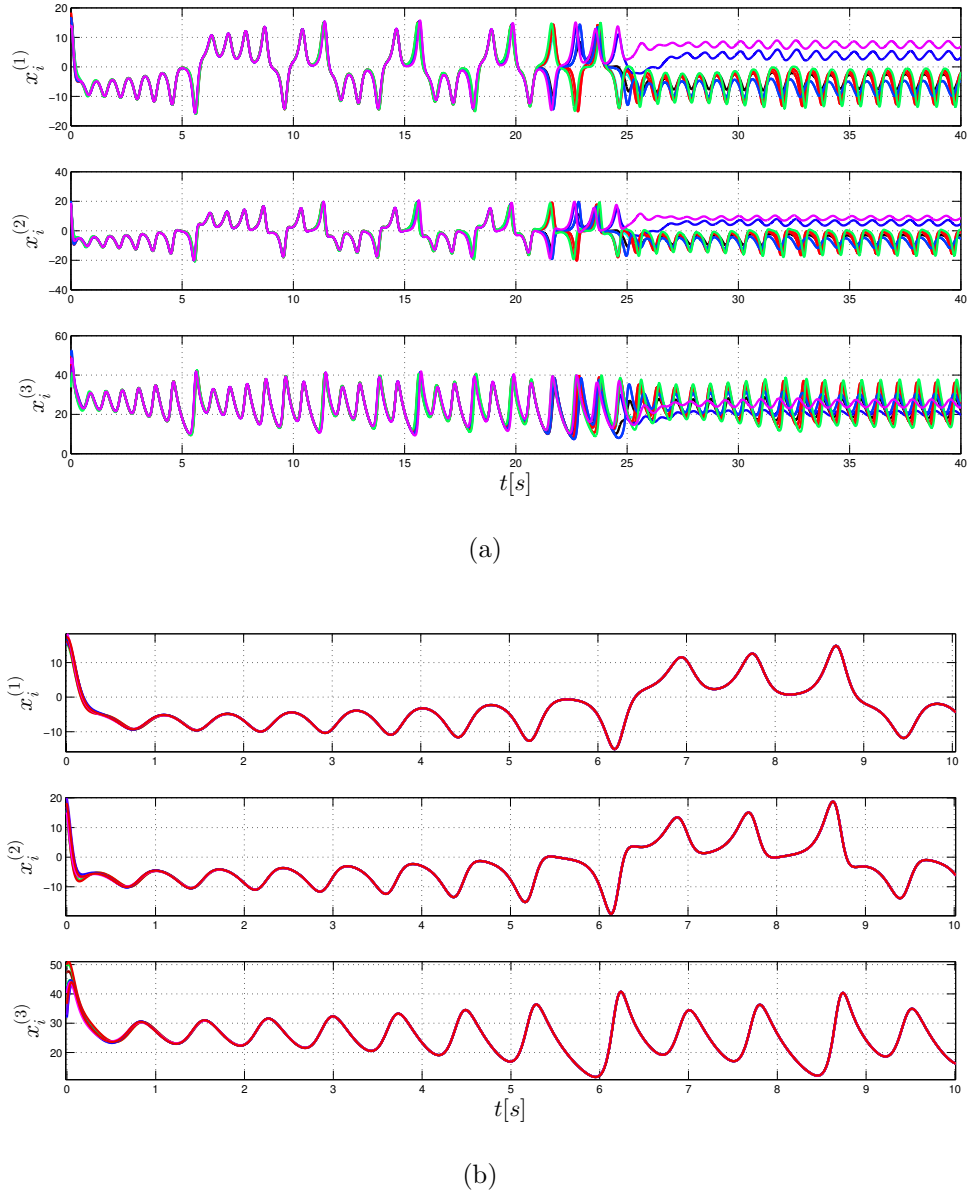


Figure 2-9.: Time response of a network of 10 chaotic Lorenz for (a) $\alpha = 3$ and (b) $\alpha = 4$.

CHAPTER 3

PID Consensus in Heterogeneous Linear Multi-Agent Networks

As we point out in the last Section, the study of consensus in networks has been carried out mostly for trivial and homogeneous dynamics in the nodes. Nevertheless, heterogeneity is a principal ingredient in real and man-made networks. Therefore, as a simple scenario for studying heterogeneous networks, we consider a multi-agent system of N nodes (agents) governed by heterogeneous first-order linear dynamics of the form

$$\dot{x}_i(t) = \rho_i x_i(t) + \delta_i + u_i(t), \quad i \in \mathcal{N} \quad (3-1)$$

where $x_i(t) \in \mathbb{R}$ represents the state of the i -th agent, $\rho_i \in \mathbb{R}$ is the agent pole determining its uncoupled dynamics, $\delta_i \in \mathbb{R}$ is some constant disturbance (or constant external input) acting on each node, and $u_i(t) \in \mathbb{R}$ is the distributed control input through which agent i communicates with its neighboring agents. Note that without any control input, the node dynamics can either be stable ($\rho_i < 0$) with different equilibria given by $x_i^* := -\delta_i/\rho_i$, or unstable ($\rho_i > 0$), while the constant term δ_i can be used to represent different quantities in applications. For example, it can model constant power injections in power grids [28] or noise in minimal models of flocks of birds [79].

Definition 3.0.2. (*Admissible consensus*) A multi-agent network of N heterogeneous agents described by (3-1) is said to reach admissible consensus if, for any set of initial conditions $x_i(0) = x_{i0}$,

$$\lim_{t \rightarrow \infty} |x_j(t) - x_i(t)| = 0, \quad |u_i(t)| < +\infty, \quad \forall t \geq 0, \quad i \in \mathcal{N} \quad (3-2)$$

If, instead $\lim_{t \rightarrow \infty} |x_j(t) - x_i(t)| \leq \varepsilon$ for $\varepsilon > 0$ and $|u_i(t)| < +\infty$, $\forall t \geq 0$, $\forall i, j \in \mathcal{N}$, the network is said to achieve ε -admissible consensus.

Here we study the case where, rather than controlling the agents via classical proportional (diffusive) strategy, agents in the network are controlled by distributed PID control given by

$$u_i(t) = - \sum_{j=1}^N w_{ij} \left(\alpha (x_j(t) - x_i(t)) + \beta \int_0^t (x_j(\tau) - x_i(\tau)) d\tau + \gamma (\dot{x}_j(t) - \dot{x}_i(t)) \right) \quad (3-3)$$

where w_{ij} represents the associate weight of a link between node i and j of a graph $\mathcal{G} := (\mathcal{N}, \mathcal{E})$. We do not consider self-loops, that is $w_{ii} = 0$, and the constants $\alpha, \beta, \gamma \in \mathbb{R}^+$ are additional parameters modulating globally the contribution of the proportional, integral and derivative actions. Using the Laplacian matrix of the graph \mathcal{G} , we can recast (3-3) as

$$u_i(t) = - \sum_{j=1}^N \mathcal{L}_{ij} \left(\alpha x_j(t) + \beta \int_0^t x_j(\tau) d\tau + \gamma \dot{x}_j(t) \right) \quad (3-4)$$

where \mathcal{L}_{ij} are the elements of the network Laplacian.

Now we first present the proportional-integral case, to then study the full distributed PID control.

3.1. Distributed PI control

In this section we neglect the derivative action in (3-4), this is setting $\gamma = 0$ so that we obtain a distributed PI strategy. Hence, defining $\mathbf{P} := \text{diag}\{\rho_1, \dots, \rho_N\}$, $\Delta := [\delta_1, \dots, \delta_N]^T$, the stack vector of node states $\mathbf{x}(t) = [x_1(t), \dots, x_N(t)]^T$ and integral states

$$\mathbf{z}(t) = [z_1(t), \dots, z_N(t)]^T := -\beta \mathcal{L} \int_0^t \mathbf{x}(\tau) d\tau \quad (3-5)$$

the overall dynamics of the closed-loop network can be written as

$$\begin{bmatrix} \dot{\mathbf{x}}(t) \\ \dot{\mathbf{z}}(t) \end{bmatrix} = \underbrace{\begin{bmatrix} \mathbf{P} - \alpha \mathcal{L} & \mathbf{I}_N \\ -\beta \mathcal{L} & \mathbf{0}_{N \times N} \end{bmatrix}}_{\mathbf{A}} \begin{bmatrix} \mathbf{x}(t) \\ \mathbf{z}(t) \end{bmatrix} + \begin{bmatrix} \Delta \\ \mathbf{0}_{N \times 1} \end{bmatrix} \quad (3-6)$$

Then, the problem is finding conditions on the control gains α, β , the network structure \mathcal{L} and node dynamics \mathbf{P} , such that the closed-loop network (3-6) achieves admissible consensus.

3.1.1. Consensus equilibrium

First we prove that the PI strategy is able to guarantee consensus. In particular we prove that the closed-loop network (3-6) has a unique equilibrium which solves the admissible consensus problem.

Proposition 3.1.1. *The closed-loop network (3-6) has a unique equilibrium given by $\mathbf{x}^* := x_\infty \mathbb{1}_N$ with $x_\infty := -\sum_{k=1}^N \delta_k / \sum_{k=1}^N \rho_k$, and $\mathbf{z}^* := -(\mathbf{P}\mathbf{x}^* + \Delta)$.*

Proof. The proof follows immediately by setting the left-hand side of (3-6) to zero and noticing that $\mathcal{L} \in \Omega$ (see Lemma 2.2.1) so that $\mathbf{x}^* = a\mathbb{1}_N$, $\forall a \in \mathbb{R}$ and $\mathbf{z}^* = -(a\mathbf{P}\mathbb{1}_N + \Delta)$. By definition (3-5), and from the fact that $\mathcal{L} \in \Omega$, we also have $\mathbb{1}_N^T \mathbf{z}(t) = 0$, then $\mathbb{1}_N^T \mathbf{z}^* = 0$ and we obtain

$$a = -\mathbb{1}_N^T \Delta / \mathbb{1}_N^T \mathbf{P} \mathbb{1}_N = -\left(\sum_{k=1}^N \delta_k\right) \left(\sum_{k=1}^N \rho_k\right)^{-1}$$

Hence, setting $x_\infty = a$ completes the proof. \square

To prove convergence of the closed-loop network (3-6), we have to prove that equilibrium in Proposition (3.1.1) is globally asymptotically stable. We start by shifting the origin via the state transformation $\mathbf{y}(t) := \mathbf{z}(t) + \Delta$ so that (3-6) becomes

$$\begin{bmatrix} \dot{\mathbf{x}}(t) \\ \dot{\mathbf{y}}(t) \end{bmatrix} = \underbrace{\begin{bmatrix} \mathbf{P} - \alpha \mathcal{L} & \mathbf{I}_N \\ -\beta \mathcal{L} & \mathbb{0}_{N \times N} \end{bmatrix}}_{\mathbf{A}} \begin{bmatrix} \mathbf{x}(t) \\ \mathbf{y}(t) \end{bmatrix} \quad (3-7)$$

Therefore, convergence is equivalent to prove that the matrix \mathbf{A} is Hurwitz stable. To this aim we split the proof into two stages. Firstly, the system describing the error dynamics to the consensus state is derived and some of its generic properties are described. Secondly, the two cases of homogeneous and heterogeneous nodes are treated separately in order to complete the proof of convergence.

3.1.2. Block decomposition of \mathcal{L}

First, we present a decomposition of the Laplacian matrix that will be crucial for the derivations reported in the rest of the manuscript. Note that such a decomposition can be avoided sometimes when proving consensus in homogeneous networks, but it is particularly useful to prove convergence in the presence of heterogeneous nodes.

As the Laplacian matrix is symmetric (the graph is undirected), according to Schur's lemma, there exists an orthogonal matrix, say $\mathbf{V} := (1/\sqrt{N})\mathbf{U}$ such that $\mathcal{L} = \mathbf{V}\Lambda\mathbf{V}^{-1} = \mathbf{U}\Lambda\mathbf{U}^{-1}$, where $\Lambda = \text{diag}\{0, \lambda_2, \dots, \lambda_N\}$. Note that the eigenvectors of \mathcal{L} are column vectors of \mathbf{V} (or equivalently row vectors of \mathbf{V}^{-1}). As suggested in [41], without loss of generality, we can express the orthogonal matrix \mathbf{U} and its inverse in the following block form

$$\mathbf{U} = \begin{bmatrix} 1 & \mathbf{Q}_{12} \\ \mathbb{1}_{N-1} & \mathbf{Q}_{22} \end{bmatrix}, \quad \mathbf{U}^{-1} = \begin{bmatrix} r_{11} & \mathbf{R}_{12} \\ \mathbf{R}_{21} & \mathbf{R}_{22} \end{bmatrix}, \quad (3-8)$$

where $\mathbf{Q}_{12} \in \mathbb{R}^{1 \times (N-1)}$, $\mathbf{Q}_{22} \in \mathbb{R}^{(N-1) \times (N-1)}$, $r_{11} \in \mathbb{R}$, $\mathbf{R}_{12} \in \mathbb{R}^{1 \times (N-1)}$, $\mathbf{R}_{21} \in \mathbb{R}^{(N-1) \times 1}$, $\mathbf{R}_{22} \in \mathbb{R}^{(N-1) \times (N-1)}$ are blocks of appropriate dimensions and

$$r_{11} = \frac{1}{N}, \quad \mathbf{R}_{12} = \frac{1}{N}\mathbb{1}_{N-1}^T, \quad (3-9)$$

Moreover, as $\mathbf{V}^{-1} = \mathbf{V}^T$, it follows that $\mathbf{R}_{21} = (1/N)\mathbf{Q}_{12}^T$ and $\mathbf{R}_{22} = (1/N)\mathbf{Q}_{22}^T$. Thus, we can recast \mathbf{U} as

$$\mathbf{U} = \begin{bmatrix} 1 & N\mathbf{R}_{21}^T \\ \mathbb{1}_{N-1} & N\mathbf{R}_{22}^T \end{bmatrix}, \quad (3-10)$$

Also, since $\mathbf{U}^{-1}\mathbf{U} = \mathbf{I}_N$, the blocks in the definition of \mathbf{U} and \mathbf{U}^{-1} must fulfill the following conditions:

$$\mathbf{R}_{21} + \mathbf{R}_{22}\mathbb{1}_{N-1} = \mathbb{0}_{(N-1) \times 1} \quad (3-11)$$

$$\mathbf{R}_{21}\mathbf{R}_{21}^T + \mathbf{R}_{22}\mathbf{R}_{22}^T = \frac{1}{N}\mathbf{I}_{N-1} \quad (3-12)$$

$$r_{11}\mathbf{R}_{21}^T + \mathbf{R}_{12}\mathbf{R}_{22}^T = \mathbb{0}_{1 \times (N-1)} \quad (3-13)$$

Note that, solving (3-11) for \mathbf{R}_{21} and (3-13) for \mathbf{R}_{21}^T , using (3-9), we can also write

$$\mathbf{R}_{21}\mathbf{R}_{21}^T = \mathbf{R}_{22}\mathbb{1}_{N-1}\mathbb{1}_{N-1}^T\mathbf{R}_{22}^T \quad (3-14)$$

Moreover, $\|\mathbf{V}^{-1}\| = \sqrt{\lambda_{\max}((\mathbf{V}^{-1})^T\mathbf{V}^{-1})}$ (see (2-4)). Also, as $\mathbf{V}^{-1} = \mathbf{V}^T$ and $\mathbf{V}\mathbf{V}^T = \mathbf{I}_N$ one has $\|\mathbf{U}^{-1}\| = \frac{1}{\sqrt{N}}$ and therefore its block \mathbf{R}_{22} is such that

$$\|\mathbf{R}_{22}\| \leq \|\mathbf{U}^{-1}\| = 1/\sqrt{N} \quad (3-15)$$

Finally, $\|\mathbf{R}_{22}\mathbb{1}_{N-1}\| \leq \sqrt{N-1}\|\mathbf{R}_{22}\|$ (see Theorem 5.6.2 of [67]), then expressing \mathbf{R}_{21} from (3-11) and using (3-15), we find that

$$\|\mathbf{R}_{21}\| \leq \sqrt{N-1}\|\mathbf{R}_{22}\| \leq \sqrt{(N-1)/N} \quad (3-16)$$

Proposition 3.1.2. *The matrix \mathbf{R}_{22} has full rank.*

Proof. From the definition, \mathbf{U} is full rank and $\det(\mathbf{U}) \neq 0$. Then, from (3-10) one has (see Prop. 2.8.3 in [6])

$$\det(\mathbf{U}) = \det(N\mathbf{R}_{22}^T - N\mathbb{1}_{N-1}\mathbf{R}_{21}^T)$$

Now, from (3-11), $\mathbf{R}_{21}^T = -\mathbb{1}_{N-1}^T\mathbf{R}_{22}^T$. Therefore,

$$\det(\mathbf{U}) = N \det(\mathbf{I}_{N-1} + \mathbb{1}_{N-1}\mathbb{1}_{N-1}^T) \det(\mathbf{R}_{22}^T) \neq 0$$

which implies that the rank of \mathbf{R}_{22} is full. \square

3.1.3. Error dynamics

To study convergence to the consensus equilibrium, we consider the state transformation $\mathbf{e}(t) = \mathbf{U}^{-1}\mathbf{x}(t)$. Indeed, using the block representation of \mathbf{U}^{-1} in (3-8) and letting $\bar{\mathbf{e}}(t) = [e_2(t), \dots, e_N(t)]$, $\bar{\mathbf{x}}(t) = [x_2(t), \dots, x_N(t)]$ we obtain

$$e_1(t) = r_{11}x_1(t) + \mathbf{R}_{12}\bar{\mathbf{x}}(t) \quad (3-17a)$$

$$\bar{\mathbf{e}}(t) = \mathbf{R}_{21}x_1(t) + \mathbf{R}_{22}\bar{\mathbf{x}}(t) \quad (3-17b)$$

Note that by adding and subtracting the term $\mathbf{R}_{22}x_1(t)\mathbb{1}_{N-1}$ to (3-17b), and using property (3-11), one has

$$\bar{\mathbf{e}}(t) = \mathbf{R}_{22}(\bar{\mathbf{x}}(t) - x_1(t)\mathbb{1}_{N-1})$$

It is important to highlight that $\bar{\mathbf{e}}(t) = \mathbb{0}_{(N-1)\times 1}$ if and only if $\bar{\mathbf{x}}(t) - x_1(t)\mathbb{1}_{N-1} = \mathbb{0}_{(N-1)\times 1}$ since \mathbf{R}_{22} is full rank (Proposition 3.1.2) [This also implies that, when consensus is achieved all nodes must converge to $x_1(t)$]. Then, admissible consensus is achieved if $\lim_{t \rightarrow \infty} \|\bar{\mathbf{e}}(t)\| = 0$ and $\|\mathbf{z}(t)\| < +\infty, \forall t > 0$.

Now, recasting (3-7), in the new coordinates $\mathbf{e}(t)$ and $\mathbf{w}(t) = \mathbf{U}^{-1}\mathbf{y}(t)$, and using Lemma 2.2.1, we get

$$\begin{bmatrix} \dot{e}_1(t) \\ \dot{\bar{\mathbf{e}}}(t) \end{bmatrix} = \left(\boldsymbol{\Psi} - \begin{bmatrix} 0 & \mathbb{0}_{1 \times N-1} \\ \mathbb{0}_{N-1 \times 1} & \alpha \bar{\Lambda} \end{bmatrix} \right) \mathbf{e}(t) + \begin{bmatrix} 0 \\ \bar{\mathbf{w}}(t) \end{bmatrix} \quad (3-18a)$$

$$\dot{\bar{\mathbf{w}}}(t) = -\beta \bar{\Lambda} \bar{\mathbf{e}}(t) \quad (3-18b)$$

where $\bar{\mathbf{w}}(t) = [w_2(t), \dots, w_N(t)]$, and $\bar{\Lambda} = \text{diag}\{\lambda_2, \dots, \lambda_N\}$. Note that the equation for $w_1(t)$ can be neglected as it has trivial dynamics with null initial conditions and represents an uncontrollable and unobservable state. Moreover, $\boldsymbol{\Psi}$ is a block matrix defined as

$$\boldsymbol{\Psi} = \begin{bmatrix} \psi_{11} & \boldsymbol{\Psi}_{12} \\ \boldsymbol{\Psi}_{21} & \boldsymbol{\Psi}_{22} \end{bmatrix} := \mathbf{U}^{-1}\mathbf{P}\mathbf{U} = \mathbf{U}^{-1} \begin{bmatrix} \rho_1 & \mathbb{0}_{1 \times (N-1)} \\ \mathbb{0}_{(N-1) \times 1} & \bar{\mathbf{P}} \end{bmatrix} \mathbf{U} \quad (3-19)$$

with $\bar{\mathbf{P}} := \text{diag}\{\rho_2, \dots, \rho_N\}$. Also, using properties (3-11)-(3-14), we can write (see Appendix A.1 for the derivation, considering $\tilde{\mathcal{L}}^{-1} = \mathbf{I}_N$ since $\gamma = 0$)

$$\psi_{11} = (1/N) \sum_{k=1}^N \rho_k \quad (3-20)$$

$$\Psi_{12} = \bar{\rho} \mathbf{R}_{22}^T = \Psi_{21}^T \quad (3-21)$$

$$\Psi_{22} = N \mathbf{R}_{22} (\rho_1 \mathbf{1}_{N-1} \mathbf{1}_{N-1}^T + \bar{\mathbf{P}}) \mathbf{R}_{22}^T \quad (3-22)$$

where

$$\bar{\rho} := [\rho_2 - \rho_1, \dots, \rho_N - \rho_1] \quad (3-23)$$

Case 1: Homogeneous node dynamics

We first complete the proof of convergence for the homogeneous case, that is we assume all nodes share identical uncoupled dynamics ($\rho_i = \rho_j = -\rho^*$ for all $i, j \in \mathcal{N}$), but are affected by different constant disturbances δ_i .

Theorem 3.1.1. *The closed-loop network (3-6) with homogeneous nodes i.e., $\rho_i = \rho_j = -\rho^*$, $\rho^* \in \mathbb{R}^+$ for $i, j \in \mathcal{N}$, achieves admissible consensus for any positive values of α and β . Moreover, all node states converge asymptotically to $x_\infty := (1/N) \sum_{k=1}^N \delta_k / \rho^*$*

Proof. Firstly note that when all nodes share the same dynamics we have that $\bar{\rho} = \mathbf{0}_{1 \times (N-1)}$ in (3-23); hence, $\Psi_{12} = \Psi_{21}^T = \mathbf{0}_{1 \times (N-1)}$ in (3-21). Moreover, $\bar{\mathbf{P}} = -\rho^* \mathbf{I}_{N-1}$ and, using properties (3-12) and (3-14), $\Psi_{22} = -\rho^* \mathbf{I}_{N-1}$. Then, (3-18a) becomes an uncoupled equation, this is the dynamics of e_1 does not depends from the rest, and under the assumptions $e_1(t)$ exponentially converges to zero. Now, for the dynamics of $\bar{\mathbf{e}}(t)$ and $\bar{\mathbf{w}}(t)$, let's consider the transverse candidate Lyapunov function

$$V(\bar{\mathbf{e}}, \bar{\mathbf{w}}) = \frac{1}{2} (\beta \bar{\mathbf{e}}^T \bar{\Lambda} \bar{\mathbf{e}} + \bar{\mathbf{w}}^T \bar{\mathbf{w}}) \quad (3-24)$$

differentiating V along the trajectories of (3-18), one has $\dot{V} = -\beta \bar{\mathbf{e}}^T \bar{\Lambda} (\alpha \bar{\Lambda} + \rho^* \mathbf{I}_{N-1}) \bar{\mathbf{e}}$, which is clearly negative definite for any positive value of α and β . As the function is also radially unbounded, we can conclude that the origin is a globally exponentially stable equilibrium and the closed-loop network converge to the equilibrium shown in Proposition 3.1.1, and the proof is complete. \square

Remark 3.1.1. Note that:

- An alternative proof of Theorem 3.1.1 can be found in [34] and [2] for identical and nonidentical disturbances, respectively. However, our proof also allows to consider the more generic case of heterogeneous node dynamics as we will present in the next section.

- Network (3-6) still achieves admissible consensus if the nodes are unstable ($\rho^* \in \mathbb{R}^-$), since a suitable α can be chosen such that $\alpha\bar{\Lambda} + \rho^*\mathbf{I}_{N-1}$ remains positive; however, the average trajectory $e_1(t)$ will be unstable and the system will exhibit unbounded admissible consensus; that is, $\lim_{t \rightarrow \infty} (x_i(t) - x_j(t)) = 0$ but $\lim_{t \rightarrow \infty} x_i(t) \rightarrow \infty$ for all $i, j \in \mathcal{N}$.
- The aim of the distributed PI action is to guarantee that the nodes disagreement tends to zero at steady-state despite the presence of the disturbances. Therefore it should not be surprising that when these are present, consensus is indeed achieved but on a value that is dependent on their magnitude.
- The proof of the theorem does not apply as is if the nodes are simple integrators ($\rho_i = \rho_j = 0$). In this case, Corollary 3.2.1 must be used instead.

Example 5. Consider the multi-agent system (3-1) with homogeneous node dynamics $\rho_i = -2$ for all $i \in \mathcal{N}$ and $\delta_i = 1$ for i being an odd index and $\delta_i = 0$ otherwise. Therefore, under distributed PI (3-4) ($\gamma = 0$) strategy, and using Theorem (3.1.1) we can conclude that the homogeneous multi-agent network reaches consensus for any value of α and β .

Without loss of generality we choose $\alpha = \beta = 1$ and unitary link-weights. This is $w_{ij} = 1$ if there is an associate edge between nodes i and j and $w_{ij} = 0$ otherwise. Thus, from Proposition 3.1.1 we have that $x_\infty := -\sum_{k=1}^N \delta_k / \sum_{k=1}^N \rho_k = 0.25$; therefore, $\mathbf{x}^* := 0.25\mathbf{1}_N$ and

$$\mathbf{z}^* := -(\mathbf{P}\mathbf{x}^* + \boldsymbol{\Delta}) = [-0.5, 0.5, -0.5, 0.5, -0.5, 0.5, -0.5, 0.5, -0.5, 0.5]^T$$

The time response of the closed-loop heterogeneous network is depicted in Figures 3-1 and 3-2, considering different network topologies. Note that the speed of convergence to the consensus equilibrium increases when the algebraic connectivity λ_2 also increases.

Case 2: Heterogeneous Node Dynamics

Here we consider the case where at least one pole is different from all others, and the disturbances δ_i are generically nonidentical.

Theorem 3.1.2. *The heterogeneous multi-agent system (3-1) controlled by the distributed PID strategy (3-4), achieves admissible consensus for any $\beta > 0$ and $\gamma \geq 0$ if the following conditions hold*

$$\psi_{11} = (1/N) \sum_{k=1}^N \rho_k < 0, \quad (3-25a)$$

$$\alpha\lambda_2 > \frac{1}{N} \left(\max_i \{|\rho_i|\} + \frac{\bar{\rho}\bar{\rho}^T}{|\psi_{11}|} \right) \quad (3-25b)$$

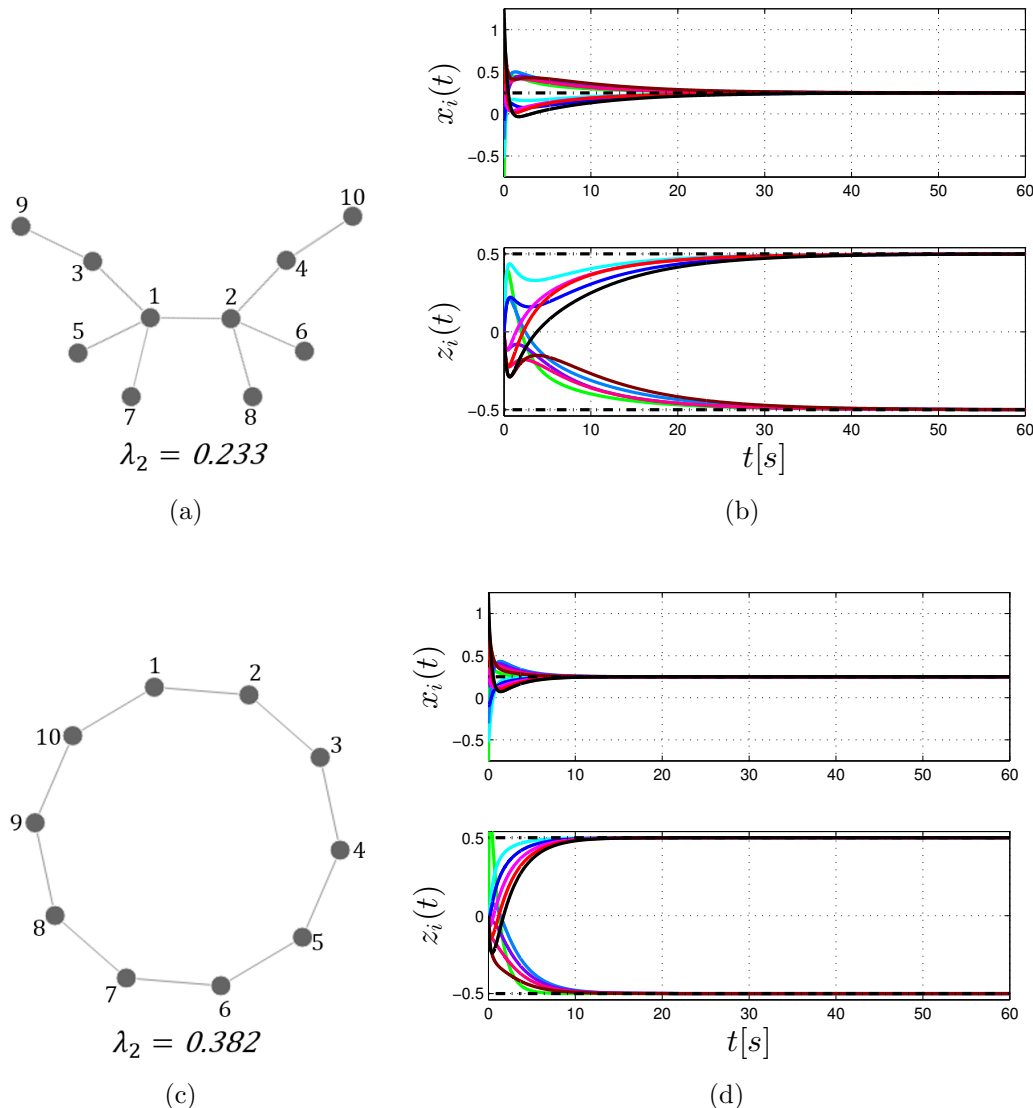


Figure 3-1.: Time response of the PI controlled multi-agent system for: (a),(b) three, (c),(d) star network topologies. The dashed-lines represent the equilibrium value.

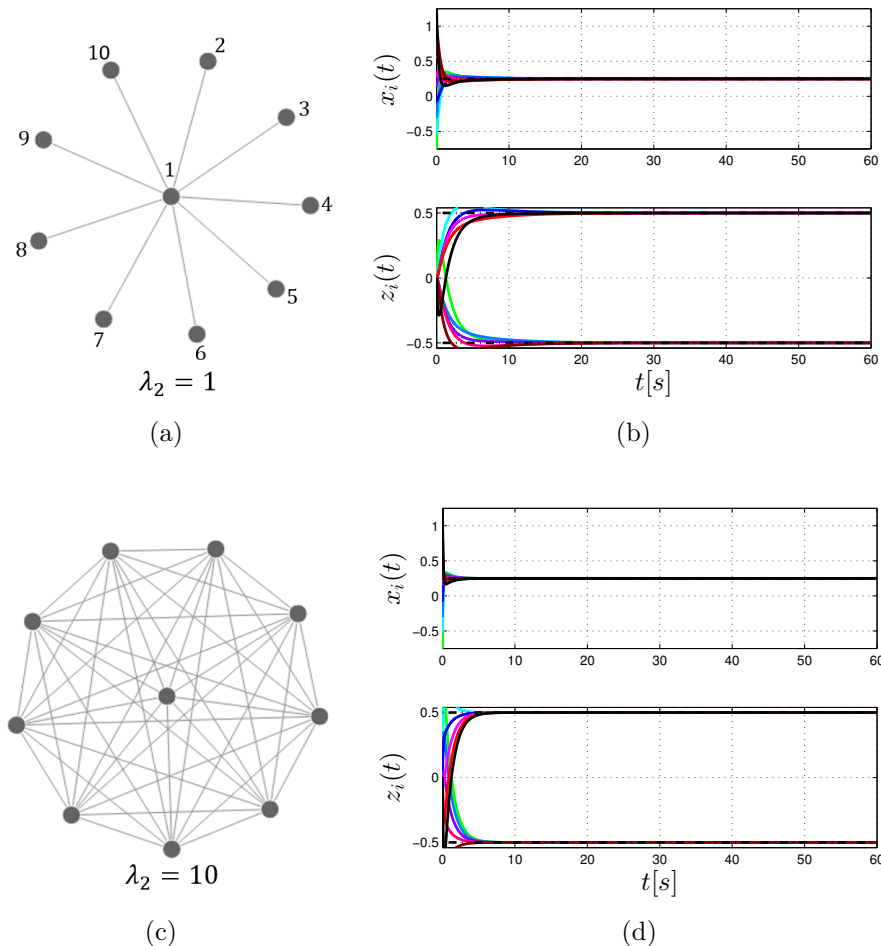


Figure 3-2: Time response of the PI controlled multi-agent system for: (a),(b) star, (c),(d) all-to-all network topologies. The dashed-lines represent the equilibrium value.

Moreover, all node states converge to x_∞ as defined in Prop. 3.1.1.

Proof. Consider the following candidate Lyapunov function:

$$V = \frac{1}{2} \left(e_1^2 + \bar{\mathbf{e}}^T \bar{\mathbf{e}} + \frac{1}{\beta} \bar{\mathbf{w}}^T \bar{\Lambda}^{-1} \bar{\mathbf{w}} \right) \quad (3-26)$$

where $\bar{\Lambda} := \text{diag}\{\lambda_2, \dots, \lambda_N\}$; therefore, V is a positive definite and radially unbounded function. Differentiating V along the trajectories of (3-18) yields

$$\dot{V} = \psi_{11} e_1^2 + \bar{\mathbf{e}}^T \Psi_{22} \bar{\mathbf{e}} - \alpha \bar{\mathbf{e}}^T \bar{\Lambda} \bar{\mathbf{e}} + e_1 \bar{\mathbf{e}}^T (\Psi_{12}^T + \Psi_{21})$$

and, using (3-21), we get

$$\dot{V} = \psi_{11} e_1^2 + \bar{\mathbf{e}}^T \Psi_{22} \bar{\mathbf{e}} - \alpha \bar{\mathbf{e}}^T \bar{\Lambda} \bar{\mathbf{e}} + \underbrace{2e_1 \bar{\mathbf{e}}^T \mathbf{R}_{22} \bar{\rho}^T}_{g(e_1, \bar{\mathbf{e}})} \quad (3-27)$$

Now, by setting $\mathbf{Q}^T = \mathbf{R}_{22}$, $\zeta_1^T = \bar{\mathbf{e}}^T$, and $\zeta_2 = \bar{e}_1 \bar{\rho}^T$ in (2-2), we can upper-bound $g(e_1, \bar{\mathbf{e}})$ as follows

$$g(e_1, \bar{\mathbf{e}}) \leq \varepsilon \bar{\mathbf{e}}^T \mathbf{Q}^T \mathbf{Q} \bar{\mathbf{e}} + \frac{\bar{\rho} \bar{\rho}^T}{\varepsilon} e_1^2$$

This yields that from (3-27) we get

$$\dot{V} \leq \left(\psi_{11} + \frac{\bar{\rho} \bar{\rho}^T}{2\varepsilon} \right) e_1^2 + \bar{\mathbf{e}}^T \Psi_{22} \bar{\mathbf{e}} - \alpha \bar{\mathbf{e}}^T \bar{\Lambda} \bar{\mathbf{e}} + \frac{\varepsilon}{2} \bar{\mathbf{e}}^T \mathbf{Q}^T \mathbf{Q} \bar{\mathbf{e}} \quad (3-28)$$

From (3-19), we obtain $\|\Psi + \Psi^T\| \leq 2\|\mathbf{U}\|^2 \|\mathbf{P}\|$. Moreover, we have $\|\mathbf{P}\| = \max_i \{|\rho_i|\}$ and, from (3-15), $\|\mathbf{U}\|^2 = (1/N)$. Then, $\|\Psi + \Psi^T\| \leq (2/N) \max_i \{|\rho_i|\}$.

Using (2-5) we then find that $\lambda_{\max}(\Psi_{22} + \Psi_{22}^T) \leq \lambda_{\max}(\Psi + \Psi^T)$ so that

$$\bar{\mathbf{e}}^T \Psi_{22} \bar{\mathbf{e}} = (1/2) \bar{\mathbf{e}}^T (\Psi_{22} + \Psi_{22}^T) \bar{\mathbf{e}} \leq (1/N) \max_i \{|\rho_i|\} \bar{\mathbf{e}}^T \bar{\mathbf{e}}$$

Also, as $-\bar{\mathbf{e}}^T \bar{\Lambda} \bar{\mathbf{e}} \leq -\lambda_2 \bar{\mathbf{e}}^T \bar{\mathbf{e}}$, we obtain

$$\dot{V} \leq \left(\psi_{11} + \frac{\bar{\rho} \bar{\rho}^T}{\varepsilon} \right) e_1^2 + \left(\frac{1}{N} \max_i \{|\rho_i|\} - \alpha \lambda_2 + \frac{\varepsilon}{N} \right) \bar{\mathbf{e}}^T \bar{\mathbf{e}} \quad (3-29)$$

Now, \dot{V} is negative definite if the terms $\xi_1 := \psi_{11} + \bar{\rho} \bar{\rho}^T / \varepsilon$ and $\xi_2 := (1/N) \max_i \{|\rho_i|\} - \alpha \lambda_2 + (\varepsilon/2N)$ are both negative.

From the assumptions, we have that $\psi_{11} < 0$, therefore $\xi_1 < 0$ is ensured if we choose $\varepsilon > \bar{\rho} \bar{\rho}^T / |\psi_{11}|$ [this is always possible as ε is an arbitrary positive constant in (2-2)]. Then the condition $\xi_2 < 0$ can be fulfilled by selecting the control gains so as to satisfy (3-25b). Therefore, all agents in (3-1) achieves admissible consensus to x_∞ as defined in Prop. 3.1.1 which completes the proof. \square

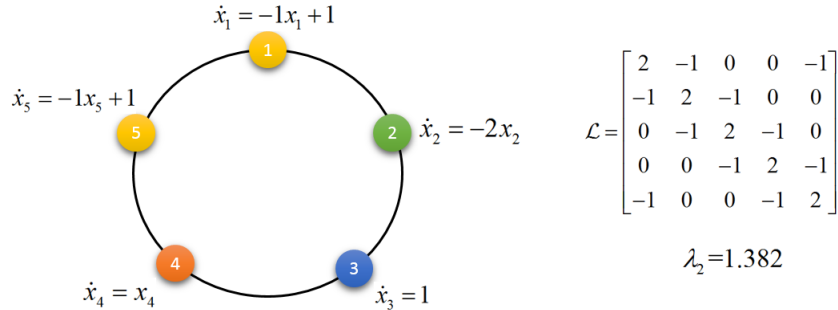


Figure 3-3.: Heterogeneous ring network controlled by distributed PI strategy.

Example 6. Consider the heterogeneous ring network shown in Figure 3-3 where all link weights are one

From Theorem 3.1.2 we have that $\psi_{11} = (1/N) \sum_{k=1}^N \rho_k = -0.6 < 0$; therefore, condition (3-25a) is fulfilled. Next, from (3-23) we have that $\bar{\rho} := [-1, 1, 2, 0]$ and $\max_i \{|\rho_i|\} = 2$. Hence $\alpha \lambda_2 > 1.066$. From Figure 3-3 we have that $\lambda_2 = 1.382$ and the heterogeneous multi-agent network reaches admissible consensus if $\alpha > 0.7713$. The consensus equilibrium can be computed using Proposition 3.1.1, then

$$x_\infty = -\frac{\sum_{k=1}^N \delta_k}{\sum_{k=1}^N \rho_k} = 1$$

so that $\mathbf{x}^* := \mathbb{1}_N$ and

$$\mathbf{z}^* = -(\mathbf{P}\mathbf{x}^* + \Delta) = [0, 2, -1, -1, 0]^T \quad (3-30)$$

The evolution of the closed-loop network setting $\alpha = \beta = 1$, is shown in Figure 3-4 where consensus is achieved to the predicted value $(\mathbf{x}^*, \mathbf{z}^*)$

3.2. Distributed PID control

In this section we consider the multi-agent system (3-1) controlled by distributed PID (3-4). Then the overall dynamics of the closed-loop network can be written as (using the notation introduced in the PI section)

$$\begin{bmatrix} \tilde{\mathcal{L}}\dot{\mathbf{x}}(t) \\ \dot{\mathbf{z}}(t) \end{bmatrix} = \begin{bmatrix} \mathbf{P} - \alpha \mathcal{L} & \mathbf{I}_N \\ -\beta \mathcal{L} & \mathbb{0}_{N \times N} \end{bmatrix} \begin{bmatrix} \mathbf{x}(t) \\ \mathbf{z}(t) \end{bmatrix} + \begin{bmatrix} \Delta \\ \mathbb{0}_{N \times 1} \end{bmatrix} \quad (3-31)$$

where $\tilde{\mathcal{L}} := \mathbf{I}_N + \gamma \mathcal{L}$ is the matrix encoding the derivative gain. Next we derive some properties of the matrix $\tilde{\mathcal{L}}$ that will be useful through the manuscript.

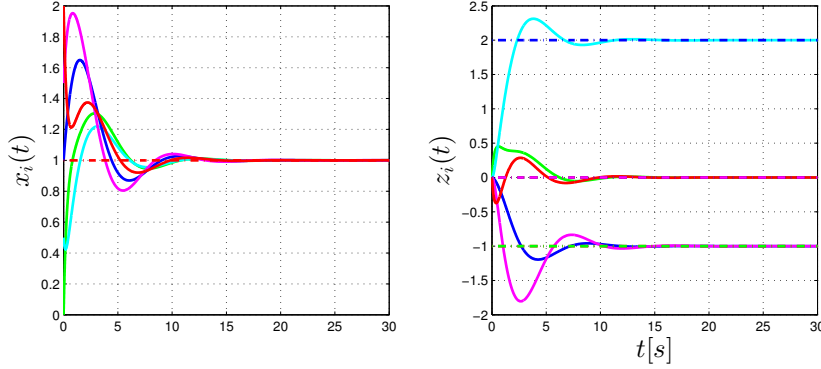


Figure 3-4.: Time response of the closed-loop heterogeneous network of Fig. 3-3 controlled by distributed PI strategy with $\alpha = \beta = 1$. The dashed-lines represent the equilibrium value.

3.2.1. Properties of $\tilde{\mathcal{L}}$

From the definition and the properties of \mathcal{L} , we immediately have that $\tilde{\mathcal{L}}$ is invertible and its eigenvalues are $\tilde{\lambda}_i = 1 + \gamma\lambda_i, \forall i \in \mathcal{N}$. We can prove the following Lemma that will be useful for the convergence analysis

Lemma 3.2.1. *If $\mathcal{L} \in \Omega$, then $\tilde{\mathcal{L}}^{-1}$ has positive real eigenvalues that can be given in descending order as $1 \geq 1/(\gamma\lambda_2 + 1) \geq \dots \geq 1/(\gamma\lambda_N + 1)$. Moreover, the product $\tilde{\mathcal{L}}^{-1}\mathcal{L}$ is itself in Ω and can be expressed as*

$$\tilde{\mathcal{L}}^{-1}\mathcal{L} = \mathbf{U}\Gamma\mathbf{U}^{-1}, \quad \Gamma = \begin{bmatrix} 0 & \mathbb{0}_{1 \times (N-1)} \\ \mathbb{0}_{(N-1) \times 1} & \bar{\Gamma} \end{bmatrix} \quad (3-32)$$

with

$$\bar{\Gamma} = \text{diag}\{\lambda_2 / (\gamma\lambda_2 + 1), \dots, \lambda_N / (\gamma\lambda_N + 1)\} \quad (3-33)$$

Proof. From the definition of $\tilde{\mathcal{L}}$ we can write $\tilde{\mathcal{L}} = \mathbf{U}\mathbf{U}^{-1} + \gamma\mathbf{U}\Lambda\mathbf{U}^{-1}$, and letting $\Sigma := \text{diag}\{1, \gamma\lambda_2 + 1, \dots, \gamma\lambda_N + 1\}$ yields $\tilde{\mathcal{L}} = \mathbf{U}\Sigma\mathbf{U}^{-1}$. Note that this is the eigen-decomposition of a symmetric matrix and $\tilde{\mathcal{L}}^{-1} = \mathbf{U}\Sigma^{-1}\mathbf{U}^{-1}$ where

$$\Sigma^{-1} := \text{diag}\{1, 1 / (\gamma\lambda_2 + 1), \dots, 1 / (\gamma\lambda_N + 1)\} \quad (3-34)$$

Thus, we obtain $\tilde{\mathcal{L}}^{-1}\mathcal{L} = \mathbf{U}\Gamma\mathbf{U}^{-1}$ with $\Gamma := \Sigma^{-1}\Lambda$ and the proof is complete. \square

Also, rewriting $\tilde{\mathcal{L}}^{-1}$ in block form, we have

$$\tilde{\mathcal{L}}^{-1} = \begin{bmatrix} \hat{l}_{11} & \hat{\mathcal{L}}_{12} \\ \hat{\mathcal{L}}_{21} & \hat{\mathcal{L}}_{22} \end{bmatrix} \quad (3-35)$$

where $\hat{l}_{11} \in \mathbb{R}$, $\hat{\mathcal{L}}_{12} \in \mathbb{R}^{1 \times N-1}$, $\hat{\mathcal{L}}_{21} \in \mathbb{R}^{N-1 \times 1}$, and $\hat{\mathcal{L}}_{22} \in \mathbb{R}^{N-1 \times N-1}$ are blocks of appropriate dimension. Moreover, from Lemma 2.2.1, $\mathcal{L}\mathbf{1}_N = \mathbb{0}_{N \times 1}$; therefore, $\tilde{\mathcal{L}}\mathbf{1}_N = \mathbf{1}_N$. Hence, multiplying both sides by $\tilde{\mathcal{L}}^{-1}$ we have $\tilde{\mathcal{L}}^{-1}\tilde{\mathcal{L}}\mathbf{1}_N = \tilde{\mathcal{L}}^{-1}\mathbf{1}_N$ so that $\tilde{\mathcal{L}}^{-1}\mathbf{1}_N = \mathbf{1}_N$. Therefore, the blocks in (3-35) must satisfy the conditions:

$$\hat{\mathcal{L}}_{12}\mathbf{1}_{N-1} = \hat{\mathcal{L}}_{21}^T\mathbf{1}_{N-1} = 1 - \hat{l}_{11} \quad (3-36)$$

$$\hat{\mathcal{L}}_{22}\mathbf{1}_{N-1} = \mathbf{1}_{N-1} - \hat{\mathcal{L}}_{21} \quad (3-37)$$

$$\mathbf{1}_{N-1}\mathbf{1}_{N-1}^T\hat{\mathcal{L}}_{22} = \mathbf{1}_{N-1}\mathbf{1}_{N-1}^T - \mathbf{1}_{N-1}\hat{\mathcal{L}}_{12} \quad (3-38)$$

$$\hat{\mathbf{H}}\mathbf{1}_{N-1} = \hat{l}_{11}\mathbf{1}_{N-1} - \hat{\mathcal{L}}_{21} \quad (3-39)$$

where

$$\hat{\mathbf{H}} := \hat{\mathcal{L}}_{22} - \mathbf{1}_{N-1}\hat{\mathcal{L}}_{12} \quad (3-40)$$

Moreover, from Lemma 3.2.1 we have that $\mathbf{U}^{-1}\tilde{\mathcal{L}}^{-1}\mathbf{U} = \Sigma^{-1}$. Using the block representation of \mathbf{U} and \mathcal{L}^{-1} we have

$$\begin{bmatrix} r_{11} & \mathbf{R}_{12} \\ \mathbf{R}_{21} & \mathbf{R}_{22} \end{bmatrix} \begin{bmatrix} \hat{l}_{11} & \hat{\mathcal{L}}_{12} \\ \hat{\mathcal{L}}_{21} & \hat{\mathcal{L}}_{22} \end{bmatrix} \begin{bmatrix} 1 & N\mathbf{R}_{21}^T \\ \mathbf{1}_{N-1} & N\mathbf{R}_{22}^T \end{bmatrix} = \Sigma^{-1} \quad (3-41)$$

Letting $\mathbf{M} := \mathbf{U}^{-1}\tilde{\mathcal{L}}\mathbf{U}$, and

$$\bar{\Sigma}^{-1} := \text{diag}\{1/(\gamma\lambda_2 + 1), \dots, 1/(\gamma\lambda_N + 1)\} \quad (3-42)$$

some straightforward algebra yields

$$\begin{bmatrix} M_{11} & \mathbf{M}_{12} \\ \mathbf{M}_{21} & \mathbf{M}_{22} \end{bmatrix} = \begin{bmatrix} 1 & \mathbb{0}_{1 \times (N-1)} \\ \mathbb{0}_{(N-1) \times 1} & \bar{\Sigma}^{-1} \end{bmatrix}$$

where

$$\begin{aligned} M_{11} &= r_{11}(\hat{l}_{11} + \hat{\mathcal{L}}_{12}\mathbf{1}_{N-1}) + \mathbf{R}_{12}(\hat{\mathcal{L}}_{21} + \hat{\mathcal{L}}_{22}\mathbf{1}_{N-1}) \\ \mathbf{M}_{12} &= Nr_{11}(\hat{l}_{11}\mathbf{R}_{21}^T + \hat{\mathcal{L}}_{12}\mathbf{R}_{22}^T) + N\mathbf{R}_{12}(\hat{\mathcal{L}}_{21}\mathbf{R}_{21}^T + \hat{\mathcal{L}}_{22}\mathbf{R}_{22}^T) \\ \mathbf{M}_{21} &= \mathbf{R}_{21}(\hat{l}_{11} + \hat{\mathcal{L}}_{12}\mathbf{1}_{N-1}) + \mathbf{R}_{22}(\hat{\mathcal{L}}_{21} + \hat{\mathcal{L}}_{22}\mathbf{1}_{N-1}) \\ \mathbf{M}_{22} &= N\mathbf{R}_{21}(\hat{l}_{11}\mathbf{R}_{21}^T + \hat{\mathcal{L}}_{12}\mathbf{R}_{22}^T) + N\mathbf{R}_{22}(\hat{\mathcal{L}}_{21}\mathbf{R}_{21}^T + \hat{\mathcal{L}}_{22}\mathbf{R}_{22}^T) \end{aligned}$$

Equating the blocks we have that $\mathbf{M}_{22} = \bar{\Sigma}^{-1}$, and some algebraic manipulations yield

$$\mathbf{R}_{21}\hat{l}_{11}\mathbf{R}_{21}^T + \mathbf{R}_{21}\hat{\mathcal{L}}_{12}\mathbf{R}_{22}^T + \mathbf{R}_{22}\hat{\mathcal{L}}_{21}\mathbf{R}_{21}^T + \mathbf{R}_{22}\hat{\mathcal{L}}_{22}\mathbf{R}_{22}^T = \frac{1}{N}\bar{\Sigma}^{-1}$$

Now, adding and subtracting $\widehat{l}_{11}\mathbf{R}_{21}\mathbb{1}_{N-1}^T\mathbf{R}_{22}^T$ one gets

$$\widehat{l}_{11}\mathbf{R}_{21}(\mathbf{R}_{21}^T + \mathbb{1}_{N-1}^T\mathbf{R}_{22}^T) - \widehat{l}_{11}\mathbf{R}_{21}\mathbb{1}_{N-1}^T\mathbf{R}_{22}^T + \mathbf{R}_{21}\widehat{\mathcal{L}}_{12}\mathbf{R}_{22}^T + \mathbf{R}_{22}\widehat{\mathcal{L}}_{21}\mathbf{R}_{21}^T + \mathbf{R}_{22}\widehat{\mathcal{L}}_{22}\mathbf{R}_{22}^T = \frac{1}{N}\bar{\Sigma}^{-1}$$

From property (3-13) one has that $\mathbf{R}_{21}^T + \mathbb{1}_{N-1}^T\mathbf{R}_{22}^T = \mathbb{0}$. Also, using (3-11), we have $\mathbf{R}_{21} = -\mathbf{R}_{22}\mathbb{1}_{N-1}$ so that the equation above can be recast as

$$\mathbf{R}_{22}\widehat{\mathcal{L}}_{22}\mathbf{R}_{22}^T - \mathbf{R}_{22}\mathbb{1}_{N-1}\widehat{\mathcal{L}}_{12}\mathbf{R}_{22}^T - \mathbf{R}_{22}\widehat{\mathcal{L}}_{21}\mathbb{1}_{N-1}^T\mathbf{R}_{22}^T + \widehat{l}_{11}\mathbf{R}_{22}\mathbb{1}_{N-1}^T\mathbf{R}_{22}^T = \frac{1}{N}\bar{\Sigma}^{-1}$$

Finally regrouping terms we obtain

$$\frac{1}{N}\bar{\Sigma}^{-1} = \mathbf{R}_{22}\left(\widehat{\mathbf{H}} + (\widehat{l}_{11}\mathbb{1}_{N-1} - \widehat{\mathcal{L}}_{21})\mathbb{1}_{N-1}^T\right)\mathbf{R}_{22}^T \quad (3-43)$$

3.2.2. Closed-loop network

Defining the stack vector of integral states

$$\mathbf{s}(t) = [s_1(t), \dots, s_N(t)]^T := \tilde{\mathcal{L}}^{-1}\mathbf{z}(t) \quad (3-44)$$

the overall dynamics of the closed-loop network can be written as (using the notation introduced previously)

$$\begin{bmatrix} \dot{\mathbf{x}}(t) \\ \dot{\mathbf{s}}(t) \end{bmatrix} = \begin{bmatrix} \tilde{\mathcal{L}}^{-1}(\mathbf{P} - \alpha\mathcal{L}) & \mathbf{I}_N \\ -\beta\tilde{\mathcal{L}}^{-1}\mathcal{L} & \mathbb{0}_{N \times N} \end{bmatrix} \begin{bmatrix} \mathbf{x}(t) \\ \mathbf{s}(t) \end{bmatrix} + \begin{bmatrix} \tilde{\mathcal{L}}^{-1}\Delta \\ \mathbb{0}_{N \times N} \end{bmatrix} \quad (3-45)$$

Then, the problem is finding conditions on the control gains α, β and γ , the network structure and node dynamics such that the closed-loop network (3-45) achieves admissible consensus.

Proposition 3.2.1. *The closed-loop network (3-45) has a unique equilibrium given by $\mathbf{x}^* := x_\infty\mathbb{1}_N$ with $x_\infty := -\sum_{k=1}^N \delta_k / \sum_{k=1}^N \rho_k$, and $\mathbf{s}^* := -\tilde{\mathcal{L}}^{-1}(\mathbf{P}\mathbf{x}^* + \Delta)$.*

Proof. The proof follows immediately by setting the left-hand side of (3-45) to zero and noticing that $\tilde{\mathcal{L}}^{-1}\mathcal{L} \in \Omega$ (see Lemma 3.2.1) so that $\mathbf{x}^* = a\mathbb{1}_N, \forall a \in \mathbb{R}$ and $\mathbf{s}^* = -\tilde{\mathcal{L}}^{-1}(a\mathbf{P}\mathbb{1}_N + \Delta)$. By definition (3-5) and (3-44) one has that $s(t) = -\beta\tilde{\mathcal{L}}^{-1}\mathcal{L}$. Hence, from the fact that $\tilde{\mathcal{L}}^{-1}\mathcal{L} \in \Omega$, we also have $\mathbb{1}_N^T\mathbf{s}(t) = 0$, then $\mathbb{1}_N^T\mathbf{s}^* = 0$ and we obtain

$$a = -\mathbb{1}_N^T\Delta / \mathbb{1}_N^T\mathbf{P}\mathbb{1}_N = -\left(\sum_{k=1}^N \delta_k\right) \left(\sum_{k=1}^N \rho_k\right)^{-1}$$

Hence, setting $x_\infty = a$ completes the proof. \square

Remark 3.2.1. Comparing the equilibrium points of the PI and PID shown in Propositions (3.1.1) and (3.2.1) respectively, we note that the node states converge to the same constant value. However, the integral action in the PID case depends on $\tilde{\mathcal{L}}$. This represents an important aspect, since the equilibrium point of the integral term will be the amount of energy (control effort) needed by the controller, to compensate the heterogeneity among nodes. Therefore, the control effort can be substantially reduced by manipulating γ or the network structure.

Error dynamics

To study convergence to the consensus equilibrium, we consider the state transformation $\mathbf{e}(t) = \mathbf{U}^{-1}\mathbf{x}(t)$. Now, recasting (3-45), in the new coordinates $\mathbf{e}(t)$ and $\mathbf{w}(t) = \mathbf{U}^{-1}\mathbf{s}(t)$, and using Lemma 3.2.1, we get

$$\begin{bmatrix} e_1(t) \\ \bar{\mathbf{e}}(t) \end{bmatrix} = \left(\Psi - \begin{bmatrix} 0 & \mathbf{0}_{1 \times (N-1)} \\ \mathbf{0}_{(N-1) \times 1} & \alpha \bar{\Gamma} \end{bmatrix} \right) \mathbf{e}(t) + \mathbf{w}(t) + \tilde{\Delta} \quad (3-46a)$$

$$\dot{\bar{\mathbf{w}}}(t) = -\beta \bar{\Gamma} \bar{\mathbf{e}}(t) \quad (3-46b)$$

where $\bar{\mathbf{w}}(t) = [w_2(t), \dots, w_N(t)]$ and $\Psi := \mathbf{U}^{-1} \tilde{\mathcal{L}}^{-1} \mathbf{P} \mathbf{U}$. (Note that the equation for $w_1(t)$ can be neglected as it has trivial dynamics with null initial conditions and represents an uncontrollable and unobservable state.) Furthermore, $\tilde{\Delta} := \mathbf{U}^{-1} \tilde{\mathcal{L}}^{-1} \Delta = [\mathbf{q}^T \ \hat{\mathbf{R}}^T]^T \Delta$, where $\mathbf{q} \in \mathbb{R}^{1 \times N}$, $\hat{\mathbf{R}} \in \mathbb{R}^{(N-1) \times N}$ are given by

$$\begin{bmatrix} \mathbf{q} \\ \hat{\mathbf{R}} \end{bmatrix} = \begin{bmatrix} r_{11} \hat{l}_{11} + \mathbf{R}_{12} \hat{\mathcal{L}}_{21} & r_{11} \hat{\mathcal{L}}_{12} + \mathbf{R}_{12} \hat{\mathcal{L}}_{22} \\ \mathbf{R}_{21} \hat{l}_{11} + \mathbf{R}_{22} \hat{\mathcal{L}}_{21} & \mathbf{R}_{21} \hat{\mathcal{L}}_{12} + \mathbf{R}_{22} \hat{\mathcal{L}}_{22} \end{bmatrix}$$

From the definition of \mathbf{R}_{12} in (3-9) and using (3-36) we obtain

$$\mathbf{q} = [r_{11} \ \mathbf{R}_{12}] = \frac{1}{N} \mathbb{1}_N^T \quad (3-47)$$

Also, it follows from (3-11) that $\mathbf{R}_{21} = -\mathbf{R}_{22} \mathbb{1}_{N-1}$ and again using (3-36) one has $\hat{\mathbf{R}} = [\mathbf{R}_{22}(\hat{\mathcal{L}}_{21} - \hat{l}_{11} \mathbb{1}_{N-1}) \ \mathbf{R}_{22}(\hat{\mathcal{L}}_{22} - \mathbb{1}_{N-1} \hat{\mathcal{L}}_{12})]$. Thus, using (3-39) we obtain

$$\hat{\mathbf{R}} = \mathbf{R}_{22} \hat{\mathbf{H}} [-\mathbb{1}_{N-1} \ \mathbf{I}_{N-1}] \quad (3-48)$$

Moreover, the matrix Ψ is a block matrix that can be expressed as

$$\Psi = \mathbf{U}^{-1} \tilde{\mathcal{L}}^{-1} \mathbf{P} \mathbf{U} = \begin{bmatrix} \psi_{11} & \Psi_{12} \\ \Psi_{21} & \Psi_{22} \end{bmatrix} = \mathbf{U}^{-1} \begin{bmatrix} \hat{l}_{11} & \hat{\mathcal{L}}_{12} \\ \hat{\mathcal{L}}_{21} & \hat{\mathcal{L}}_{22} \end{bmatrix} \begin{bmatrix} \rho_1 & \mathbf{0}_{1 \times (N-1)} \\ \mathbf{0}_{(N-1) \times 1} & \bar{\mathbf{P}} \end{bmatrix} \mathbf{U} \quad (3-49)$$

with $\bar{\mathbf{P}} := \text{diag}\{\rho_2, \dots, \rho_N\}$.

Using properties (3-11)-(3-14) and (3-36)-(3-38), some algebraic manipulation yields (see Appendix A.1 for the derivation)

$$\psi_{11} := (1/N) \sum_{k=1}^N \rho_k \quad (3-50)$$

$$\boldsymbol{\Psi}_{12} := \bar{\boldsymbol{\rho}} \mathbf{R}_{22}^T \quad (3-51)$$

$$\boldsymbol{\Psi}_{21} := \mathbf{R}_{22} \hat{\mathbf{H}} \bar{\boldsymbol{\rho}}^T \quad (3-52)$$

$$\boldsymbol{\Psi}_{22} := N \mathbf{R}_{22} \hat{\mathbf{H}} (\bar{\mathbf{P}} + \rho_1 \mathbb{1}_{N-1} \mathbb{1}_{N-1}^T) \mathbf{R}_{22}^T \quad (3-53)$$

where

$$\bar{\boldsymbol{\rho}} := [\rho_2 - \rho_1, \dots, \rho_N - \rho_1] \quad (3-54)$$

Finally, shifting the origin of (3-46) via the further state transformation

$$\begin{bmatrix} \hat{e}_1(t) \\ \hat{\mathbf{e}}(t) \\ \hat{\mathbf{w}}(t) \end{bmatrix} = \begin{bmatrix} e_1(t) \\ \bar{\mathbf{e}}(t) \\ \bar{\mathbf{w}}(t) \end{bmatrix} + \begin{bmatrix} (1/\psi_{11}) \mathbf{q}^T \\ \mathbb{0}_{N-1 \times N} \\ \hat{\mathbf{R}} - (1/\psi_{11}) \boldsymbol{\Psi}_{21} \mathbf{q}^T \end{bmatrix} \Delta \quad (3-55)$$

we obtain

$$\begin{bmatrix} \dot{\hat{e}}_1(t) \\ \dot{\hat{\mathbf{e}}}(t) \\ \dot{\hat{\mathbf{w}}}(t) \end{bmatrix} = \begin{bmatrix} \psi_{11} & \boldsymbol{\Psi}_{12} & \mathbb{0}_{(N-1) \times (N-1)} \\ \boldsymbol{\Psi}_{21} & \boldsymbol{\Psi}_{22} - \alpha \bar{\Gamma} & \mathbb{I}_{N-1} \\ 0 & -\beta \bar{\Gamma} & \mathbb{0}_{(N-1) \times (N-1)} \end{bmatrix} \begin{bmatrix} \hat{e}_1(t) \\ \hat{\mathbf{e}}(t) \\ \hat{\mathbf{w}}(t) \end{bmatrix} \quad (3-56)$$

Now, we can address the admissible consensus problem for (3-45) in terms of finding conditions on α , β and γ that render the origin a stable equilibrium point of (3-56).

Before studying this problem in the two cases of homogeneous or heterogeneous nodes, we first obtain an upper bound on the integral states that apply for both. By definition we have that $\mathbf{s}(t) = \mathbf{U}\mathbf{w}$, thus

$$s_1(t) = w_1(t) + N \mathbf{R}_{21}^T \bar{\mathbf{w}}(t) \quad (3-57a)$$

$$\bar{\mathbf{s}}(t) = \mathbb{1}_{N-1} w_1(t) + N \mathbf{R}_{22}^T \bar{\mathbf{w}}(t) \quad (3-57b)$$

where $\bar{\mathbf{s}}(t) = [s_2(t), \dots, s_N(t)]$. Neglecting w_1 for the same reason given above and using (3-16), we find from (3-57) that $\|s_1(t)\| \leq \sqrt{N(N-1)} \|\bar{\mathbf{w}}(t)\|$ and $\|\bar{\mathbf{s}}(t)\| \leq \sqrt{N} \|\bar{\mathbf{w}}(t)\|$. Hence, we can conclude that the integral action remains bounded and

$$\|\mathbf{s}(t)\| \leq \sqrt{N(N-1)} \|\bar{\mathbf{w}}(t)\|$$

Therefore, asymptotically, we have

$$s_\infty := \lim_{t \rightarrow \infty} \|\mathbf{s}(t)\| \leq \sqrt{N(N-1)} \lim_{t \rightarrow \infty} \|\bar{\mathbf{w}}(t)\| \quad (3-58)$$

An upper bound for s_∞ can be obtained by noticing that, if the origin of (3-56) is stable, then

$$\lim_{t \rightarrow \infty} \bar{\mathbf{s}}(t) = (1/\psi_{11} \Psi_{21} \mathbf{q}^T - \widehat{\mathbf{R}}) \Delta \quad (3-59)$$

so that

$$\lim_{t \rightarrow \infty} \|\bar{\mathbf{s}}(t)\| \leq \left(1/|\psi_{11}| \|\Psi_{21}\| \|\mathbf{q}\| + \|\widehat{\mathbf{R}}\| \right) \|\Delta\| \quad (3-60)$$

Then, using (3-48) and (3-15) yields

$$\|\widehat{\mathbf{R}}\| \leq \|\mathbf{R}_{22}\| \|\widehat{\mathbf{H}}\| \|[-\mathbb{1}_{N-1} \ \mathbf{I}_{N-1}]\| \leq \sqrt{N} \|\mathbf{R}_{22}\| \|\widehat{\mathbf{H}}\| \leq \|\widehat{\mathbf{H}}\| \quad (3-61)$$

Also, from (3-52) we have that $\|\Psi_{21}\| \leq \|\mathbf{R}_{22}\| \|\bar{\rho}\| \|\widehat{\mathbf{H}}\|$. Then, using property (3-15) again, from (3-60), we can write

$$\lim_{t \rightarrow \infty} \|\bar{\mathbf{s}}(t)\| \leq \|\widehat{\mathbf{H}}\| \left(1 + \frac{\|\bar{\rho}\|}{N|\psi_{11}|} \right) \|\Delta\| \quad (3-62)$$

Finally, combining (3-62) with (3-58) yields

$$s_\infty \leq \sqrt{N(N-1)} \|\widehat{\mathbf{H}}\| \left(1 + \frac{\|\bar{\rho}\|}{N|\psi_{11}|} \right) \|\Delta\| \quad (3-63)$$

Note that $\|\widehat{\mathbf{H}}\|$ is a function of γ and therefore varying γ controls the upper bound on $\mathbf{s}(t)$ and consequently can be used to reduce the control effort. Specifically, we can prove the following result.

Proposition 3.2.2. *The spectral norm of $\widehat{\mathbf{H}}$ can be upper bounded as*

$$\|\widehat{\mathbf{H}}\| \leq \frac{N}{\gamma \lambda_2 + 1} \quad (3-64)$$

Proof. From Lemma 3.2.1 we have that $\tilde{\mathcal{L}}^{-1} = \mathbf{U} \Sigma^{-1} \mathbf{U}^{-1}$. Then, using for each matrix its block representation as shown in (3-41), we have

$$\widehat{l}_{11} = r_{11} + N \mathbf{R}_{21}^T \bar{\Sigma}^{-1} \mathbf{R}_{21} \quad (3-65)$$

$$\widehat{\mathcal{L}}_{12} = \mathbf{R}_{12} + N \mathbf{R}_{21}^T \bar{\Sigma}^{-1} \mathbf{R}_{22} \quad (3-66)$$

$$\widehat{\mathcal{L}}_{21} = r_{11} \mathbb{1}_{N-1} + N \mathbf{R}_{22}^T \bar{\Sigma}^{-1} \mathbf{R}_{21} \quad (3-67)$$

$$\widehat{\mathcal{L}}_{22} = \mathbb{1}_{N-1} \mathbf{R}_{12} + N \mathbf{R}_{22}^T \bar{\Sigma}^{-1} \mathbf{R}_{22} \quad (3-68)$$

Replacing (3-66), (3-68) in (3-40) and taking into account that $\mathbf{R}_{12} = 1/N \mathbb{1}_{N-1}^T$ and $\mathbf{R}_{21}^T = -\mathbb{1}_{N-1}^T \mathbf{R}_{22}$ [from (3-11)], we have

$$\begin{aligned}\hat{\mathbf{H}} &= N \mathbf{R}_{22}^T \bar{\Sigma}^{-1} \mathbf{R}_{22} - N \mathbb{1}_{N-1} \mathbf{R}_{21}^T \bar{\Sigma}^{-1} \mathbf{R}_{22} \\ &= N \mathbf{R}_{22}^T \bar{\Sigma}^{-1} \mathbf{R}_{22} + N \mathbb{1}_{N-1} \mathbb{1}_{N-1}^T \mathbf{R}_{22}^T \bar{\Sigma}^{-1} \mathbf{R}_{22} \\ &= N(\mathbf{I}_{N-1} + \mathbb{1}_{N-1} \mathbb{1}_{N-1}^T) \mathbf{R}_{22}^T \bar{\Sigma}^{-1} \mathbf{R}_{22}\end{aligned}\quad (3-69)$$

From (3-42) we have that $\|\bar{\Sigma}^{-1}\| = 1/(\gamma\lambda_2 + 1)$ and $\|\hat{\mathbf{H}}\| \leq N^2 \|\mathbf{R}_{22}\|^2 (1/(\gamma\lambda_2 + 1))$. Therefore, using (3-15) we obtain (3-64) and the proof is complete. \square

3.2.3. Homogeneous node dynamics

We first complete the proof of convergence for the homogeneous case, that is we assume all nodes share identical uncoupled dynamics.

Theorem 3.2.1. *The closed-loop network (3-45) with $\rho_i = -\rho^*$, $\rho^* \in \mathbb{R}^+ \forall i \in \mathcal{N}$ achieves admissible consensus for any positive value of α , β and γ . Moreover, all node states converge asymptotically to $x_\infty = (1/N) \sum_{k=1}^N \delta_k / \rho^*$ with*

$$s_\infty \leq \frac{\sqrt{N^3(N-1)}}{\gamma\lambda_2 + 1} \|\Delta\| \quad (3-70)$$

Proof. Firstly, note that when all nodes share the same dynamics we have $\bar{\rho} = \mathbb{0}_{1 \times (N-1)}$ in (3-54). Consequently, Ψ_{12} and Ψ_{21} as defined by (3-51) and (3-52) are both null vectors so that the dynamics of \hat{e}_1 in (3-56) is independent from all the other variables, and converges to zero.

We can then study independently, the dynamics of $\hat{e}(t)$ and $\hat{w}(t)$ by considering the transverse candidate Lyapunov function

$$V(\hat{e}, \hat{w}) = (\beta/2) \hat{e}^T \bar{\Gamma} \hat{e} + (1/2) \hat{w}^T \hat{w} \quad (3-71)$$

which is positive definite and radially unbounded for any $\beta, \gamma > 0$. Then differentiating V along the trajectories of (3-56) one has $\dot{V} = -\beta \hat{e}^T \bar{\Gamma} (\alpha \bar{\Gamma} - \Psi_{22}) \hat{e}$. As all poles are identical, $\bar{P} = -\rho^* \mathbf{I}_{N-1}$; hence, expression (3-53) can be written as

$$\Psi_{22} = -\rho^* N (\mathbf{R}_{22} \hat{\mathbf{H}} \mathbf{R}_{22}^T + \mathbf{R}_{22} \hat{\mathbf{H}} \mathbb{1}_{N-1} \mathbb{1}_{N-1}^T \mathbf{R}_{22}^T) \quad (3-72)$$

and, using properties (3-39) and (3-43), we obtain $\Psi_{22} = -\rho^* \hat{\Sigma}^{-1}$.

Then $\dot{V} = -\beta \hat{e}^T \bar{\Gamma} \left\{ \alpha \bar{\Gamma} + \rho^* \hat{\Sigma}^{-1} \right\} \hat{e}$, which is negative definite for any positive value of α , β and γ . Therefore, (3-45) achieves admissible consensus. Moreover, all nodes will converge

to x_∞ as defined in Prop. 3.2.1 with $\sum_{k=1}^N \rho_k = -N\rho^*$. To estimate the upper bound on the integral states, we consider (3-63) with $\bar{\rho} = \mathbb{0}_{1 \times (N-1)}$ and using Proposition 3.2.2 we obtain expression (3-70). \square

Note that network (3-45) still achieves admissible consensus if the nodes are unstable ($\rho^* \in \mathbb{R}^-$), since a suitable α can be chosen such that $\alpha\bar{\Gamma} + \rho^*\bar{\Sigma}^{-1}$ remains positive definite; however, the average trajectory $\hat{e}_1(t)$ will be unstable and the system will exhibit unbounded admissible consensus; that is, $\lim_{t \rightarrow \infty} (x_i(t) - x_j(t)) = 0$ but $\lim_{t \rightarrow \infty} x_i(t) \rightarrow \infty$ for all $i, j \in \mathcal{N}$. By comparing the PID and PI ($\gamma = 0$) strategies discussed above, we observe that the most notable difference is the presence of the factor $N/(\gamma\lambda_2 + 1)$ in the expression of the upper bound of the integral term when PID is used instead of PI. Such a factor can be varied by selecting the gain of the derivative action. This can be done by taking into account the size (N) and structure of the network encoded by λ_2 , in order to avoid possible saturation of those integral terms and avoid the need for anti-windup strategies that can be difficult to implement across the network.

Theorem 3.2.2. *(Convergence Rate) The closed-loop network (3-45) with homogeneous node dynamics ($\rho_i = -\rho^*$), reaches admissible consensus with a convergence rate, say μ , that can be estimated as*

$$\mu = \left| \max_{2 \leq k \leq N} \left(\operatorname{Re} \left(-\frac{b}{2} + \frac{\sqrt{b^2 - \frac{4\beta\lambda_k}{\gamma\lambda_k+1}}}{2} \right) \right) \right| \quad (3-73)$$

where $b = (\alpha\lambda_k + \rho^*)/(\gamma\lambda_k + 1)$

Proof. The proof is based on straightforward linear algebra [63]. Indeed, as all poles are identical, we have from (3-72) that $\Psi_{22} = -\rho^*\hat{\Sigma}^{-1}$. Thus, one has from (3-56) that

$$\begin{bmatrix} \dot{\hat{e}}(t) \\ \dot{\hat{w}}(t) \end{bmatrix} = \underbrace{\begin{bmatrix} -(\rho^*\bar{\Sigma}^{-1} + \alpha\bar{\Gamma}) & \mathbf{I}_{N-1} \\ -\beta\bar{\Gamma} & \mathbb{0} \end{bmatrix}}_{\tilde{\mathbf{A}}} \begin{bmatrix} \hat{e}(t) \\ \hat{w}(t) \end{bmatrix}$$

The rate of convergence can be estimated by computing the dominant eigenvalue(s) of the dynamic matrix $\tilde{\mathbf{A}}$ defined above. Specifically, say η a generic eigenvalue of $\tilde{\mathbf{A}}$ and $\mathbf{v} = [\mathbf{v}_x \ \mathbf{v}_z]^T$ its corresponding eigenvector such that $\tilde{\mathbf{A}}\mathbf{v} = \eta\mathbf{v}$. Then, using the definition of $\tilde{\mathbf{A}}$ we obtain

$$-(\rho^*\bar{\Sigma}^{-1} + \alpha\bar{\Gamma})\mathbf{v}_x + \mathbf{v}_z = \eta\mathbf{v}_x \quad (3-74a)$$

$$-\beta\bar{\Gamma}\mathbf{v}_x = \eta\mathbf{v}_z \quad (3-74b)$$

Thus combining (3-74b) and (3-74a), we get

$$-\left(\frac{\alpha\eta + \beta}{\eta}\right)\bar{\Gamma}\mathbf{v}_x = (\eta\mathbf{I}_{N-1} + \rho^*\bar{\Sigma}^{-1})\mathbf{v}_x$$

From their definitions, it is easy to see that all matrices on both sides are diagonal; hence, component-wise we obtain

$$-(\alpha\eta + \beta)\frac{\lambda_k}{\gamma\lambda_k + 1} = \eta\left(\eta + \frac{\rho^*}{\gamma\lambda_k + 1}\right), k \in \{2, \dots, N\}$$

Therefore, the eigenvalues of matrix $\tilde{\mathbf{A}}$ are the $2(N - 1)$ solutions of the equations

$$\eta_k^2 + \eta_k\frac{(\alpha\lambda_k + \rho^*)}{\gamma\lambda_k + 1} + \frac{\beta\lambda_k}{\gamma\lambda_k + 1} = 0, k \in \{2, \dots, N\}$$

Finally, letting $\mu := |\eta_{max}| = \left| \max_k \{ \Re(\eta_k^\pm) \} \right|$ we obtain (3-73). \square

Remark 3.2.2. Note that

- The convergence rate depends on the network structure (via λ_2) as in the case of classical consensus problems, e.g. [56], but also on the node dynamics (ρ^*), and the controller gains (α , β and γ).
- In general, increasing the value of γ yields lower values of b in (3-73) and therefore the convergence rate may become slower. This indicates the presence of a trade-off between speed of convergence and bounds on the integral action that needs to be taken into account during the design stage.

Now, we consider distributed proportional-derivative (PD) strategy obtained by setting $\beta = 0$ in (3-4).

Theorem 3.2.3. Network (3-45) with homogeneous node dynamics, controlled by the distributed PD protocol obtained by selecting $\alpha > 0$, $\beta = 0$ and $\gamma > 0$ in (3-4) achieves ε -admissible consensus with

$$\varepsilon = \frac{\gamma\lambda_N + 1}{\gamma\lambda_2 + 1} \frac{N}{\alpha\lambda_N + \rho^*} \|\Delta\| \quad (3-75)$$

Proof. Equation (3-46a) without the integral action ($\beta = 0$) and homogeneous nodes can be written as the two uncoupled equations

$$\dot{e}_1(t) = \psi_{11}e_1(t) + q\Delta \quad (3-76)$$

$$\dot{\bar{e}}(t) = D\bar{e} + \hat{R}\Delta \quad (3-77)$$

where $\mathbf{D} = (\Psi_{22} - \alpha\widehat{\Gamma})$. Note that, $\psi_{11} = -\rho^*$ and, using property (3-43) as done in the proof of Theorem 3.2.1, we have $\Psi_{22} = -\rho^*\widehat{\Sigma}^{-1}$ and $\mathbf{D} = -(\alpha\bar{\Gamma} + \rho^*\widehat{\Sigma}^{-1})$ which is a negative definite, invertible matrix. Thus, $\lim_{t \rightarrow \infty} \bar{\mathbf{x}}^\perp(t) = -\mathbf{D}^{-1}\widehat{\mathbf{R}}\Delta$. To get an expression for the upper bound, we notice that, using (3-61), we can write

$$\left\| -\mathbf{D}^{-1}\widehat{\mathbf{R}}\Delta \right\| \leq \left\| \widehat{\mathbf{H}} \right\| \left\| (\alpha\bar{\Gamma} + \rho^*\widehat{\Sigma}^{-1})^{-1} \right\| \|\Delta\|$$

From (3-33) and (3-42), we know that $\bar{\Gamma}$ and $\bar{\Sigma}^{-1}$ are diagonal matrices and so is the matrix $\alpha\bar{\Gamma} + \rho^*\widehat{\Sigma}^{-1}$ with entries $(\alpha\lambda_k + \rho^*)/(\gamma\lambda_k + 1)$, $\forall k \in \{2, \dots, N\}$. Therefore, the diagonal elements of $(\alpha\bar{\Gamma} + \rho^*\widehat{\Sigma}^{-1})^{-1}$ are given by $(\gamma\lambda_k + 1)/(\alpha\lambda_k + \rho^*)$. From Lemma 2.4.1, we then have that $\left\| (\alpha\bar{\Gamma} + \rho^*\widehat{\Sigma}^{-1})^{-1} \right\| = (\gamma\lambda_N + 1)/(\alpha\lambda_N + \rho^*)$ since λ_N is the maximum eigenvalue of \mathcal{L} . Finally, using Prop. 3.2.2, we obtain (3-75). \square

As expected, the bound ε on the consensus error can be considerably reduced by increasing the gain of the proportional action (α) while it might be adversely affected by the gain of the derivative action. Indeed as for classical PID control, the presence of a distributed derivative action has little or no beneficial effect on the magnitude of the steady-state error. Also, it is clear that the network structure encoded by λ_2 and λ_N has an effect on the overall error bound.

Example 7. We consider the multi-agent system of Example 5 controlled by distributed PD instead of PI. The evolution of the node dynamics can be seen in Fig. 3-5 where ε -admissible consensus is achieved. Note that as predicted theoretically the bound ε can be adjusted by varying the network topology.

We conclude our investigation of the homogeneous case by studying distributed PID control for simple integrators, this is $\rho_i = 0, \forall i \in \mathcal{N}$

Corollary 3.2.1. (*Network of simple integrators*) Under controller dynamics (3-4), a multi-agent system of N agents (3-1) in the absence of disturbances with nodes characterized by infinite time constants i.e. $\rho_i = 0$, achieves admissible consensus for any positive value of α , β and γ . Moreover, if $\mathbf{s}(0) = 0$ all node states converge to the average consensus value $x_\infty(t) = (1/N) \sum_{k=1}^N x_k(0)$ as t approaches infinity.

Proof. The closed-loop network can be written as

$$\begin{bmatrix} \dot{\mathbf{x}}(t) \\ \dot{\mathbf{s}}(t) \end{bmatrix} = \tilde{\mathbf{A}} \begin{bmatrix} \mathbf{x}(t) \\ \mathbf{s}(t) \end{bmatrix}, \quad \tilde{\mathbf{A}} = \begin{bmatrix} -\alpha\tilde{\mathcal{L}}^{-1}\mathcal{L} & \mathbf{I}_N \\ -\beta\tilde{\mathcal{L}}^{-1}\mathcal{L} & \mathbf{0}_{N \times N} \end{bmatrix}$$

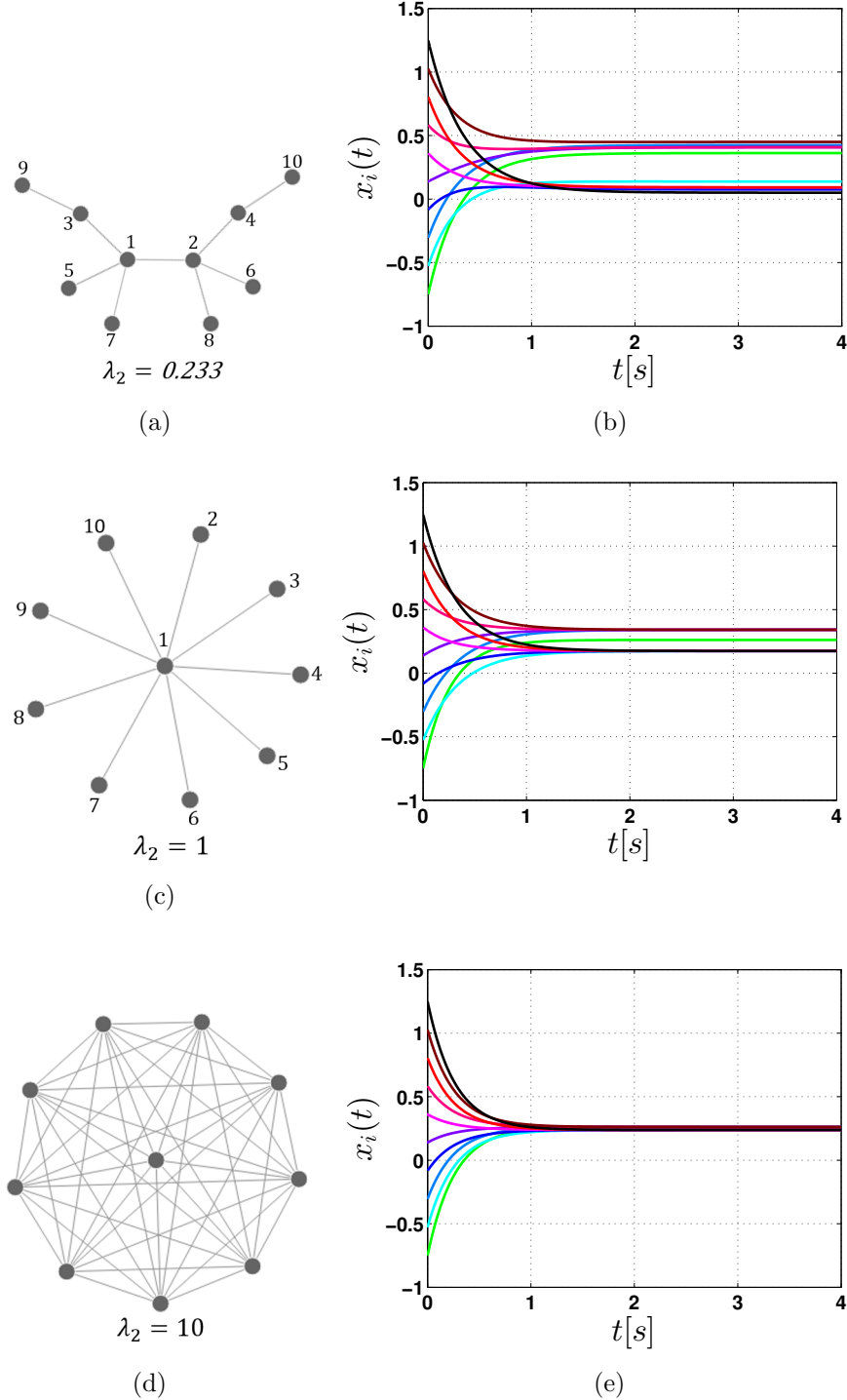


Figure 3-5.: Time response of the PD controlled multi-agent system for different network topologies with $\alpha = 4$ and $\gamma = 1$

Then, using the properties of the determinant of a block matrix as done in [66, 2], the characteristic equation of $\tilde{\mathbf{A}}$ can be written as $\det\left(\left(\alpha\tilde{\lambda} + \beta\right)\tilde{\mathcal{L}}^{-1}\mathcal{L} + \tilde{\lambda}^2\mathbf{I}_N\right) = 0$. Also, from Lemma 3.2.1 the characteristic equation of $\tilde{\mathcal{L}}^{-1}\mathcal{L}$ is $\det\left(\tilde{\mathcal{L}}^{-1}\mathcal{L} - \bar{\lambda}\mathbf{I}_N\right) = 0$ with solutions $\bar{\lambda} = \Gamma_{ii} \geq 0$, $i = \{1, \dots, N\}$.

Then, following a similar derivation as in [2] (proof of Theorem 1, p. 2078), one has $\tilde{\lambda}^2 + \Gamma_{ii}\alpha\tilde{\lambda} + \Gamma_{ii}\beta = 0$ with solutions $\tilde{\lambda}_1 = \tilde{\lambda}_2 = 0$ for $\Gamma_{11} = 0$ and $\tilde{\lambda} \in \mathbb{C}$ otherwise.

Note that the algebraic multiplicity of the zero eigenvalue is equal to 2 and all other eigenvalues are positive. Consequently, we can rewrite $\tilde{\mathbf{A}}$ into Jordan canonical form as

$$\tilde{\mathbf{A}} = \mathbf{W}\mathbf{J}\mathbf{W}^{-1} = \mathbf{W} \begin{bmatrix} 0 & 1 & \mathbf{0}_{1 \times 2N-2} \\ 0 & 0 & \mathbf{0}_{1 \times 2N-2} \\ \mathbf{0}_{2N-2 \times 1} & \mathbf{0}_{2N-2 \times 1} & \bar{\mathbf{J}} \end{bmatrix} \mathbf{W}^{-1}$$

where $\mathbf{W} = [\mathbf{w}_1^T, \dots, \mathbf{w}_{2N}^T]^T$ and $\mathbf{W}^{-1} = [\mathbf{v}_1^T, \dots, \mathbf{v}_{2N}^T]^T$ are matrices composed by the right and left eigenvectors of $\tilde{\mathbf{A}}$ and $\bar{\mathbf{J}}$ is the Jordan upper diagonal block matrix corresponding to the $2(N-1)$ nonzero eigenvalues of $\tilde{\mathbf{A}}$. Without loss of generality we choose $\mathbf{w}_1 = [\mathbf{1}_N^T \ \mathbf{0}_{1 \times N}]^T$, $\mathbf{w}_2 = [\mathbf{0}_{1 \times N} \ \mathbf{1}_N^T]^T$, $\mathbf{v}_1 = (1/N)[\mathbf{1}_N^T \ \mathbf{0}_{1 \times N}]^T$ and $\mathbf{v}_2 = (1/N)[\mathbf{0}_{1 \times N} \ \mathbf{1}_N^T]^T$ as generalized right and left eigenvectors. Therefore, the system solution can be written as

$$\begin{bmatrix} \mathbf{x}(t) \\ \mathbf{s}(t) \end{bmatrix} = e^{\tilde{\mathbf{A}}t} \begin{bmatrix} \mathbf{x}(0) \\ \mathbf{s}(0) \end{bmatrix} \text{ where}$$

$$e^{\tilde{\mathbf{A}}t} = \mathbf{W}e^{\mathbf{J}t}\mathbf{W}^{-1} = \mathbf{W} \begin{bmatrix} 1 & t & \mathbf{0}_{1 \times (2N-2)} \\ 0 & 1 & \mathbf{0}_{1 \times (2N-2)} \\ \mathbf{0}_{(2N-2) \times 1} & \mathbf{0}_{(2N-2) \times 1} & e^{\bar{\mathbf{J}}t} \end{bmatrix} \mathbf{W}^{-1}$$

Noticing that for a large t

$$\lim_{t \rightarrow \infty} \begin{bmatrix} \mathbf{x}(t) \\ \mathbf{s}(t) \end{bmatrix} = (1/N) \begin{bmatrix} \mathbf{1}_N \mathbf{1}_N^T & t \cdot \mathbf{1}_N \mathbf{1}_N^T \\ \mathbf{0}_{N \times N} & \mathbf{1}_N \mathbf{1}_N^T \end{bmatrix} \begin{bmatrix} \mathbf{x}(0) \\ \mathbf{s}(0) \end{bmatrix}$$

thus we have that for any initial condition $\mathbf{x}(0)$ and $\mathbf{s}(0) = 0$, the

$$\lim_{t \rightarrow \infty} \mathbf{x}(t) = (1/N) \sum_{k=1}^N x_k(0)$$

and $\lim_{t \rightarrow \infty} \mathbf{s}(t) = 0$ and the proof is complete. \square

3.2.4. Heterogeneous node dynamics

Next we consider the case where at least one pole ρ_i in (3-45) is different from the others, and the disturbances δ_i are generically nonidentical.

Theorem 3.2.4. *The heterogeneous group of agents (3-1) controlled by the distributed PID strategy (3-4), achieves admissible consensus for any $\beta > 0$ and $\gamma \geq 0$ if the following conditions hold*

$$\psi_{11} = (1/N) \sum_{k=1}^N \rho_k < 0, \quad (3-78a)$$

$$\alpha \frac{\lambda_2}{\gamma \lambda_2 + 1} > \frac{1}{N} \left(\max_i \{|\rho_i|\} + \frac{\bar{\rho} \bar{\rho}^T}{4 |\psi_{11}|} \|\mathbf{H}_1\|^2 \right) \quad (3-78b)$$

where $\mathbf{H}_1 := \mathbf{I}_{N-1} + \widehat{\mathbf{H}}$. Moreover, all node states converge to x_∞ as defined in Prop. 3.2.1, and the integral actions remain bounded by s_∞ given in (3-63).

Proof. Consider the following candidate Lyapunov function:

$$V = \frac{1}{2} \left(\widehat{e}_1^2 + \widehat{\mathbf{e}}^T \widehat{\mathbf{e}} + \frac{1}{\beta} \widehat{\mathbf{w}}^T \bar{\Gamma}^{-1} \widehat{\mathbf{w}} \right) \quad (3-79)$$

where $\bar{\Gamma}^{-1} := \text{diag}\{(\gamma \lambda_2 + 1)/\lambda_2, \dots, (\gamma \lambda_N + 1)/\lambda_N\}$. Differentiating V along the trajectories of (3-56) yields

$$\dot{V} = \psi_{11} \widehat{e}_1^2 + \widehat{\mathbf{e}}^T \Psi_{22} \widehat{\mathbf{e}} - \alpha \widehat{\mathbf{e}}^T \bar{\Gamma} \widehat{\mathbf{e}} + \widehat{e}_1 \widehat{\mathbf{e}}^T (\Psi_{12}^T + \Psi_{21})$$

and, using (3-51) and (3-52), we get

$$\dot{V} = \psi_{11} \widehat{e}_1^2 + \widehat{\mathbf{e}}^T \Psi_{22} \widehat{\mathbf{e}} - \alpha \widehat{\mathbf{e}}^T \bar{\Gamma} \widehat{\mathbf{e}} + \underbrace{\widehat{e}_1 \widehat{\mathbf{e}}^T \mathbf{R}_{22} \mathbf{H}_1 \bar{\rho}^T}_{g(\widehat{e}_1, \widehat{\mathbf{e}})} \quad (3-80)$$

Now, by setting $\mathbf{Q}^T = \mathbf{R}_{22} \mathbf{H}_1$, $\zeta_1^T = \widehat{\mathbf{e}}^T$, and $\zeta_2 = \widehat{e}_1 \bar{\rho}^T$ in (2-2), we can upper-bound $g(\widehat{e}_1, \widehat{\mathbf{e}})$ as follows

$$g(\widehat{e}_1, \widehat{\mathbf{e}}) \leq \frac{\varepsilon}{2} \widehat{\mathbf{e}}^T \mathbf{Q}^T \mathbf{Q} \widehat{\mathbf{e}} + \frac{\bar{\rho} \bar{\rho}^T}{2\varepsilon} \widehat{e}_1^2$$

This yields that from (3-80) we get

$$\dot{V} \leq \left(\psi_{11} + \frac{\bar{\rho} \bar{\rho}^T}{2\varepsilon} \right) \widehat{e}_1^2 + \widehat{\mathbf{e}}^T \Psi_{22} \widehat{\mathbf{e}} - \alpha \widehat{\mathbf{e}}^T \bar{\Gamma} \widehat{\mathbf{e}} + \frac{\varepsilon}{2} \widehat{\mathbf{e}}^T \mathbf{Q}^T \mathbf{Q} \widehat{\mathbf{e}} \quad (3-81)$$

From (3-19), we obtain $\|\Psi + \Psi^T\| \leq 2\|\mathbf{U}\|^2 \|\mathbf{P}\| \|\tilde{\mathcal{L}}^{-1}\|$. Moreover, we have $\|\tilde{\mathcal{L}}^{-1}\| = |\lambda_{\max}(\tilde{\mathcal{L}}^{-1})| = 1$, $\|\mathbf{P}\| = \max_i \{|\rho_i|\}$ and, from (3-15), $\|\mathbf{U}\|^2 = (1/N)$. Then, $\|\Psi + \Psi^T\| \leq (2/N) \max_i \{|\rho_i|\}$.

Using property (2-5) we then find that $\lambda_{\max}(\Psi_{22} + \Psi_{22}^T) \leq \lambda_{\max}(\Psi + \Psi^T)$ so that

$$\widehat{\mathbf{e}}^T \Psi_{22} \widehat{\mathbf{e}} = (1/2) \widehat{\mathbf{e}}^T (\Psi_{22} + \Psi_{22}^T) \widehat{\mathbf{e}} \leq (1/N) \max_i \{|\rho_i|\} \widehat{\mathbf{e}}^T \widehat{\mathbf{e}}$$

Also, as $-\widehat{\mathbf{e}}^T \bar{\Gamma} \widehat{\mathbf{e}} \leq -\lambda_2 / (\gamma \lambda_2 + 1) \widehat{\mathbf{e}}^T \widehat{\mathbf{e}}$, we obtain

$$\dot{V} \leq \left(\psi_{11} + \frac{\bar{\rho} \bar{\rho}^T}{2\varepsilon} \right) \widehat{x}_1^2 + \left(\frac{1}{N} \max_i \{|\rho_i|\} - \alpha \frac{\lambda_2}{\gamma \lambda_2 + 1} + \frac{\varepsilon}{2N} \|\mathbf{H}_1\|^2 \right) \widehat{\mathbf{x}}^T \widehat{\mathbf{x}} \quad (3-82)$$

Now, \dot{V} is negative definite if the terms $\xi_1 := \psi_{11} + \bar{\rho} \bar{\rho}^T / (2\varepsilon)$ and $\xi_2 := (1/N) \max_i \{|\rho_i|\} - \alpha \lambda_2 / (\gamma \lambda_2 + 1) + (\varepsilon/2N) \|\mathbf{H}_1\|^2$ are both negative.

From the assumptions, we have that $\psi_{11} < 0$, therefore $\xi_1 < 0$ is ensured if we choose $\varepsilon > \bar{\rho} \bar{\rho}^T / (2|\psi_{11}|)$ [this is always possible as ε is an arbitrary positive constant in (2-2)]. Then the condition $\xi_2 < 0$ can be fulfilled by selecting the control gains so as to satisfy (3-78b). Therefore, all agents in (3-1) achieves admissible consensus to x_∞ as defined in Prop. 3.2.1, and the integral actions remain bounded by (3-63) with $\|\widehat{\mathbf{H}}\|$ being bounded by (3-64) which completes the proof. \square

By comparing the PI and PID strategies we note that the convergence conditions (3-3) and (3-78b) differ by the term $\|\mathbf{H}_1\|^2/4$, which includes the derivative gain γ .

Example 8. For the sake of comparison we continue with the Example 6 where just PI actions were deployed in the heterogeneous multi-agent system. Here we include also the derivative action. Therefore, setting $\gamma = 1$ we have that

$$\tilde{\mathcal{L}} = \begin{bmatrix} 3 & -1 & 0 & 0 & -1 \\ -1 & 3 & -1 & 0 & 0 \\ 0 & -1 & 3 & -1 & 0 \\ 0 & 0 & -1 & 3 & -1 \\ -1 & 0 & 0 & -1 & 3 \end{bmatrix}, \tilde{\mathcal{L}}^{-1} = \begin{bmatrix} 0.4545 & 0.1818 & 0.0909 & 0.0909 & 0.1818 \\ 0.1818 & 0.4545 & 0.1818 & 0.0909 & 0.0909 \\ 0.0909 & 0.1818 & 0.4545 & 0.1818 & 0.0909 \\ 0.0909 & 0.0909 & 0.1818 & 0.4545 & 0.1818 \\ 0.1818 & 0.0909 & 0.0909 & 0.1818 & 0.4545 \end{bmatrix}$$

from (3-40) we find that

$$\widehat{\mathbf{H}} = \begin{bmatrix} 0.2727 & 0.0909 & 0 & -0.0909 \\ 0 & 0.3636 & 0.0909 & -0.0909 \\ -0.0909 & 0.0909 & 0.3636 & 0 \\ -0.0909 & 0 & 0.0909 & 0.2727 \end{bmatrix}$$

hence, $\|\mathbf{H}_1\| = 2.6504$ and the heterogeneous multi-agent system under distributed PID, reaches admissible consensus if $\alpha \lambda_2 / (\lambda_2 + 1) > 1.5708$. For the network structure considered in Example 6, we have that $\lambda_2 = 1.382$ so that $\alpha > 3.844$. The consensus equilibrium can be computed using Proposition 3.2.1, yielding $\mathbf{x}^* = \mathbb{1}_N$ and

$$\mathbf{s}^* = -\tilde{\mathcal{L}}^{-1}(\mathbf{P}\mathbf{x}^* + \Delta) = [0.1818, 0.6364, -0.2727, -0.4545, -0.0909]^T \quad (3-83)$$

Computing the norm of (3-30) and (3-83) we find that $\|\mathbf{z}^*\| = 2.4495$ and $\|\mathbf{s}^*\| = 0.8528$ respectively. Therefore a substantial reduction in the integral term has been obtained by

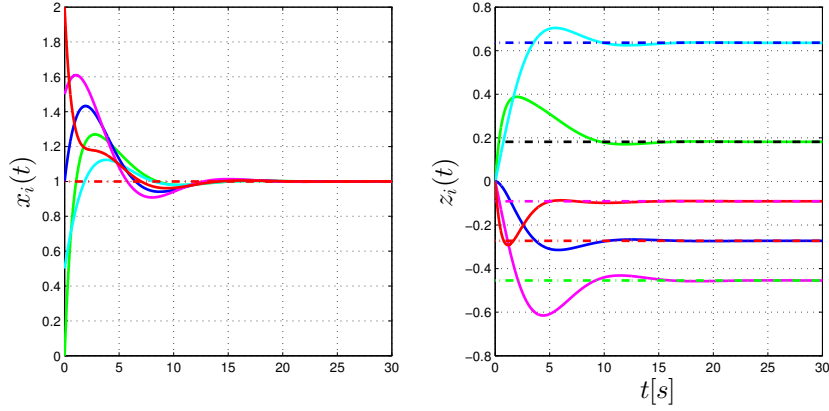


Figure 3-6.: Time response of the closed-loop heterogeneous network of Fig. 3-3 controlled by distributed PID strategy with $\alpha = 4$, and $\gamma = \beta = 1$. The dashed-lines represent the equilibrium constant value

considering a derivative action. In fact as shown in the upper-bound (3-63), the integral action at steady state can be reduced by increasing the value of γ . This confirms the fact that the derivative action can be used to decrease the amount of energy needed by the integral action to compensate heterogeneity among the nodes.

The evolution of the closed-loop network setting $\alpha = 4$ and $\beta = 1$, is shown in Figure 3-6 where consensus is achieved to the predicted value $(\mathbf{x}^*, \mathbf{s}^*)$.

CHAPTER 4

Multiplex PI Control for Networks of Heterogeneous Agents

In this chapter we extend the idea presented in Section 3.1, to the case where general linear dynamics are considered in each node and also proportional and integral actions can be independently deployed on different links. Specifically, we consider the problem of achieving consensus in a network of N agents governed by open-loop heterogeneous dynamics of the form

$$\dot{\mathbf{x}}_i(t) = \mathbf{A}_i \mathbf{x}_i(t) + \boldsymbol{\delta}_i - \sigma \sum_{j=1}^N \mathcal{C}_{ij} \mathbf{x}_j(t) + \mathbf{u}_i(t), i \in \mathcal{N} \quad (4-1)$$

where $\mathbf{x}_i(t) \in \mathbb{R}^{n \times 1}$ represents the state of the i -th agent, $\mathbf{A}_i \in \mathbb{R}^{n \times n}$ is the intrinsic node dynamic matrix, $\boldsymbol{\delta}_i \in \mathbb{R}^{n \times 1}$ is some constant disturbance (or constant external input) acting on each node, σ is a non-negative constant modelling the global coupling strength among any pair of nodes, \mathcal{C} is the (possibly disconnected) Laplacian matrix of the weighted graph $\mathcal{G}_C := (\mathcal{N}, \mathcal{E}_C)$ representing the open-loop network to be controlled, and $\mathbf{u}_i(t) \in \mathbb{R}^{n \times 1}$ is the control input.

Definition 4.0.1. *Network (4-1) is said to achieve admissible consensus if for any set of initial conditions $x_i(0) = x_{i0}$, and $\forall t \geq 0$*

$$\lim_{t \rightarrow \infty} \|\mathbf{x}_j(t) - \mathbf{x}_i(t)\| = 0, \|\mathbf{u}_i(t)\| < +\infty, i, j \in \mathcal{N}$$

The problem we shall solve is to find bounded and distributed control inputs $\mathbf{u}_i(t)$, such that all states $\mathbf{x}_i(t)$ converge asymptotically towards each other, i.e. admissible consensus.

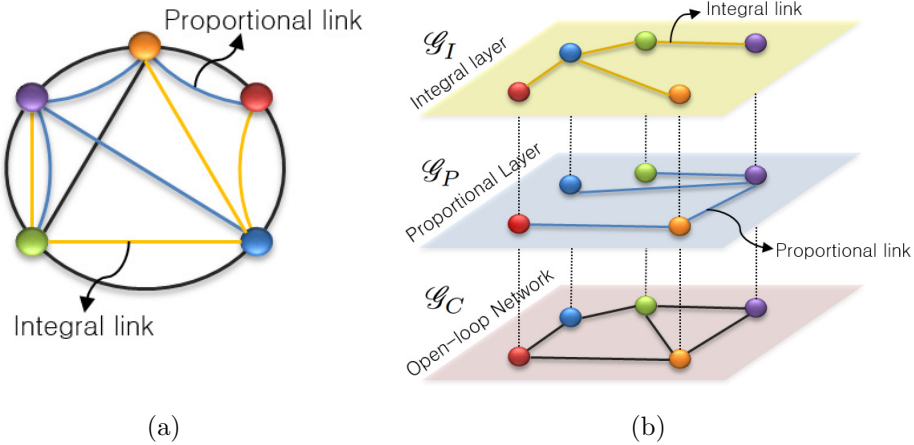


Figure 4-1: (a): The network to be controlled is represented by black links and the blue and yellow connections represent the additional proportional and integral links that are used for control. (b) Multiplex representation of a network controlled by proportional and integral distributed controllers.

To solve this problem, we propose the use of a distributed multiplex PI control strategy, obtained by setting:

$$\mathbf{u}_i(t) = -\alpha \sum_{j=1}^N w_{ij}(\mathbf{x}_j(t) - \mathbf{x}_i(t)) - \beta \sum_{j=1}^N g_{ij} \int_0^t (\mathbf{x}_j(\tau) - \mathbf{x}_i(\tau)) d\tau \quad (4-2)$$

where the non-negative constants $w_{ij} \geq 0$ and $g_{ij} \geq 0$ represent the control strengths of the proportional and integral control actions respectively (we do not consider self-loops, that is $w_{ii} = g_{ii} = 0$). It is important to highlight that this controller allows the deployment of proportional and integral actions independently from each other ($w_{ij} = 0$ or $g_{ij} = 0$ for some $i, j \in \mathcal{N}$, $i \neq j$). The constants $\alpha, \beta \in \mathbb{R}^+$ are additional parameters modulating globally the contribution of each control layer with respect to each other.

Equation (4-2) effectively defines two control layers each represented by a different weighted graph $\mathcal{G}_P := (\mathcal{N}, \mathcal{E}_P)$ for the proportional layer and $\mathcal{G}_I := (\mathcal{N}, \mathcal{E}_I)$ for the integral layer, where \mathcal{E}_P and \mathcal{E}_I are the set of edges with associated weights w_{ij} and g_{ij} respectively.

As depicted in Fig. 4-1 the resulting control strategy is therefore a multiplex distributed control strategy, with a multiplex graph $\mathcal{M} = (\mathcal{G}, \mathcal{D})$ where $\mathcal{G} := \{\mathcal{G}_C, \mathcal{G}_P, \mathcal{G}_I\}$. Moreover, in (4-2) the layers do not interact between them so that \mathcal{D} is an empty set. Next, we define

$$\widehat{\mathcal{C}} := (\mathcal{C} \otimes \mathbf{I}_n), \widehat{\mathcal{P}} := (\mathcal{P} \otimes \mathbf{I}_n), \widehat{\mathcal{I}} := (\mathcal{I} \otimes \mathbf{I}_n), \mathbf{x}(t) = [\mathbf{x}_1^T(t), \dots, \mathbf{x}_N^T(t)]^T,$$

$$\mathbf{z}(t) = [\mathbf{z}_1^T(t), \dots, \mathbf{z}_N^T(t)]^T := -\beta \widehat{\mathcal{I}} \int_0^t \mathbf{x}(\tau) d\tau \quad (4-3)$$

Then, the overall dynamics of the closed-loop network can be written as

$$\begin{bmatrix} \dot{\mathbf{x}}(t) \\ \dot{\mathbf{z}}(t) \end{bmatrix} = \begin{bmatrix} \widehat{\mathbf{A}} - \mathcal{H} & \mathbf{I}_{nN} \\ -\beta \widehat{\mathcal{I}} & \mathbb{0}_{(nN \times nN)} \end{bmatrix} \begin{bmatrix} \mathbf{x}(t) \\ \mathbf{z}(t) \end{bmatrix} + \begin{bmatrix} \Delta \\ \mathbb{0}_{(nN \times 1)} \end{bmatrix} \quad (4-4)$$

where $\widehat{\mathbf{A}} \in \mathbb{R}^{nN \times nN}$ is a block diagonal matrix given by $\widehat{\mathbf{A}} := \text{diag}\{\mathbf{A}_1, \dots, \mathbf{A}_N\}$, $\mathcal{H} := \sigma \widehat{\mathcal{C}} + \alpha \widehat{\mathcal{P}}$, and $\Delta \in \mathbb{R}^{nN \times 1}$ is the vector of constant disturbances, $\Delta := [\delta_1^T, \dots, \delta_N^T]^T$.

Thus, the problem becomes that of finding conditions on the node dynamics, the gains σ , α , and β , and most importantly the structural properties of the open-loop network layer \mathcal{G}_C and control layers \mathcal{G}_P and \mathcal{G}_I , so as to guarantee emergence of admissible consensus in the closed-loop network (4-4).

4.1. Consensus equilibrium

In this section we first show that the collective dynamics of the multiplex closed-loop network (4-4) has a unique equilibrium which is the solution of the admissible consensus problem. Then we derive some sufficient conditions guaranteeing asymptotic stability of such equilibrium.

Proposition 4.1.1. *If the matrix $\Psi_{11} := (1/N) \sum_{k=1}^N \mathbf{A}_k$ is non-singular, then the closed-loop network (4-4) has a unique equilibrium $\mathbf{x}^* := (\mathbb{1}_N \otimes \mathbf{x}_\infty)$ and $\mathbf{z}^* := -(\widehat{\mathbf{A}} \mathbf{x}^* + \Delta)$ where*

$$\mathbf{x}_\infty := -(1/N) \Psi_{11}^{-1} \sum_{k=1}^N \delta_k \quad (4-5)$$

Proof. Setting the left-hand side of (4-4) to zero one has that $\mathbf{x}^* = (\mathbb{1}_N \otimes \mathbf{v})$, $\forall \mathbf{v} \in \mathbb{R}^{n \times 1}$ and $\mathbf{z}^* = -(\widehat{\mathbf{A}}(\mathbb{1}_N \otimes \mathbf{v}) + \Delta)$. From (4-3), we also have that $(\mathbb{1}_N^T \otimes \mathbf{I}_n) \mathbf{z}(t) = \mathbb{0}_{nN \times 1}$, then $(\mathbb{1}_N^T \otimes \mathbf{I}_n) \mathbf{z}^* = \mathbb{0}_{nN \times 1}$ and we obtain

$$\begin{aligned} (\mathbb{1}_N^T \otimes \mathbf{I}_n) \widehat{\mathbf{A}} (\mathbb{1}_N \otimes \mathbf{v}) &= -(\mathbb{1}_N^T \otimes \mathbf{I}_n) \Delta \\ (1/N) \sum_{k=1}^N \mathbf{A}_k \mathbf{v} &= -(1/N) \sum_{k=1}^N \delta_k \end{aligned}$$

then $\mathbf{v} = -(1/N) \Psi_{11}^{-1} \sum_{k=1}^N \delta_k = \mathbf{x}_\infty$ completes the proof. \square

Remark 4.1.1. Note indeed that if controller (4-2) is able to render this equilibrium stable, it is also able to guarantee consensus of all node states $\mathbf{x}(t)$ to a constant vector \mathbf{x}_∞ using bounded control energy. Also, the emergent behaviour from the collective dynamics of the network, follows an “exo-system” given by $\dot{\mathbf{s}}(t) = \Psi_{11}\mathbf{s}(t) + (1/N) \sum_{k=1}^N \boldsymbol{\delta}_k$. This result for perturbed heterogeneous agents establishes a connection with [78] where internal models in networks are studied.

Now, to prove convergence, it suffices to guarantee that $(\mathbf{x}^*, \mathbf{z}^*)$ is globally asymptotically stable. We start by shifting the origin via the state transformation $\mathbf{y}(t) := \mathbf{z}(t) + \Delta$ so that (4-4) becomes

$$\begin{bmatrix} \dot{\mathbf{x}}(t) \\ \dot{\mathbf{y}}(t) \end{bmatrix} = \begin{bmatrix} \widehat{\mathbf{A}} - \mathcal{H} & \mathbf{I}_{nN} \\ -\beta \widehat{\mathcal{L}} & \mathbb{O}_{(nN \times nN)} \end{bmatrix} \begin{bmatrix} \mathbf{x}(t) \\ \mathbf{y}(t) \end{bmatrix} \quad (4-6)$$

Next, we present a decomposition of the Laplacian matrix that will be crucial for the derivations reported in the rest of the paper. As presented in the last Section such a decomposition is particularly useful to prove convergence in the presence of heterogeneous nodes.

4.2. Error dynamics

First we provide two important lemmas that will be used for determining the error dynamics of the consensus solution. The first one is the generalization of the block decomposition of \mathcal{L} presented in Section 3.1.2.

Lemma 4.2.1. Let $\mathcal{L} \in \Omega$ be the Laplacian matrix of a generic undirected and connected graph \mathcal{G} , then \mathcal{L} can be written in block form as $\mathcal{L} = \mathbf{R}\mathbf{A}\mathbf{R}^{-1}$, where \mathbf{R} is an orthonormal matrix defined with its inverse as

$$\mathbf{R} = \begin{bmatrix} 1 & N\mathbf{R}_{21}^T \\ \mathbb{1}_{N-1} & N\mathbf{R}_{22}^T \end{bmatrix}, \quad \mathbf{R}^{-1} = \begin{bmatrix} r_{11} & \mathbf{R}_{12} \\ \mathbf{R}_{21} & \mathbf{R}_{22} \end{bmatrix} \quad (4-7)$$

with

$$r_{11} = \frac{1}{N}, \quad \mathbf{R}_{12} = \frac{1}{N} \mathbb{1}_{N-1}^T, \quad (4-8)$$

$\mathbf{R}_{21} \in \mathbb{R}^{(N-1) \times 1}$, $\mathbf{R}_{22} \in \mathbb{R}^{(N-1) \times (N-1)}$ being blocks of appropriate dimensions,

$$\mathbf{\Lambda} = \text{diag}\{0, \lambda_2(\mathcal{L}), \dots, \lambda_N(\mathcal{L})\}$$

with $0 = \lambda_1(\mathcal{L}) < \lambda_2(\mathcal{L}) \leq \dots \leq \lambda_N(\mathcal{L})$ being the eigenvalues of \mathcal{L} in ascending order. Also, the blocks in \mathbf{R} and \mathbf{R}^{-1} must fulfill the following conditions

$$r_{11}\mathbf{I}_n + (\mathbf{R}_{12}\mathbb{1}_{N-1} \otimes \mathbf{I}_n) = \mathbf{I}_n \quad (4-9)$$

$$(\mathbf{R}_{21} \otimes \mathbf{I}_n) + (\mathbf{R}_{22}\mathbb{1}_{N-1} \otimes \mathbf{I}_n) = \mathbb{0}_{(n(N-1) \times 1)} \quad (4-10)$$

$$(\mathbf{R}_{21}\mathbf{R}_{21}^T \otimes \mathbf{I}_n) + (\mathbf{R}_{22}\mathbf{R}_{22}^T \otimes \mathbf{I}_n) = \frac{1}{N}(\mathbf{I}_{N-1} \otimes \mathbf{I}_n) \quad (4-11)$$

$$r_{11}(\mathbf{R}_{21}^T \otimes \mathbf{I}_n) + (\mathbf{R}_{12}\mathbf{R}_{22}^T \otimes \mathbf{I}_n) = \mathbb{0}_{(1 \times n(N-1))} \quad (4-12)$$

$$(\mathbf{R}_{21}\mathbf{R}_{21}^T \otimes \mathbf{I}_n) = (\mathbf{R}_{22}\mathbb{1}_{N-1}\mathbb{1}_{N-1}^T\mathbf{R}_{22}^T \otimes \mathbf{I}_n) \quad (4-13)$$

$$\|(\mathbf{R}_{22} \otimes \mathbf{I}_n)\| \leq \frac{1}{\sqrt{N}} \quad (4-14)$$

$$\|\mathbf{R}_{21}\| \leq \sqrt{N-1} \|\mathbf{R}_{22}\| \leq \sqrt{(N-1)/N} \quad (4-15)$$

$$N\mathbf{R}_{22}^T = (\mathbf{I}_{N-1} + \mathbb{1}_{N-1}\mathbb{1}_{N-1}^T)^{-1}\mathbf{R}_{22}^{-1} \quad (4-16)$$

Lemma 4.2.2. Let $\mathbf{Q} = \mathbf{R}\Lambda_1\mathbf{R}^{-1}$ and $\mathbf{S} = \mathbf{T}\Lambda_2\mathbf{T}^{-1}$ be two generic Laplacian matrices belonging to the set Ω , where \mathbf{R} and \mathbf{T} are block matrices with the same structure as in (4-7) and Λ_k , $k \in \{1, 2\}$ are diagonal matrices containing the eigenvalues of \mathbf{Q} and \mathbf{S} respectively. Then,

$$(\mathbf{R}^{-1}\mathbf{S}\mathbf{R} \otimes \mathbf{I}_n) = \begin{bmatrix} \mathbb{0}_{(n \times n)} & \mathbb{0}_{(n \times (nN-1))} \\ \mathbb{0}_{((nN-1) \times n)} & (\mathbf{\Xi}\bar{\Lambda}_2\mathbf{\Xi}^T \otimes \mathbf{I}_n) \end{bmatrix} \quad (4-17)$$

where $\mathbf{\Xi} = N\mathbf{R}_{22}(\mathbb{1}_{N-1}\mathbb{1}_{N-1}^T + \mathbf{I}_{N-1})\mathbf{T}_{22}^T$ and $\bar{\Lambda}_2 = \text{diag}\{\lambda_2(\mathbf{S}), \dots, \lambda_N(\mathbf{S})\}$. Moreover, $\mathbf{\Xi}\bar{\Lambda}_2\mathbf{\Xi}^T$ is a symmetric matrix.

Proof. Multiplying both sides of $\mathbf{S} = \mathbf{T}\Lambda_2\mathbf{T}^{-1}$ by \mathbf{R}^{-1} and \mathbf{R} , yields $\mathbf{R}^{-1}\mathbf{S}\mathbf{R} = \mathbf{R}^{-1}\mathbf{T}\Lambda_2\mathbf{T}^{-1}\mathbf{R}$. Now using the block form of \mathbf{R} and \mathbf{T} as shown in Lemma 4.2.1 one gets

$$\begin{aligned} \mathbf{R}^{-1}\mathbf{S}\mathbf{R} &= \begin{bmatrix} r_{11} & \mathbf{R}_{12} \\ \mathbf{R}_{21} & \mathbf{R}_{22} \end{bmatrix} \begin{bmatrix} 1 & N\mathbf{T}_{21}^T \\ \mathbb{1}_{N-1} & N\mathbf{T}_{22}^T \end{bmatrix} \begin{bmatrix} 0 & \mathbb{0}_{1 \times (N-1)} \\ \mathbb{0}_{(N-1) \times 1} & \bar{\Lambda}_2 \end{bmatrix} \\ &\cdot \begin{bmatrix} t_{11} & \mathbf{T}_{12} \\ \mathbf{T}_{21} & \mathbf{T}_{22} \end{bmatrix} \begin{bmatrix} 1 & N\mathbf{R}_{21}^T \\ \mathbb{1}_{N-1} & N\mathbf{R}_{22}^T \end{bmatrix} \end{aligned}$$

where $\bar{\Lambda}_2 = \text{diag}\{\lambda_2(\mathbf{S}), \dots, \lambda_N(\mathbf{S})\}$. By definition $t_{11} = r_{11}$ and $\mathbf{T}_{12} = \mathbf{R}_{12}$ (see (3-9)), and by some matrix manipulation we obtain

$$\begin{aligned} \mathbf{R}^{-1}\mathbf{S}\mathbf{R} &= \begin{bmatrix} r_{11} + \mathbf{R}_{12}\mathbb{1}_{N-1} & N(t_{11}\mathbf{T}_{21}^T + \mathbf{T}_{12}\mathbf{T}_{22}^T) \\ \mathbf{R}_{21} + \mathbf{R}_{22}\mathbb{1}_{N-1} & N(\mathbf{R}_{21}\mathbf{T}_{21}^T + \mathbf{R}_{22}\mathbf{T}_{22}^T) \end{bmatrix} \\ &\quad \begin{bmatrix} 0 & \mathbb{0}_{1 \times (N-1)} \\ \mathbb{0}_{(N-1) \times 1} & \bar{\Lambda}_2 \end{bmatrix}. \end{aligned} \quad (4-18)$$

$$\begin{bmatrix} t_{11} + \mathbf{T}_{12}\mathbb{1}_{N-1} & N(r_{11}\mathbf{R}_{21}^T + \mathbf{R}_{12}\mathbf{R}_{22}^T) \\ \mathbf{T}_{21} + \mathbf{T}_{22}\mathbb{1}_{N-1} & N(\mathbf{T}_{21}\mathbf{R}_{21}^T + \mathbf{T}_{22}\mathbf{R}_{22}^T) \end{bmatrix}$$

We next simplify each block of all matrices. Then, from (3-11) we have that $r_{11} + \mathbf{R}_{12}\mathbb{1}_{N-1} = t_{11} + \mathbf{T}_{12}\mathbb{1}_{N-1} = 1$. While, from (3-12)

$$\mathbf{R}_{21} + \mathbf{R}_{22}\mathbb{1}_{N-1} = \mathbf{T}_{21} + \mathbf{T}_{22}\mathbb{1}_{N-1} = \mathbb{0}_{(N-1 \times 1)}$$

and using (3-14)

$$N(t_{11}\mathbf{T}_{21}^T + \mathbf{T}_{12}\mathbf{T}_{22}^T) = N(r_{11}\mathbf{R}_{21}^T + \mathbf{R}_{12}\mathbf{R}_{22}^T) = \mathbb{0}_{(1 \times N-1)}$$

Note also that $\mathbf{R}_{21} = -\mathbf{R}_{22}\mathbb{1}_{N-1}$ and $\mathbf{T}_{21} = -\mathbf{T}_{22}\mathbb{1}_{N-1}$. Thus, the blocks

$$\boldsymbol{\Xi}_1 := N(\mathbf{R}_{21}\mathbf{T}_{21}^T + \mathbf{R}_{22}\mathbf{T}_{22}^T) = N\mathbf{R}_{22}(\mathbb{1}_{N-1}\mathbb{1}_{N-1}^T + \mathbf{I}_{N-1})\mathbf{T}_{22}^T \quad (4-19)$$

and,

$$\boldsymbol{\Xi}_2 := N(\mathbf{T}_{21}\mathbf{R}_{21}^T + \mathbf{T}_{22}\mathbf{R}_{22}^T) = N\mathbf{T}_{22}(\mathbb{1}_{N-1}\mathbb{1}_{N-1}^T + \mathbf{I}_{N-1})\mathbf{R}_{22}^T \quad (4-20)$$

Consequently, we have $\boldsymbol{\Xi}_1 = \boldsymbol{\Xi}_2^T$ and letting $\boldsymbol{\Xi} = \boldsymbol{\Xi}_1$, the Kronecker product $(\mathbf{R}^{-1}\mathbf{S}\mathbf{R} \otimes \mathbf{I}_n)$ yields (4-17). Finally, to prove that $\boldsymbol{\Xi}\bar{\Lambda}_2\boldsymbol{\Xi}^T$ is a symmetric matrix we have to show that $\boldsymbol{\Xi}^T$ is an orthonormal matrix. Then, from (4-19) and from the fact that \mathbf{R}_{22} is an invertible (full rank) matrix [12] one has

$$\boldsymbol{\Xi}^{-1} = \frac{1}{N}(\mathbf{T}_{22}^T)^{-1}(\mathbb{1}_{N-1}\mathbb{1}_{N-1}^T + \mathbf{I}_{N-1})^{-1}\mathbf{R}_{22}^{-1}$$

and using property (4-16) we obtain

$$\boldsymbol{\Xi}^{-1} = N\mathbf{T}_{22}(\mathbb{1}_{N-1}\mathbb{1}_{N-1}^T + \mathbf{I}_{N-1})\mathbf{R}_{22}^T = \boldsymbol{\Xi}^T$$

which completes the proof. \square

Assuming that the graphs in all layers of \mathcal{M} are connected, using Lemma 4.2.1 we can write $\mathcal{C} = \mathbf{R}\Lambda_C\mathbf{R}^{-1}$, $\mathcal{P} = \mathbf{U}\Lambda_P\mathbf{U}^{-1}$ and $\mathcal{I} = \mathbf{Q}\Lambda_I\mathbf{Q}^{-1}$. Next we define the error dynamics given by the state transformation $\mathbf{e}(t) = (\mathbf{R}^{-1} \otimes \mathbf{I}_n)\mathbf{x}(t)$; therefore, using the block representation of \mathbf{R}^{-1} and letting $\bar{\mathbf{e}}(t) := [\mathbf{e}_2^T(t), \dots, \mathbf{e}_N^T(t)]^T$ and $\bar{\mathbf{x}}(t) := [\mathbf{x}_2^T(t), \dots, \mathbf{x}_N^T(t)]^T$, we obtain

$$\mathbf{e}_1(t) = r_{11}\mathbf{x}_1(t) + (\mathbf{R}_{12} \otimes \mathbf{I}_n)\bar{\mathbf{x}}(t) \quad (4-21)$$

$$\bar{\mathbf{e}}(t) = (\mathbf{R}_{21} \otimes \mathbf{I}_n)\mathbf{x}_1(t) + (\mathbf{R}_{22} \otimes \mathbf{I}_n)\bar{\mathbf{x}}(t) \quad (4-22)$$

Thus expressing $(\mathbf{R}_{21} \otimes \mathbf{I}_n)$ from (4-10) and substituting in (3-17b) yields

$$\bar{\mathbf{e}}(t) = (\mathbf{R}_{22} \otimes \mathbf{I}_n)(\bar{\mathbf{x}}(t) - (\mathbb{1}_{N-1} \otimes \mathbf{I}_n)\mathbf{x}_1(t))$$

note that $\bar{\mathbf{e}}(t) = \emptyset$ if and only if $\bar{\mathbf{x}}(t) - (\mathbb{1}_{N-1} \otimes \mathbf{I}_n)\mathbf{x}_1(t) = \emptyset$ since \mathbf{R}_{22} is a full rank matrix [12]. Then, admissible consensus is achieved if $\lim_{t \rightarrow \infty} \bar{\mathbf{e}}(t) = \emptyset$ and $\|\mathbf{y}(t)\| < +\infty, \forall t > 0$. Now, recasting (4-6) in the new coordinates $\mathbf{e}(t)$ and $\mathbf{w}(t) := \mathbf{R}^{-1}\mathbf{y}(t)$, and letting

$$\bar{\Lambda}_C := \text{diag}\{\lambda_2(\mathcal{C}), \dots, \lambda_N(\mathcal{C})\}$$

$$\bar{\Lambda}_P := \text{diag}\{\lambda_2(\mathcal{P}), \dots, \lambda_N(\mathcal{P})\}$$

$$\bar{\Lambda}_I := \text{diag}\{\lambda_2(\mathcal{I}), \dots, \lambda_N(\mathcal{I})\}$$

we get

$$\begin{aligned} \dot{\mathbf{e}}(t) &= (\Psi - \widehat{\mathcal{H}}) \mathbf{e}(t) + \begin{bmatrix} \emptyset_{n \times 1} \\ \bar{\mathbf{w}}(t) \end{bmatrix} \\ \dot{\bar{\mathbf{w}}}(t) &= -\beta(\mathbf{\Xi}_I \bar{\Lambda}_2 \mathbf{\Xi}_I^T \otimes \mathbf{I}_n) \bar{\mathbf{e}}(t) \end{aligned} \quad (4-23)$$

where $\bar{\mathbf{w}}(t) := [\mathbf{w}_2^T(t), \dots, \mathbf{w}_N^T(t)]^T$. Note that the dynamics of $\mathbf{w}_1(t)$ can be neglected as it is trivial with null initial conditions and represents an uncontrollable and unobservable state. The quantities in (4-23) are defined as follows

- Ψ is a block matrix defined as

$$\begin{aligned} \Psi &:= \begin{bmatrix} \Psi_{11} & \Psi_{12} \\ \Psi_{21} & \Psi_{22} \end{bmatrix} = (\mathbf{R}^{-1} \otimes \mathbf{I}_n) \bar{\mathbf{A}} (\mathbf{R} \otimes \mathbf{I}_n) = \\ &(\mathbf{R}^{-1} \otimes \mathbf{I}_n) \begin{bmatrix} \mathbf{A}_1 & \emptyset_{(n \times n(N-1))} \\ \emptyset_{(n(N-1) \times n)} & \bar{\mathbf{A}} \end{bmatrix} (\mathbf{R} \otimes \mathbf{I}_n) \end{aligned}$$

where $\bar{\mathbf{A}} := \text{diag}\{\mathbf{A}_2, \dots, \mathbf{A}_N\}$ is a block diagonal matrix. Using properties (4-9)-(4-12), we can write (see Appendix A.2 for the derivation)

$$\Psi_{11} = (1/N) \sum_{k=1}^N \mathbf{A}_k \quad (4-24)$$

$$\Psi_{12} = \mathbf{P}_1 (\mathbf{R}_{22}^T \otimes \mathbf{I}_n) \quad (4-25)$$

$$\Psi_{21} = (\mathbf{R}_{22} \otimes \mathbf{I}_n) \mathbf{P}_2 \quad (4-26)$$

$$\Psi_{22} = N(\mathbf{R}_{22} \otimes \mathbf{I}_n) \mathbf{H} (\mathbf{R}_{22}^T \otimes \mathbf{I}_n) \quad (4-27)$$

with

$$\mathbf{H} := (\mathbb{1}_{N-1} \mathbb{1}_{N-1}^T \otimes \mathbf{A}_1) + \bar{\mathbf{A}} \quad (4-28)$$

$$\mathbf{P}_1 := [\mathbf{A}_2 - \mathbf{A}_1, \dots, \mathbf{A}_N - \mathbf{A}_1] \quad (4-29)$$

$$\mathbf{P}_2 := [\mathbf{A}_2^T - \mathbf{A}_1^T, \dots, \mathbf{A}_N^T - \mathbf{A}_1^T]^T \quad (4-30)$$

- the matrix $\Xi_I = N\mathbf{R}_{22}(\mathbb{1}_{N-1}\mathbb{1}_{N-1}^T + \mathbf{I}_{N-1})\mathbf{Q}_{22}^T$ was obtained using Lemma 4.2.2 for $(\mathbf{R}^{-1} \otimes \mathbf{I}_n)\widehat{\mathcal{I}}(\mathbf{R} \otimes \mathbf{I}_n)$.
- $\widehat{\mathcal{H}} := (\mathbf{R}^{-1} \otimes \mathbf{I}_n)\mathcal{H}(\mathbf{R} \otimes \mathbf{I}_n)$ and using again Lemma 4.2.2 yields

$$\widehat{\mathcal{H}} = \begin{bmatrix} 0 & \mathbb{0}_{1 \times (N-1)} \\ \mathbb{0}_{(N-1) \times 1} & \sigma\bar{\Lambda}_C + \alpha\Xi_P\bar{\Lambda}_P\Xi_P^T \end{bmatrix} \otimes \mathbf{I}_n$$

with $\Xi_P = N\mathbf{R}_{22}(\mathbb{1}_{N-1}\mathbb{1}_{N-1}^T + \mathbf{I}_{N-1})\mathbf{U}_{22}^T$.

4.3. Convergence theorem

Theorem 4.3.1. Consider the multiplex network (4-4) and assume that the graphs in each layer of \mathcal{M} are connected; then, admissible consensus is achieved for any integral graph topology \mathcal{G}_I with $\beta > 0$, if the following conditions hold

i) The matrix $\Psi_{11} = (1/N) \sum_{k=1}^N \mathbf{A}_k$ together with its symmetric part Ψ'_{11} are Hurwitz,

$$ii) \quad \alpha\lambda_2(\mathcal{P}) > \frac{1}{2} \left(\frac{\mu}{N|\eta|} + \rho \right) - \sigma\lambda_2(\mathcal{C})$$

where

$$\mu := \lambda_{\max} \left(\sum_{k=2}^N (\mathbf{A}'_k - \mathbf{A}'_1)^2 \right) \tag{4-31a}$$

$$\eta := \lambda_{\max}(\Psi'_{11}) \tag{4-31b}$$

$$\rho := \max_{k \in \mathcal{N}} \{ \lambda_{\max}(\mathbf{A}'_k) \} \tag{4-31c}$$

Moreover, all nodes asymptotically converge to $\mathbf{x}_\infty = -(1/N)\Psi_{11}^{-1} \sum_{k=1}^N \boldsymbol{\delta}_k$.

Proof. Consider the candidate Lyapunov function (in what follows we remove the time dependence of the state variables to simplify the notation)

$$V = \frac{1}{2}(\mathbf{e}_1^T \mathbf{e}_1 + \bar{\mathbf{e}}^T \bar{\mathbf{e}}) + \frac{1}{2\beta} \bar{\mathbf{w}}^T (\Xi_I \bar{\Lambda}_I \Xi_I^T \otimes \mathbf{I}_n)^{-1} \bar{\mathbf{w}} \tag{4-32}$$

From Lemma 4.2.2 we know that $\Xi_I \bar{\Lambda}_I \Xi_I^T$ is an eigendecomposition of a symmetric matrix with positive eigenvalues, which are the diagonal entries of $\bar{\Lambda}_I$; therefore, its inverse exist and it is also a positive definite matrix. Consequently, (4-32) is a positive definite and radially unbounded function. Then, differentiating V along the trajectories of (4-23) and using expressions (4-25) and (4-26), one has

$$\dot{V} = V_1(\mathbf{e}_1) + V_2(\bar{\mathbf{e}}) + V_3(\bar{\mathbf{e}}) + V_4(\mathbf{e}_1, \bar{\mathbf{e}}) \tag{4-33}$$

where,

$$V_1(\mathbf{e}_1) = \mathbf{e}_1^T \Psi_{11} \mathbf{e}_1 \quad (4-34)$$

$$V_2(\bar{\mathbf{e}}) = \bar{\mathbf{e}}^T \Psi_{22} \bar{\mathbf{e}} \quad (4-35)$$

$$V_3(\bar{\mathbf{e}}) = -\bar{\mathbf{e}}^T (\sigma(\bar{\Lambda}_C \otimes \mathbf{I}_n) + \alpha(\Xi_P \bar{\Lambda}_P \Xi_P^T \otimes \mathbf{I}_n)) \bar{\mathbf{e}} \quad (4-36)$$

$$V_4(\mathbf{e}_1, \bar{\mathbf{e}}) = \mathbf{e}_1^T (\mathbf{P}_1 + \mathbf{P}_2^T) (\mathbf{R}_{22}^T \otimes \mathbf{I}_n) \bar{\mathbf{e}} \quad (4-37)$$

Now, we proceed to find an upper-bound for each of the terms in (4-33). From the assumptions we know that $\Psi_{11} + \Psi_{11}^T$ is Hurwitz; therefore, using (4-31b) and property (2-3), one has that $V_1(\mathbf{e}_1) \leq -(1/2) |\eta| \mathbf{e}_1^T \mathbf{e}_1$

Next, consider the symmetric matrix $\Psi + \Psi^T = (\mathbf{R}^{-1} \otimes \mathbf{I}_n)(\hat{\mathbf{A}} + \hat{\mathbf{A}}^T)(\mathbf{R} \otimes \mathbf{I}_n)$. Then, it immediately follows that $\lambda_{\max}(\Psi + \Psi^T) = \rho$, where ρ is given in (4-31c). Now, we can write $V_2(\bar{\mathbf{e}}) = (1/2) \bar{\mathbf{e}}^T \Psi_{22}' \bar{\mathbf{e}}$, and from the fact that Ψ_{22} is a principal sub-matrix of Ψ , by using property (2-5) one has $V_2(\bar{\mathbf{e}}) \leq \rho \bar{\mathbf{e}}^T \bar{\mathbf{e}}$.

From Lemma 4.2.2 we know that $\Xi_P \bar{\Lambda}_P \Xi_P^T$ is a symmetric positive definite matrix. Hence, using (2-3) we have that $V_3(\bar{\mathbf{e}}) \leq -(\sigma \lambda_2(\mathcal{C}) + \alpha \lambda_2(\mathcal{P})) \bar{\mathbf{e}}^T \bar{\mathbf{e}}$.

Finally, setting $\zeta_1 = \mathbf{e}_1$, $\zeta_2 = \bar{\mathbf{e}}$, $\mathbf{Q}_1^T := \mathbf{P}_1 + \mathbf{P}_2^T$ and $\mathbf{Q}_2 := \mathbf{R}_{22}^T \otimes \mathbf{I}_n$ and using (2-2) yields

$$\begin{aligned} V_4(\mathbf{e}_1, \bar{\mathbf{e}}) &< \frac{\varepsilon}{2} \mathbf{e}_1^T \mathbf{Q}_1^T \mathbf{Q}_1 \mathbf{e}_1 + \frac{1}{2\varepsilon} \bar{\mathbf{e}}^T \mathbf{Q}_2^T \mathbf{Q}_2 \bar{\mathbf{e}} \\ &< \frac{\varepsilon}{2} \mathbf{e}_1^T \sum_{k=2}^N (\mathbf{A}'_k - \mathbf{A}'_1)^2 \mathbf{e}_1 + \frac{1}{2\varepsilon} \bar{\mathbf{e}}^T \mathbf{Q}_2^T \mathbf{Q}_2 \bar{\mathbf{e}} \end{aligned}$$

We can further simplify this expression by noticing that $\mathbf{Q}_2^T \mathbf{Q}_2$ is a symmetric matrix and using (2-3), (2-4), and (4-14), we can write $\bar{\mathbf{e}}^T \mathbf{Q}_2^T \mathbf{Q}_2 \bar{\mathbf{e}} \leq \|\mathbf{Q}_2\|^2 \bar{\mathbf{e}}^T \bar{\mathbf{e}} \leq (1/N) \bar{\mathbf{e}}^T \bar{\mathbf{e}}$. Then, using (4-31a) yields $V_4(\mathbf{e}_1, \bar{\mathbf{e}}) \leq (\varepsilon\mu)/2 \mathbf{e}_1^T \mathbf{e}_1 + 1/(2N\varepsilon) \bar{\mathbf{e}}^T \bar{\mathbf{e}}$. Exploiting all the bounds we found for each term in (4-33) yields

$$\begin{aligned} \dot{V} &\leq (1/2) (\varepsilon\mu - |\eta|) \mathbf{e}_1^T \mathbf{e}_1 - (\sigma \lambda_2(\mathcal{C}) + \alpha \lambda_2(\mathcal{P})) \bar{\mathbf{e}}^T \bar{\mathbf{e}} + \left(\frac{1}{2N\varepsilon} + \frac{\rho}{2} \right) \bar{\mathbf{e}}^T \bar{\mathbf{e}} \\ &\leq \xi_1 \mathbf{e}_1^T \mathbf{e}_1 + \xi_2 \bar{\mathbf{e}}^T \bar{\mathbf{e}} \end{aligned} \quad (4-38)$$

where $\xi_1 := \varepsilon\mu - |\eta| < 0$ and $\xi_2 := 1/(2N\varepsilon) + \rho/2 - \sigma \lambda_2(\mathcal{C}) - \alpha \lambda_2(\mathcal{P}) < 0$. Now, $\xi_1 < 0$ is ensured if $\varepsilon < |\eta|/\mu$. Also, $\xi_2 < 0$ if condition ii) is fulfilled. Therefore, under the hypotheses, all agents in (4-1) achieve admissible consensus to \mathbf{x}_∞ as defined in (4-5). \square

Remark 4.3.1.

- Note that for this type of heterogeneous networks, two ingredients node dynamics and network topology are crucial for determining the stability of the consensus equilibrium. Therefore, our results confirm that consensus in heterogeneous networks is a trade-off

between network structure (open loop network and proportional layers) and intrinsic node dynamics as shown in [30].

- The stability problem of the whole network has been simplified. In particular, rather than studying the stability of the $2nN \times 2nN$ matrix in (4-4), only conditions i) and ii) need to be verified which only depend upon $n \times n$ matrices.
- It is important to highlight that optimal values for the proportional layer ($\alpha, \lambda_2(\mathcal{P})$) can be obtained by properly labeling node 1 so that μ is such that the quantity $\mu/(N|\eta|)$ in condition ii) is the smallest.
- The integral network together with β may be used to control heuristically the rate of convergence to the consensus equilibrium. Obtaining an analytical estimate of such a rate is a highly non-trivial problem [39], [83] but some estimations can be found in the case where the agents are one-dimensional and homogeneous [12].

Corollary 4.3.1. Let $\mathcal{G}_{cp} = \text{proj}(\mathcal{G}_C, \mathcal{G}_P)$ denote the projection graph of \mathcal{G}_C and \mathcal{G}_P with \mathcal{L}_{cp} as its associated Laplacian matrix; then, assuming \mathcal{G}_{cp} connected, the multilayer network (4-4) reaches admissible consensus if condition i) of Theorem 4.3.1 is fulfilled and $\lambda_2(\mathcal{L}_{cp}) > (1/2)(\mu/(N|\eta|) + \rho)$

Proof. Since the graph $\mathcal{G}_{cp} = \text{proj}(\mathcal{G}_C, \mathcal{G}_P)$ is connected then we have that $\mathcal{L}_{cp} = \mathbf{U}\Lambda_{cp}\mathbf{U}^T$ where \mathbf{U} is the matrix composed by the eigenvectors of \mathcal{L}_{cp} and

$$\Lambda_{cp} = \text{diag}\{0, \lambda_2(\mathcal{L}_{cp}), \dots, \lambda_N(\mathcal{L}_{cp})\}$$

Hence, we have that $\mathcal{H} = (\mathcal{L}_{cp} \otimes \mathbf{I}_n)$ in (4-4) and following a similar arguments to those presented in Section 4.1 completes the proof. \square

Corollary 4.3.2. Considering homogeneous node dynamics, i.e $\mathbf{A}_i = \mathbf{A}, i \in \mathcal{N}$ where \mathbf{A} and \mathbf{A}' are Hurwitz stable, then the closed-loop network (4-4), reaches admissible consensus for any connected proportional and integral graph topologies with $\alpha, \beta > 0$.

Proof. Firstly, note that when all nodes share the same intrinsic dynamics we have that $\mu = 0$ in (4-31a), and $\Psi_{11} = \mathbf{A}$. Hence, from the assumption, condition i) of Theorem 4.3.1 is automatically satisfied and from the fact that matrix $\mathbf{A} + \mathbf{A}^T$ is Hurwitz, one has that $\rho < 0$ in (4-31c); therefore, condition ii) of Theorem 4.3.1 is also automatically fulfilled. \square

Now consider the case where Ψ_{11} is not Hurwitz stable; then, it is possible to apply a local feedback control action to a subset of the nodes so as to render Ψ_{11} Hurwitz stable and guarantee the existence of the consensus equilibrium $(\mathbf{x}^*, \mathbf{z}^*)$ in the closed-loop network. Or, equivalently, make the network *consensuable* according to the definition given in [77]. Specifically, consensusability can be achieved by adding an extra control input, say \mathbf{v}_i , onto a fraction $K < N$ nodes so that Ψ_{11} is stable. For example, one can choose the controller

$$\mathbf{v}_i(t) = \mathbf{H}_i \mathbf{x}_i(t) \quad (4-39)$$

where $\mathbf{H}_i \in \mathbb{R}^{n \times n}$ is a gain matrix to be designed appropriately. Note that typically one could simply choose $K = 1$ so that the dynamics of just one node is altered by this self-feedback loop.

Corollary 4.3.3. *The heterogeneous network (4-1) is said to be consensuable under the distributed control action (4-39), if there exist matrices \mathbf{H}_i such that conditions i) and ii) in Theorem 4.3.1 are fulfilled.*

Remark 4.3.2. *Note that the presence of local controllers acting on some nodes can be used not only for improving the closed-loop network stability, but also to change the value of the consensus vector \mathbf{x}_∞ .*

4.4. Control algorithm

The results presented so far can be distilled into the following algorithmic steps to design the multilayer PI network control strategy proposed in this paper. Specifically,

- S1 Compute matrix $\Psi_{11} = (1/N) \sum_{k=1}^N \mathbf{A}_i$ from the open-loop network (4-1).
- S2 If matrix Ψ_{11} and Ψ'_{11} are Hurwitz stable then go to step S4, otherwise go to S3.
- S3 Design local controllers (4-39) such that Ψ_{11} together with its symmetric part Ψ'_{11} are Hurwitz. Note that matrices \mathbf{H}_i can also be properly chosen for selecting different values of the consensus vector \mathbf{x}_∞ in (4-5)
- S4 Select any connected and weighed graph \mathcal{G}_T for the integral layer e.g. a minimal spanning tree. Then compute the quantities μ , η , and ρ defined in (4-31)
- S5 Find a connected and weighed graph \mathcal{G}_P for the proportional layer and a value of the global coupling gain α such that $\alpha \lambda_2(\mathcal{P}) > (1/2)(\mu/(N|\eta|) + \rho) - c \lambda_2(\mathcal{C})$

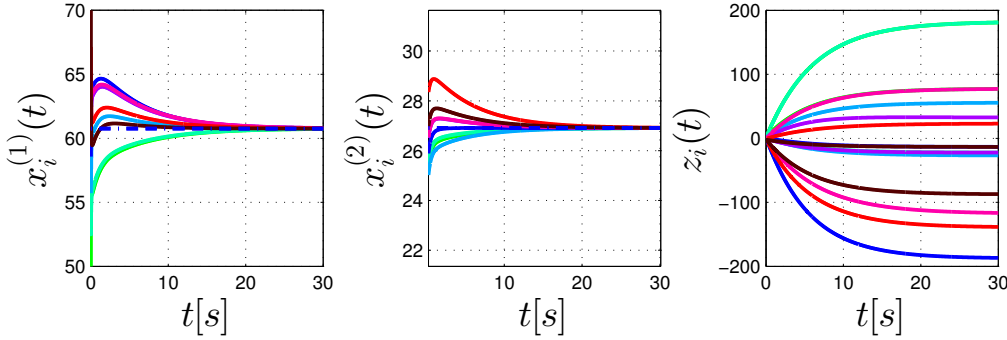


Figure 4-2.: Time response of the closed-loop multiplex network for $\alpha = 13.5$ and $\beta = 7$ where the proportional and integral networks have both ring topologies with all its weights equal to 3 and 1 respectively.

Example 9. For the sake of simplicity and without loss of generality we consider three types of node dynamics; stable (\mathbf{E}_1), oscillatory (\mathbf{E}_2) and unstable (\mathbf{E}_3)

$$\mathbf{E}_1 := \begin{bmatrix} -3 & 0 \\ 1 & -7 \end{bmatrix}, \mathbf{E}_2 := \begin{bmatrix} 0 & 1 \\ -1 & 0 \end{bmatrix}, \mathbf{E}_3 := \begin{bmatrix} 1 & 1 \\ 0 & 0.5 \end{bmatrix}$$

Then, we consider eight decoupled agents governed by (4-1), with $\sigma = 0$, $\mathbf{A}_k = \mathbf{E}_1, k \in \{1, 2, 5, 6\}$, $\mathbf{A}_k = \mathbf{E}_2, k \in \{3, 7\}$, and $\mathbf{A}_k = \mathbf{E}_3, k \in \{4, 8\}$ and disturbances $\boldsymbol{\delta}_i \in \mathbb{R}^{2 \times 1}$ given by

$$\Delta = [\boldsymbol{\delta}_1^T, \dots, \boldsymbol{\delta}_8^T]^T = [0, 50, 0, 150, 0, 5, 100, 0, 150, 150, 300, 50, -50, 200, 0, 0]$$

Note that the 8-th node does not have any perturbation. Thus, the aim is to design the multiplex PI-Controller such that all the 8 nodes achieve admissible consensus. Following the control design steps in Section 4.4, we have from S1 that matrices

$$\Psi_{11} = \begin{bmatrix} -1.25 & 0.5 \\ 0.25 & -3.375 \end{bmatrix}, \Psi'_{11} = \begin{bmatrix} -2.5 & 0.75 \\ 0.75 & -6.75 \end{bmatrix}$$

are both Hurwitz stable. Then following S4 we select a ring network of 8 nodes with unitary weights ($g_{ij} = 1 \quad \forall i, j \in \mathcal{N}$) as the connected integral network, and from (4-31) one has that $\mu = 846.4826$, $\eta = 2.3715$, and $\rho = 2.618$. From S5 we have that $\alpha \lambda_2(\mathcal{P}) > 23.6175$. Then, choosing, w.l.o.g again a ring network with $w_{ij} = 3 \quad \forall i, j \in \mathcal{N}$ so that $\lambda_2(\mathcal{P}) = 1.3244$. One has that the closed-loop network of 8 agents, achieves admissible consensus for $\alpha > 13.4392$. We choose $\alpha = 13.5$, and $\beta = 7$. The resulting evolution of the node states and integral actions is shown in Fig. 4-2, where admissible consensus is reached as expected to the predicted value $\mathbf{x}_\infty := -(1/N)\Psi_{11}^{-1} \sum_{k=1}^N \boldsymbol{\delta}_k = [60.7634, 26.9084]^T$.

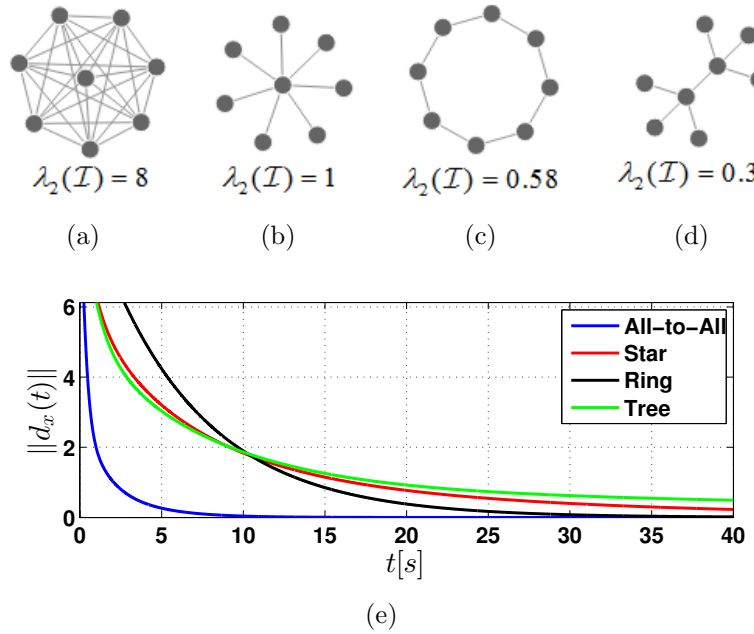


Figure 4-3: Networks with unitary weights representing different architectures for the graph in the integral control layer: (a) all-to-all, (b) star, (c) ring, and (d) Tree. (e) time response of the consensus index d_x when the topology of the integral network is varied

The admissible consensus conditions presented in Theorem 4.3.1 are independent from the graph structure of the integral layer \mathcal{G}_I that only needs to be connected. However, in general, we found that the rate of convergence to the consensus equilibrium can be affected by the specific choice of \mathcal{G}_I . To illustrate this point, we consider different structures for the graph \mathcal{G}_I as shown in Fig. 4-3. We then plot the evolution of the consensus index $d_x := \|\mathbf{x}(t) - (1/N) (\mathbb{1}_N \mathbb{1}_N^T \otimes \mathbf{I}_n) \mathbf{x}(t)\|$, where $d_x = 0$ indicates that the closed-loop network has reached admissible consensus. We observe that the structure of \mathcal{G}_I changes the speed of convergence.

Surprisingly, when the integral layer has a ring topology which has lower λ_2 than the star topology convergence is faster. Therefore, the presence of an integral layer with an independent structure from the diffusive proportional layer can be used as an extra degree of freedom to optimize performance.

CHAPTER 5

Distributed PID Control for Synchronization in Networks of Nonlinear Units

In this Chapter we address the problem of synchronizing nonlinear units by considering distributed proportional, integral and derivative actions acting among nodes. In particular we extend the previous result on linear consensus to the case of nonlinear yet identical dynamics. Specifically, consider a set of N units (agents) described by

$$\dot{\mathbf{x}}_i(t) = \mathbf{f}(\mathbf{x}_i(t)) + \mathbf{u}_i(t) \quad (5-1a)$$

$$\mathbf{y}_i(t) = \boldsymbol{\Gamma}\mathbf{x}_i(t), i \in \mathcal{N} \quad (5-1b)$$

where $\mathbf{x}_i \in \mathbb{R}^n$, $\mathbf{f}(\mathbf{x}, t) : \mathbb{R}^n \times \mathbb{R}^+ \cup \{0\} \mapsto \mathbb{R}^n$ is a nonlinear function, $\mathbf{y}_i \in \mathbb{R}^n$ is the output of each node with $\boldsymbol{\Gamma} \in \mathbb{R}^{n \times n}$, and $\mathbf{u}_i(t)$ representing a distributed controller (or interconnection term of the i -th node with its neighbour nodes). Generally, $\boldsymbol{\Gamma}$ is assumed to be a diagonal positive semi-definite matrix, representing the information that all units share with each other.

The problem is to find bounded and distributed control inputs $\mathbf{u}_i(t)$, such that all states $\mathbf{x}_i(t)$ converge asymptotically towards each other.

Definition 5.0.1. (*Admissible Synchronization*): A group of N nonlinear units (5-1), is said to reach local admissible synchronization if there exist a set of initial conditions $\mathbf{x}_i(0) = \mathbf{x}_{i0}$ such that

$$\lim_{t \rightarrow \infty} \|\mathbf{x}_j(t) - \mathbf{x}_i(t)\| = 0, \quad \|\mathbf{u}_i(t)\| < +\infty, \forall t \geq 0, \quad i \in \mathcal{N} \quad (5-2)$$

Moreover, if (5-2) holds for any set of initial conditions; then, we said that the network reaches global admissible synchronization.

As suggested in previous Chapters, to solve this problem we make use of distributed proportional, integral and derivative actions, by setting

$$u_i(t) = - \sum_{j=1}^N \mathcal{L}_{ij} \left(\alpha \mathbf{y}_j(t) + \beta \int_0^t \mathbf{y}_j(\tau) d\tau + \gamma \dot{\mathbf{y}}_j(t) \right) \quad (5-3)$$

where α , β and γ are positive constants representing the global strength of the proportional, integral and derivative contributions. Thus, the problem becomes that of finding conditions on the control gains α , β , γ , the network structure \mathcal{L} and the node dynamics $\mathbf{f}(\cdot)$ so as to guarantee convergence of all nodes towards each other, i.e, admissible synchronization.

5.1. Local stability analysis

In this section we study the stability of the synchronous network solution in presence of small perturbations. To further characterize the influence of the derivative and integral terms, we decide to analyse the PD and PI cases in a separated way. Here, the well known Master Stability Function approach (MSF) is extended for finding local synchronization conditions.

5.1.1. MSF for distributed PD

Consider the group of nonlinear units (5-1) controlled by distributed proportional and derivative actions (this is, setting $\beta = 0$ in (5-3)). Then, letting $\tilde{\mathcal{L}} := \mathbf{I}_{nN} + \gamma(\mathcal{L} \otimes \Gamma)$, the closed-loop network can be written as

$$\tilde{\mathcal{L}} \dot{\mathbf{x}}(t) = \mathbf{F}(\mathbf{x}) - \alpha(\mathcal{L} \otimes \Gamma)\mathbf{x}(t) \quad (5-4)$$

where $\mathbf{F}(\mathbf{x}) := [\mathbf{f}(\mathbf{x}_1)^T, \dots, \mathbf{f}(\mathbf{x}_N)^T]^T$ and $\mathbf{x}(t) := [\mathbf{x}_1^T(t), \dots, \mathbf{x}_N^T(t)]^T$ are the stack vectors of the nonlinear functions and node states respectively. Note that for $\gamma = 0$ (just proportional control) one has $\dot{\mathbf{x}}(t) = \mathbf{F}(\mathbf{x}) - \alpha(\mathcal{L} \otimes \Gamma)\mathbf{x}(t)$ which is the classical diffusive coupled network (2-15). As done in Section 3.2.1, we first derive some properties of the matrix $\tilde{\mathcal{L}}$ that will be useful to prove admissible synchronization

Proposition 5.1.1. *Let $\tilde{\mathcal{L}} := \mathbf{I}_{nN} + \gamma(\mathcal{L} \otimes \Gamma)$ where γ is an arbitrary non-negative constant, $\mathcal{L} \in \Omega$ and Γ is a positive semi-definite diagonal matrix. Then, the following equalities hold*

$$\tilde{\mathcal{L}}(\mathbb{1}_N \otimes \mathbb{1}_n) = \tilde{\mathcal{L}}^{-1}(\mathbb{1}_N \otimes \mathbb{1}_n) = (\mathbb{1}_N \otimes \mathbb{1}_n) \quad (5-5)$$

$$\tilde{\mathcal{L}}(\mathbb{1}_N \otimes \zeta) = \tilde{\mathcal{L}}^{-1}(\mathbb{1}_N \otimes \zeta) = (\mathbb{1}_N \otimes \zeta), \forall \zeta \in \mathbb{R}^{n \times 1} \quad (5-6)$$

$$\tilde{\mathcal{L}} = (\mathbf{U} \otimes \mathbf{I}_n)\Sigma(\mathbf{U}^T \otimes \mathbf{I}_n) \quad (5-7)$$

where Σ is a diagonal matrix given by $\Sigma = \mathbf{I}_{nN} + \gamma(\Lambda \otimes \Gamma)$

Proof. From Lemma 2.2.1, $\mathcal{L}\mathbf{1}_N = \mathbf{0}_{N \times 1}$; therefore, we immediately have $\tilde{\mathcal{L}}\mathbf{1}_{nN} = (\mathbf{I}_{nN} + \gamma(\mathcal{L} \otimes \Gamma))(\mathbf{1}_N \otimes \mathbf{1}_n) = \mathbf{1}_{nN}$. Hence, multiplying both sides by $\tilde{\mathcal{L}}^{-1}$ yields $\tilde{\mathcal{L}}^{-1}\tilde{\mathcal{L}}\mathbf{1}_{nN} = \tilde{\mathcal{L}}^{-1}\mathbf{1}_{nN}$ so that $\tilde{\mathcal{L}}^{-1}\mathbf{1}_{nN} = \mathbf{1}_{nN}$ and (5-5) is obtained. Similarly, using straightforward calculations we can obtain (5-6). Moreover, we have that $\mathcal{L} = \mathbf{U}\Lambda\mathbf{U}^T$ where $\mathbf{U}\mathbf{U}^T = \mathbf{I}_N$. Hence, we can write $\tilde{\mathcal{L}} = (\mathbf{U}\mathbf{U}^T \otimes \mathbf{I}_n) + \gamma(\mathbf{U}\Lambda\mathbf{U}^T \otimes \Gamma)$, then regrouping terms yields (5-7). \square

Now, letting $\mathcal{P} := \tilde{\mathcal{L}}^{-1}(\mathcal{L} \otimes \Gamma)$, and denoting by $\hat{\mathcal{L}}_{ij}$ and \mathcal{P}_{ij} the $n \times n$ blocks of matrices $\tilde{\mathcal{L}}^{-1}$ and \mathcal{P} respectively, yields that the equation of the i -th node of the closed-loop network (5-4) can be written as

$$\dot{\mathbf{x}}_i(t) = \sum_{j=1}^N \hat{\mathcal{L}}_{ij} \mathbf{f}(\mathbf{x}_j) - \alpha \sum_{j=1}^N \mathcal{P}_{ij} \mathbf{x}_j(t), \forall i \in \mathcal{N} \quad (5-8)$$

Note that when all nodes are synchronized, i.e., $\mathbf{x}_1(t) = \dots = \mathbf{x}_N(t) = \mathbf{s}(t)$, (5-8) becomes $\dot{\mathbf{s}}(t) = \mathbf{f}(\mathbf{s}) \sum_{j=1}^N \hat{\mathcal{L}}_{ij} - \alpha \mathbf{s}(t) \sum_{j=1}^N \mathcal{P}_{ij}$. It follows from property (5-5) that $\sum_{j=1}^N \hat{\mathcal{L}}_{ij} = 1$ and from the definition we have that \mathcal{P} is row-sum zero. This can be easily seen by considering

$$\tilde{\mathcal{L}}^{-1}(\mathcal{L} \otimes \Gamma)(\mathbf{1}_N \otimes \mathbf{1}_n) = \tilde{\mathcal{L}}^{-1}(\mathcal{L}\mathbf{1}_N \otimes \Gamma)$$

and from the fact that $\mathcal{L} \in \Omega$ we have that $\mathcal{L}\mathbf{1}_N = \mathbf{0}_{N \times 1}$. Therefore, the equation governing the synchronous motion is given by $\dot{\mathbf{s}}(t) = \mathbf{f}(\mathbf{s})$.

Following the master stability function approach, we study the stability of the synchronous solution of the closed-loop network (5-8), in presence of small perturbations $\delta\mathbf{x}(t)$. Thus, we set $\mathbf{s}(t) = \mathbf{x}_i(t) - \delta\mathbf{x}_i(t)$. It follows from Taylor series expansion that $\mathbf{f}(\delta\mathbf{x}_i + \mathbf{s}) = \mathbf{f}(\mathbf{s}) + D\mathbf{f}(\mathbf{s})\delta\mathbf{x}_i(t), \forall i \in \mathcal{N}$, where $D\mathbf{f}(\mathbf{s})$ represents the time-varying Jacobi matrix of $\mathbf{f}(\cdot)$. Therefore, using the properties of $\tilde{\mathcal{L}}$ the perturbation dynamics can be expressed as

$$\dot{\delta\mathbf{x}}_i(t) = \sum_{j=1}^N \hat{\mathcal{L}}_{ij} D\mathbf{f}(\mathbf{s}) \delta\mathbf{x}_j(t) - \alpha \sum_{j=1}^N \mathcal{P}_{ij} \delta\mathbf{x}_j(t) \quad (5-9)$$

which in compact form reads

$$\dot{\Delta}(t) = \tilde{\mathcal{L}}^{-1}(\mathbf{I}_N \otimes D\mathbf{f}(\mathbf{s})) \Delta(t) - \alpha \mathcal{P} \Delta(t) \quad (5-10)$$

where $\Delta(t) := [\delta\mathbf{x}_1^T(t), \dots, \delta\mathbf{x}_N^T(t)]^T$. Moreover, from (5-7) one has that $\tilde{\mathcal{L}}^{-1} = (\mathbf{U} \otimes \mathbf{I}_n)\Sigma^{-1}(\mathbf{U}^T \otimes \mathbf{I}_n)$; therefore, $\mathcal{P} = \tilde{\mathcal{L}}^{-1}(\mathcal{L} \otimes \Gamma) = (\mathbf{U} \otimes \mathbf{I}_n)\Sigma^{-1}(\Lambda \otimes \Gamma)(\mathbf{U}^T \otimes \mathbf{I}_n)$. Hence, by applying the state transformation $\zeta(t) = (\mathbf{U}^T \otimes \mathbf{I}_n) \Delta(t)$ to (5-10) and using properties 2-6 one has

$$\dot{\zeta}(t) = \Sigma^{-1}((\mathbf{I}_N \otimes D\mathbf{f}(\mathbf{s})) - \alpha(\Lambda \otimes \Gamma)) \zeta(t) \quad (5-11)$$

note that (5-11) is in triangular form with N decoupled blocks

$$\dot{\zeta}_i(t) = (\mathbf{I}_n + \gamma \lambda_i \mathbf{\Gamma})^{-1} (D\mathbf{f}(\mathbf{s}) - \alpha \lambda_i \mathbf{\Gamma}) \zeta_i(t) \quad (5-12)$$

Then, letting $\tilde{\gamma} = \gamma \lambda_i$, and $\tilde{\alpha} = \alpha \lambda_i$ we have that the general equation describing the perturbed dynamics of the synchronous state for any node in the network is given by

$$\dot{\zeta}_s(t) = (\mathbf{I}_n + \tilde{\gamma} \mathbf{\Gamma})^{-1} (D\mathbf{f}(\mathbf{s}) - \tilde{\alpha} \mathbf{\Gamma}) \zeta_s(t) \quad (5-13)$$

Therefore, the local stability of the synchronous solution $\mathbf{s}(t)$ can be addressed computing the Maximum Lyapunov Exponent (MLE) of the variational equation (5-13) as a function of the parameters $\tilde{\alpha}$ and $\tilde{\gamma}$. We denote this MLE value as $\Psi(\tilde{\alpha}, \tilde{\gamma})$, which is also known as Master Stability Function (MSF) [9]. Positive values of $\Psi(\tilde{\alpha}, \tilde{\gamma})$ represent unstable modes, i.e. the networks does not exhibit synchronized motion. Moreover, negative values of $\Psi(\tilde{\alpha}, \tilde{\gamma})$ indicates that the networks exhibit local admissible synchronization.

Note from (5-13), that for $\lambda_1 = 0$ one has that $\tilde{\alpha} = 0$ and $\tilde{\gamma} = 0$. Thus, the variational equation reads $\dot{\zeta}_s(t) = D\mathbf{f}(\mathbf{s})\zeta_s(t)$, and its Lyapunov exponents are equal to those of the single uncoupled system. Hence for the next $N - 1$ nonzero eigenvalues, multiple scenarios where $\Psi(\tilde{\alpha}, \tilde{\gamma})$ intersects the zero plane can be obtained, as the ones presented in Section 2.6.1.

5.1.2. MSF for distributed PI

Here we are interested in networks under distributed PI control. This is, setting $\gamma = 0$ in (5-3). Thus, letting $\mathbf{z}_i(t) = \int_0^t \mathbf{x}_j(\tau) d\tau$ and $\mathbf{w}_i := [\mathbf{x}_i^T(t), \mathbf{z}_i^T(t)]^T$, the closed-loop network dynamics reads

$$\dot{\mathbf{w}}_i(t) = \mathbf{g}(\mathbf{w}_i) - \sum_{j=1}^N \mathcal{L}_{ij} \mathbf{H} \mathbf{w}_j(t), \forall i \in \mathcal{N} \quad (5-14)$$

where $\mathbf{g}(\mathbf{w}_i) := [\mathbf{f}(\mathbf{x}_i)^T, \mathbf{x}_i^T]^T$ and

$$\mathbf{H} := \begin{bmatrix} \alpha \mathbf{\Gamma} & \beta \mathbf{\Gamma} \\ \mathbf{0}_{n \times n} & \mathbf{0}_{n \times n} \end{bmatrix} \quad (5-15)$$

When the network reaches synchronization; this is, $\mathbf{x}_1(t) = \dots = \mathbf{x}_N(t) = \mathbf{s}(t)$, we have that $\dot{\mathbf{s}}(t) = \mathbf{g}(\mathbf{s})$, which in vector form can be written as

$$\begin{bmatrix} \dot{\mathbf{s}}_x(t) \\ \dot{\mathbf{s}}_z(t) \end{bmatrix} = \begin{bmatrix} \mathbf{f}(\mathbf{s}_x) \\ \mathbf{s}_x \end{bmatrix} \quad (5-16)$$

Then, following the MSF approach by studying the perturbed state $\mathbf{s}(t) = \mathbf{w}_i(t) - \boldsymbol{\delta}\mathbf{w}_i(t)$, and using the notation introduced in Section 5.1.1 one has

$$\dot{\Delta}(t) = ((\mathbf{I}_N \otimes D\mathbf{g}(\mathbf{s})) - (\mathcal{L} \otimes \mathbf{H})) \Delta(t) \quad (5-17)$$

Then, using again the state transformation $\zeta(t) = (\mathbf{U}^{-1} \otimes I_n) \Delta(t)$ one has

$$\dot{\zeta}(t) = ((\mathbf{I}_N \otimes D\mathbf{g}(\mathbf{s})) - (\Lambda \otimes \mathbf{H})) \zeta(t) \quad (5-18)$$

note that (5-18) has triangular form with blocks

$$\dot{\zeta}_i(t) = (D\mathbf{g}(\mathbf{s}) - \lambda_i \mathbf{H}) \zeta_i(t), \forall i \in \mathcal{N} \quad (5-19)$$

where λ_i are the eigenvalues of the Laplacian matrix. Then, letting $\tilde{\alpha} = \lambda_i \alpha$ and $\tilde{\beta} = \lambda_i \beta$ we have that the blocks of (5-19) can be represented by the generic dynamics $\zeta_s(t)$ given by

$$\dot{\zeta}_s(t) = \left(D\mathbf{g}(\mathbf{s}) - \begin{bmatrix} \tilde{\alpha} \mathbf{\Gamma} & \tilde{\beta} \mathbf{\Gamma} \\ \mathbb{0}_{n \times n} & \mathbb{0}_{n \times n} \end{bmatrix} \right) \zeta_s(t) \quad (5-20)$$

Similarly to the PD case, the local stability of the synchronous solution $\mathbf{s}(t)$ can be addressed computing the MLE of the variational equation (5-20). Hence, synchronization is guaranteed for the set of values $\tilde{\alpha}$ and $\tilde{\beta}$ such that $\Psi(\tilde{\alpha}, \tilde{\beta})$ remains negative.

Example 10. To illustrate the use of the MSF for PD and PI case, we consider the chaotic Lorenz system introduced in Example 4. Then we compute the MSF for PD and PI control by solving the variational equations (5-13) and (5-20) respectively. The two dimensional representation of the MSF for both cases is depicted in Fig. 5-1 for two different configurations of the output matrix $\mathbf{\Gamma}$.

Setting $\tilde{\gamma} = 0$ we just have distributed proportional control acting among nodes. Then, the MSF coincides with the one depicted in Fig. 2-8. In both cases Fig. 5.1(a) and Fig. 5.1(b), the proportional gain can be considerably reduced by increasing the derivative one, and even can be neglected in the second case where $\mathbf{\Gamma} = \text{diag}\{1, 0, 0\}$. Moreover, when the distributed integral control is deployed together with the proportional one, we have different results (see Fig. 5.1(c) and Fig. 5.1(d)).

This extra degree of freedom provided by the derivative or integral gain can be properly used to optimize the network performance, since low values of the control gains may decrease the control effort required to achieve synchronization. Next, we consider a network of ten Chaotic Lorenz with $\mathbf{\Gamma} = \text{diag}\{1, 0, 0\}$, where its structure is described by the graph depicted in Fig.

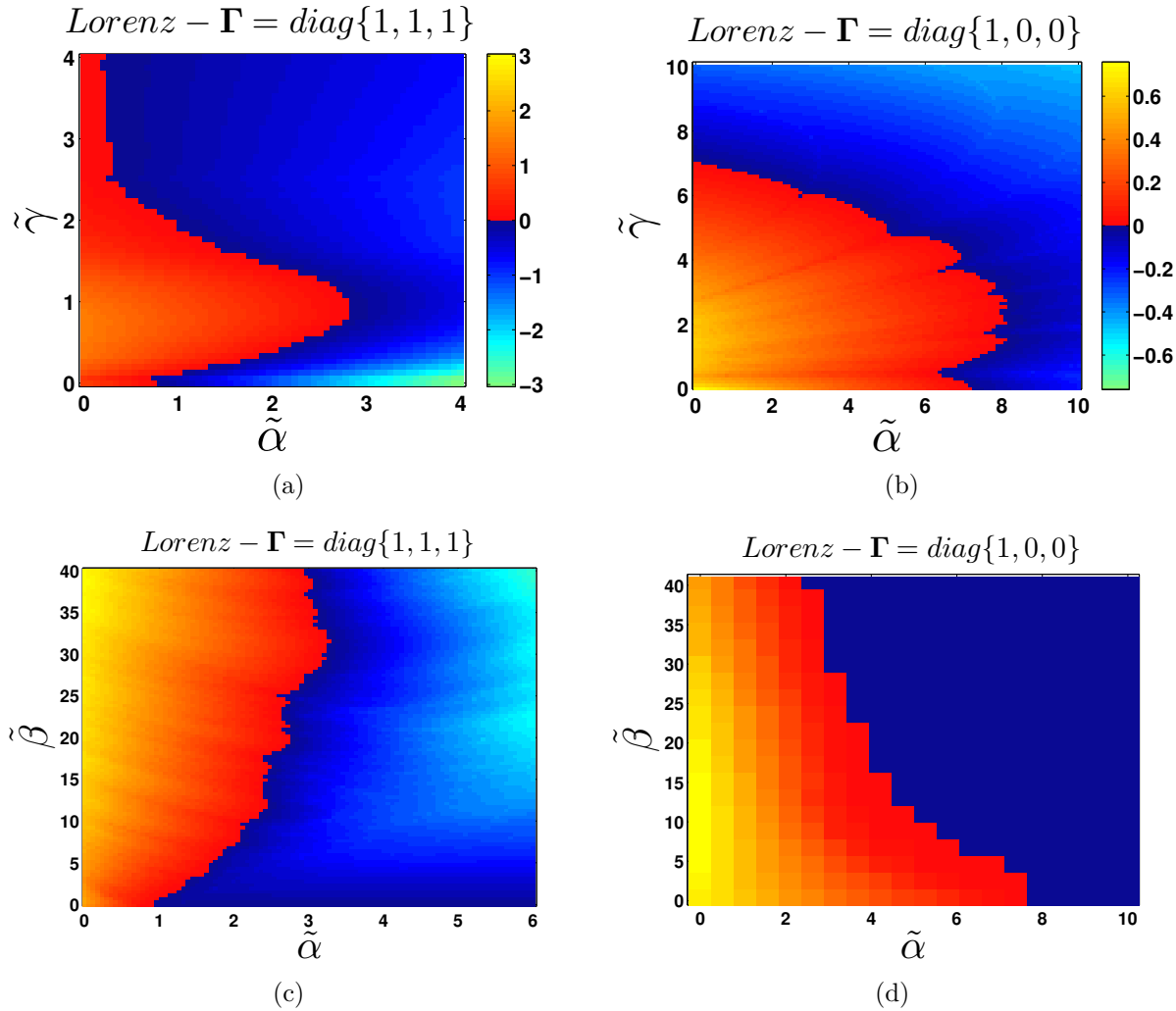


Figure 5-1: Two dimensional representation of the master stability function for Chaotic Lorenz. For each point in the plane corresponds the value of the MSF evaluated at that point, which is represented with different colors. The red-scale colors denote positive values of the MSF, while negative values are represented by the blue-scale. (a)-(b) $\Psi(\tilde{\alpha}, \tilde{\gamma})$ function computed for distributed PD control, (c)-(d) $\Psi(\tilde{\alpha}, \tilde{\beta})$ function computed for PI control.

2.5(a) where $\lambda_2 = 0.233$. Hence, accordingly to the diagram on Fig. 5.1(b), if we choose the point $\tilde{\alpha} = \tilde{\gamma} = 2$ where the MSF is positive (No synchronization), we thus have that $\alpha = \tilde{\alpha}/\lambda_2 = 8.5837$ and $\gamma = \tilde{\gamma}/\lambda_2 = 8.5837$. The time response of the network is shown in Fig. 5.2(a). If instead we set $\tilde{\alpha} = 2$ and $\tilde{\gamma} = 8$ we have that $\gamma = 34.3348$ and the network achieves synchronization as expected (Fig. 5.2(b)). Finally, we change the network structure

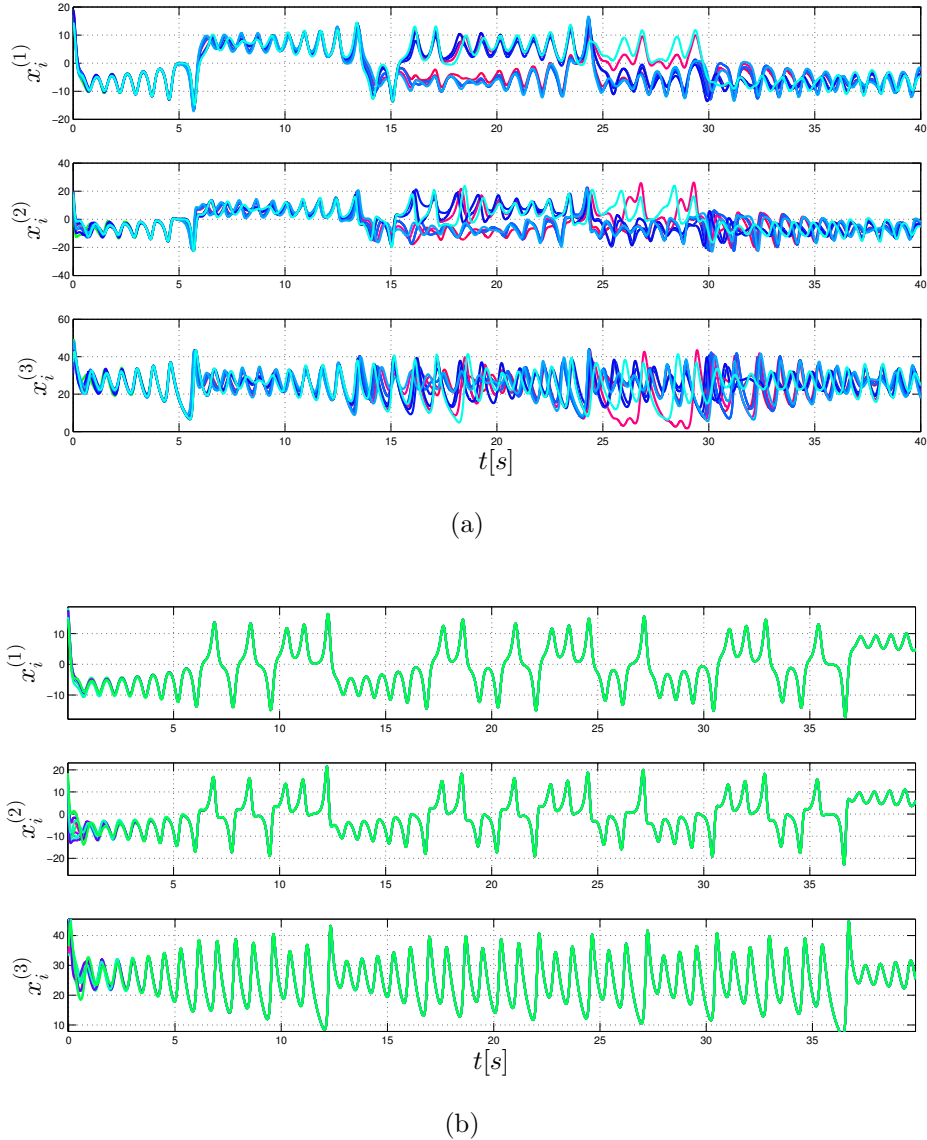


Figure 5-2.: Time response of a network of ten chaotic Lorenz. (a) $\alpha = \beta = 8.58$ (b) $\alpha = 8.58$ and $\gamma = 34.3348$

by the one depicted in Fig. 2.5(c) where $\lambda_2 = 1$. Also, we assume $\Gamma = \text{diag}\{1, 1, 1\}$ and we consider proportional-integral control. Hence, accordingly to diagram Fig. 5.1(c) we have

that setting $\alpha = 1.5$ and $\beta = 8$ the network does not exhibit local admissible synchronization as shown in Fig. 5.3(a). While selecting $\alpha = 1.5$ and $\beta = 0.5$ the network synchronizes (see Fig. 5.3(b)). Note that, varying the network structure via λ_2 affects the value of the control gains, and it suggest that there may exist an optimal network structure and values of the control gains, such that the network synchronize using minimum control energy.

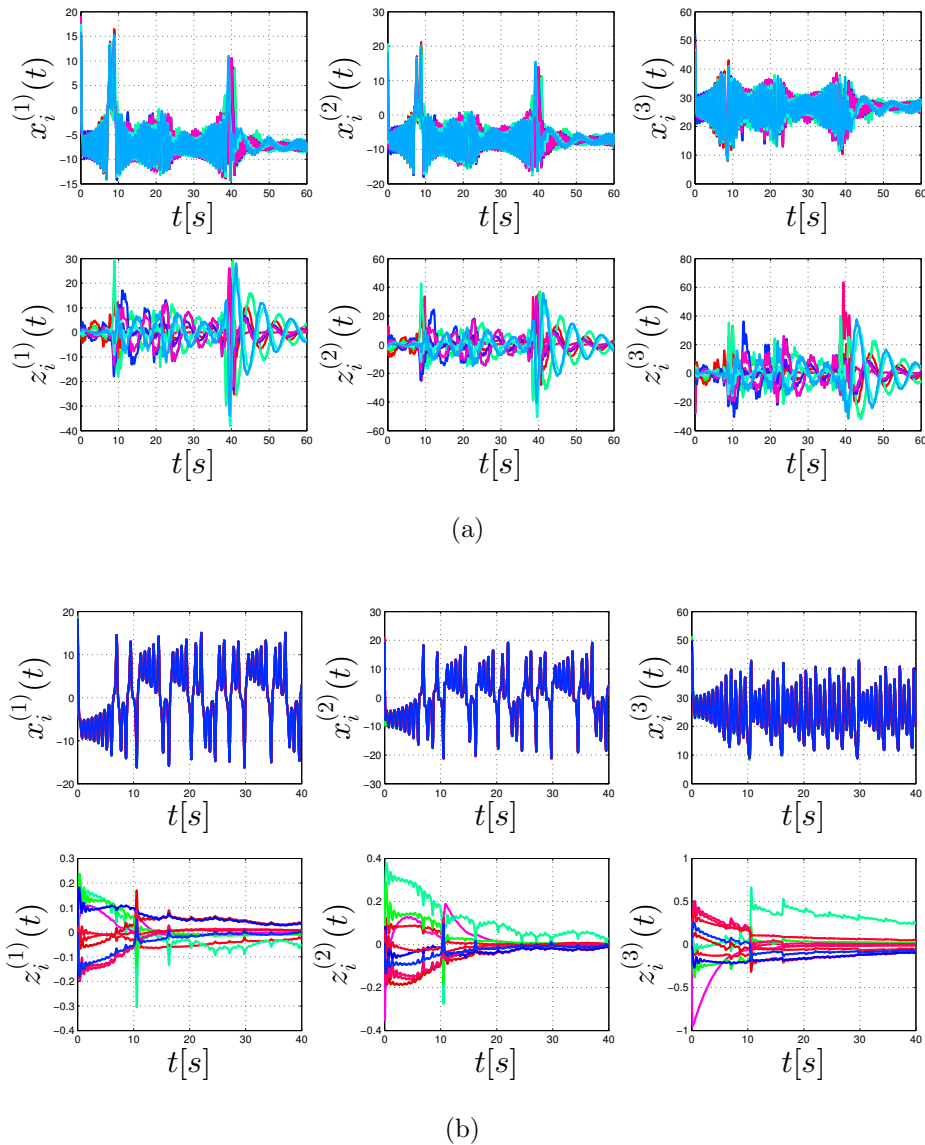


Figure 5-3.: Time response of a network of ten chaotic Lorenz. (a) $\alpha = 1.5$ and $\beta = 8$ (b) $\alpha = 1.5$ and $\beta = 0.5$

5.2. Global stability analysis

In the last section we have shown that the distributed derivative and integral action, affects the synchronization region of the network in the parameter space. Those results were obtained using the MSF; however, they are valid for a sufficiently small neighborhood of the synchronous state. In this section we are interested in providing conditions to guarantee global synchronization for PD and PI controlled networks. The conditions of global synchronization are derived under some assumptions in the nonlinear vector-fields and output matrix Γ of each unit.

5.2.1. Distributed PD control

Consider the closed-loop network (5-8). Define the disagreement dynamics as

$$\delta \mathbf{x}_i(t) = \mathbf{x}_i(t) - \hat{\mathbf{x}}(t), \hat{\mathbf{x}}(t) = \frac{1}{N} \sum_{k=1}^N \mathbf{x}_k(t), \forall i \in \mathcal{N} \quad (5-21)$$

then, one has that

$$\dot{\delta \mathbf{x}}_i(t) = -\alpha \sum_{j=1}^N \mathcal{P}_{ij} \delta \mathbf{x}_j(t) + \sum_{j=1}^N \tilde{\mathcal{L}}_{ij} \mathbf{f}(\mathbf{x}_j) - \frac{1}{N} \sum_{j=1}^N \mathbf{f}(\mathbf{x}_j), \forall i \in \mathcal{N} \quad (5-22)$$

and letting $\Delta_x(t) := [\delta \mathbf{x}_1^T(t), \dots, \delta \mathbf{x}_N^T(t)]^T$, we have that the disagreement dynamics of the whole network is

$$\dot{\Delta}_x(t) = -\alpha \mathcal{P} \Delta_x(t) + \tilde{\mathcal{L}}^{-1} \mathbf{F}(\mathbf{x}) - \frac{1}{N} (\mathbb{1}_N \mathbb{1}_N^T \otimes \mathbf{I}_n) \mathbf{F}(\mathbf{x}) \quad (5-23)$$

Therefore, the problem becomes that of finding conditions on $\mathbf{f}(\cdot)$, Γ and the control parameters, α , γ and \mathcal{L} such that the zero equilibrium of (5-23) remains globally asymptotically stable. Then, we require some assumptions in the vector-fields as well as derive some properties for the disagreement dynamics, that will be particularly useful for both PD and PI cases.

Definition 5.2.1. (*Lipchitz and QUAD conditions*) A function $\mathbf{f}(\mathbf{x}, t) : \mathbb{R}^n \times \mathbb{R}^+ \cup \{0\} \mapsto \mathbb{R}^n$ is called Lipchitz if there exist a positive constant μ such that

$$\|\mathbf{f}(\mathbf{x}, t) - \mathbf{f}(\mathbf{y}, t)\| \leq \mu \|\mathbf{x} - \mathbf{y}\|, \forall \mathbf{x}, \mathbf{y} \in \mathbb{R}^n; \forall t \geq 0 \quad (5-24)$$

if instead there exist a diagonal matrix $\mathbf{D} = \text{diag}\{d_1, \dots, d_n\}$, and a positive constant ε such that

$$(\mathbf{x} - \mathbf{y})^T (\mathbf{f}(\mathbf{x}, t) - \mathbf{f}(\mathbf{y}, t) - \mathbf{D}(\mathbf{x} - \mathbf{y})) \leq -\varepsilon (\mathbf{x} - \mathbf{y})^T (\mathbf{x} - \mathbf{y}), \forall \mathbf{x}, \mathbf{y} \in \mathbb{R}^n; \forall t \geq 0 \quad (5-25)$$

we say that the function $\mathbf{f}(\cdot)$ is QUAD(ε, \mathbf{D}).

Proposition 5.2.1. Consider the quantity $\mathbf{x} := (\boldsymbol{\Pi} \otimes \mathbf{I}_n)\mathbf{y}$ where, the matrix $\boldsymbol{\Pi} \in \Omega$ is defined as $\boldsymbol{\Pi} := \mathbf{I}_N - (1/N)\mathbf{1}_N\mathbf{1}_N^T$ and the vectors $\mathbf{x}, \mathbf{y} \in \mathbb{R}^{nN \times 1}$ are given by $\mathbf{x} := [\mathbf{x}_1^T, \dots, \mathbf{x}_N^T]^T$, and $\mathbf{y} := [\mathbf{y}_1^T, \dots, \mathbf{y}_N^T]^T$ with $\mathbf{x}_i, \mathbf{y}_i \in \mathbb{R}^{n \times 1}, \forall i \in \mathcal{N}$. The following expressions holds:

$$\mathbf{x}^T \mathbf{1}_{nN} = \sum_{i=1}^N \sum_{j=1}^N \boldsymbol{\Pi}_{ij} \mathbf{y}_j = 0 \quad (5-26)$$

$$\mathbf{x}^T (\mathbf{1}_N \otimes \boldsymbol{\zeta}) = \sum_{i=1}^N \mathbf{y}_i^T \sum_{j=1}^N \boldsymbol{\Pi}_{ij} \boldsymbol{\zeta} = 0, \forall \boldsymbol{\zeta} \in \mathbb{R}^n \quad (5-27)$$

$$\mathbf{x}^T (\mathbf{1}_N \mathbf{1}_N^T \otimes \mathbf{I}_n) = \mathbf{0}_{1 \times nN} \quad (5-28)$$

Proof. Since $\boldsymbol{\Pi} \in \Omega$ one has that $\boldsymbol{\Pi}\mathbf{1}_N = \mathbf{0}_{(1 \times N)}$; therefore, relations (5-26) and (5-27) are easily verifiable. Besides, from the definition we have that $\mathbf{x} = (\boldsymbol{\Pi} \otimes \mathbf{I}_n)\mathbf{y}$ and substituting in (5-28) yields $(\mathbf{1}_N \mathbf{1}_N^T \boldsymbol{\Pi} \otimes \mathbf{I}_n)\mathbf{y} = \mathbf{0}_{1 \times nN}$. \square

Theorem 5.2.1. A network of identical nonlinear units (5-1) satisfying the QUAD(ε, \mathbf{D}) assumption and controlled by a distributed PD strategy with $\gamma > 0$, reaches global admissible synchronization if the diagonal matrix $\mathbf{D} - \alpha \lambda_2 \boldsymbol{\Gamma}$ is negative definite.

Proof. Let's consider the candidate Lyapunov function

$$V = \frac{1}{2} \boldsymbol{\Delta}_x^T(t) \tilde{\mathcal{L}} \boldsymbol{\Delta}_x(t)$$

where $\tilde{\mathcal{L}}$ is a symmetric positive-definite matrix. This can be easily seen from (5-7) where all the eigenvalues of $\tilde{\mathcal{L}}$ are positive. Hence, V is a positive definite and radially unbounded function. Then, deriving V along the trajectories of (5-23) one has

$$\dot{V} = \boldsymbol{\Delta}_x^T(t) (-\alpha (\mathcal{L} \otimes \boldsymbol{\Gamma}) \boldsymbol{\Delta}_x(t) + \mathbf{F}(\mathbf{x}) - (1/N)(\mathbf{1}_N^T \mathbf{1}_N \otimes \mathbf{I}_n) \mathbf{F}(\mathbf{x})) \quad (5-29)$$

Moreover, from (5-21) we can write $\boldsymbol{\Delta}_x(t) := (\boldsymbol{\Pi} \otimes \mathbf{I}_n)\mathbf{x}(t)$; hence, using property (5-28), we have that $\boldsymbol{\Delta}_x^T(t)(\mathbf{1}_N \mathbf{1}_N^T \otimes \mathbf{I}_n)\mathbf{F}(\mathbf{x}) = \mathbf{0}_{1 \times nN}$. Furthermore, setting $\boldsymbol{\zeta} = \mathbf{f}(\hat{\mathbf{x}})$ in (5-27) one has $\boldsymbol{\Delta}_x^T(t)(\mathbf{1}_N \otimes \mathbf{f}(\hat{\mathbf{x}})) = 0$. Therefore, (5-29) can be recast as

$$\dot{V} = -\alpha \boldsymbol{\Delta}_x^T(t) (\mathcal{L} \otimes \boldsymbol{\Gamma}) \boldsymbol{\Delta}_x(t) + \boldsymbol{\Delta}_x^T(t) (\mathbf{F}(\mathbf{x}) - (\mathbf{1}_N \otimes \mathbf{f}(\hat{\mathbf{x}}))) \quad (5-30)$$

Letting $\mathbf{D} := \text{diag}\{d_1, \dots, d_n\}$, and adding and subtracting the term $\boldsymbol{\Delta}_x^T(t)(\mathbf{I}_N \otimes \mathbf{D})\boldsymbol{\Delta}_x(t)$ in (5-30) yields $\dot{V} = V_1 + V_2$, where

$$V_1 = \boldsymbol{\Delta}_x^T(t) (\mathbf{F}(\mathbf{x}) - (\mathbf{1}_N \otimes \mathbf{f}(\hat{\mathbf{x}}))) - (\mathbf{I}_N \otimes \mathbf{D})\boldsymbol{\Delta}_x(t) \quad (5-31)$$

$$V_2 = -\alpha \boldsymbol{\Delta}_x^T(t) (\mathcal{L} \otimes \boldsymbol{\Gamma}) \boldsymbol{\Delta}_x(t) + \boldsymbol{\Delta}_x^T(t)(\mathbf{I}_N \otimes \mathbf{D})\boldsymbol{\Delta}_x(t) \quad (5-32)$$

It follows that V_1 can be written as

$$V_1 = \sum_{i=1}^N (\mathbf{x}_i(t) - \hat{\mathbf{x}}(t))^T (\mathbf{f}(\mathbf{x}_i) - \mathbf{f}(\hat{\mathbf{x}}) - \mathbf{D}(\mathbf{x}_i(t) - \hat{\mathbf{x}}(t))) \quad (5-33)$$

from the assumption we know that $\mathbf{f}(\mathbf{x}_i)$ is QUAD(ε, \mathbf{D}); therefore,

$$\begin{aligned} V_1 &\leq -\varepsilon \sum_{i=1}^N (\mathbf{x}_i(t) - \hat{\mathbf{x}}(t))^T (\mathbf{x}_i(t) - \hat{\mathbf{x}}(t)) \\ &\leq -\varepsilon \Delta_x^T(t) \Delta_x(t) < 0 \end{aligned} \quad (5-34)$$

Now, for the linear term V_2 , we define a new state $\tilde{\Delta}(t) := (\mathbf{U}^T \otimes \mathbf{I}_n) \Delta_x(t)$ where

$$\tilde{\Delta}(t) := [\tilde{\delta \mathbf{x}}_1^T(t), \dots, \tilde{\delta \mathbf{x}}_N^T(t)]^T$$

Remember that \mathbf{U} is an orthonormal matrix which is composed by the eigenvectors of \mathcal{L} (see Lemma 2.2.1). Note that the eigenvector corresponding to the null eigenvalue of the Laplacian matrix is $\mathbf{u}_1 = (1/\sqrt{N}) \mathbb{1}_N^T$; consequently

$$\tilde{\delta \mathbf{x}}_1(t) = (1/N)(\mathbb{1}_N^T \otimes \mathbf{I}_n) \Delta_x(t) = (1/N)(\mathbb{1}_N^T \otimes \mathbf{I}_n)(\mathbf{\Pi} \otimes \mathbf{I}_n) \mathbf{x}(t) = \mathbf{0}_{n \times 1}$$

Then, neglecting this trivial state and letting $\bar{\Delta}(t) := [\tilde{\delta \mathbf{x}}_2^T(t), \dots, \tilde{\delta \mathbf{x}}_N^T(t)]^T$ and $\bar{\Lambda} := \text{diag}\{\lambda_2, \dots, \lambda_N\}$ yields

$$V_2 = \bar{\Delta}^T(t) ((\mathbf{I}_N \otimes \mathbf{D}) - \alpha(\bar{\Lambda} \otimes \mathbf{\Gamma})) \bar{\Delta}(t) \quad (5-35)$$

note that (5-35) is a block-diagonal matrix, with blocks $\mathbf{D} - \alpha \lambda_k \mathbf{\Gamma}$ for $k \in \{2, \dots, N\}$. Since $-\lambda_2$ is the largest eigenvalue of $-\bar{\Lambda}$; then, for \dot{V} to be negative definite it suffices that the diagonal matrix $\mathbf{D} - \alpha \lambda_2 \mathbf{\Gamma} \prec 0$, which concludes the proof.

□

Remark 5.2.1. Note that the condition for Global Admissible Synchronization in Theorem 5.2.1 is independent of the derivative gain γ . The condition is in fact the same obtained for the proportional case [47, 44]. This suggests that the underlying distributed proportional control, provides an conservative estimation for the PD one.

To find synchronization conditions explicitly depending on the derivative gain γ , we have to assume stronger conditions on the vector field $\mathbf{f}(\cdot)$ and the output matrix $\mathbf{\Gamma}$

Theorem 5.2.2. Under distributed PD control, a network of nonlinear units (5-1) with Lipschitz vector fields and with $\mathbf{\Gamma} = \mathbf{I}_n$, reaches global admissible synchronization if

$$\alpha > \frac{\mu(\gamma \lambda_2 + 1)}{\lambda_2} \quad (5-36)$$

Proof. Let's consider the Lyapunov function candidate

$$V = \frac{1}{2} \Delta_x^T(t) \Delta_x(t)$$

which is positive definite and radially unbounded. Then, by differentiating V along the trajectories of (5-23) one has

$$\dot{V} = \Delta_x^T(t) (-\alpha \mathcal{P} \Delta_x(t) + \tilde{\mathcal{L}}^{-1} \mathbf{F}(\mathbf{x}) - (1/N) (\mathbb{1}_N^T \mathbb{1}_N \otimes \mathbf{I}_n) \mathbf{F}(\mathbf{x})) \quad (5-37)$$

Moreover, from (5-5) we have that $\tilde{\mathcal{L}}^{-1} \mathbb{1}_{nN} = \mathbb{1}_{nN}$, and using property (5-27) we can write $\Delta_x^T(t) \tilde{\mathcal{L}}^{-1} (\mathbb{1}_N \otimes \mathbf{f}(\hat{\mathbf{x}})) = 0$. It follows also from property (5-27) and (5-28) that the quantity $\Delta_x^T(t) (\mathbb{1}_N \otimes \mathbf{f}(\hat{\mathbf{x}})) = 0$, and $\Delta_x^T(t) (\mathbb{1}_N^T \mathbb{1}_N \otimes \mathbf{I}_n) \mathbf{F}(\mathbf{x}) = \mathbb{0}_{1 \times nN}$ (see the proof of Theorem 5.2.1). Therefore, we can recast (5-37) as $\dot{V} = V_1 + V_2$, where

$$V_1 = \Delta_x^T(t) \tilde{\mathcal{L}}^{-1} (\mathbf{F}(\mathbf{x}) - (\mathbb{1}_N \otimes \mathbf{f}(\hat{\mathbf{x}}))) \quad (5-38)$$

$$V_2 = -\alpha \Delta_x^T(t) \mathcal{P} \Delta_x(t) \quad (5-39)$$

Now, we proceed to find linear upper-bounds for each one of the terms on (5-38) and (5-39). Hence, first we have that $V_1 \leq \|\Delta_x(t)\| \|\tilde{\mathcal{L}}^{-1}\| \|(\mathbf{F}(\mathbf{x}) - (\mathbb{1}_N \otimes \mathbf{f}(\hat{\mathbf{x}})))\|$. Thus, using Lemma 2.4.1 and (5-7), we have that $\|\tilde{\mathcal{L}}^{-1}\| = \max_i \left\{ |\lambda_i(\tilde{\mathcal{L}}^{-1})| \right\} = \max_i \{ |\lambda_i(\Sigma^{-1})| \} = 1$. Next, from triangular inequality we have $\|\Delta_x(t)\| \leq \zeta$, where $\zeta := \sum_{k=1}^N \|\delta \mathbf{x}_k\|$; hence, (5-38) can be recast as

$$\begin{aligned} V_1 &\leq \zeta \|(\mathbf{F}(\mathbf{x}) - (\mathbb{1}_N \otimes \mathbf{f}(\hat{\mathbf{x}})))\| \\ &\leq \zeta \sum_{i=1}^N \|\mathbf{f}(\mathbf{x}_i) - \mathbf{f}(\hat{\mathbf{x}})\| \end{aligned}$$

from the assumption we know that $\mathbf{f}(\mathbf{x}_i)$ is Lipchitz; therefore, $\|\mathbf{f}(\mathbf{x}_i) - \mathbf{f}(\hat{\mathbf{x}})\| \leq \mu \|(\mathbf{x}_i(t) - \hat{\mathbf{x}}(t))\|$ and one gets $V_1 \leq \mu \zeta^2$.

Moreover, for V_2 , we have that

$$\mathcal{P} = \tilde{\mathcal{L}}^{-1} (\mathcal{L} \otimes \Gamma) = (\mathbf{U} \otimes \mathbf{I}_n) \Sigma^{-1} (\Lambda \otimes \mathbf{I}_n) (\mathbf{U}^T \otimes \mathbf{I}_n)$$

Note that the matrix $\Sigma^{-1} (\Lambda \otimes \mathbf{I}_n)$ is a block diagonal matrix with diagonal blocks given by

$$\Sigma^{-1} (\Lambda \otimes \mathbf{I}_n) = \text{diag} \left\{ \mathbb{0}_{n \times n}, \frac{\lambda_2}{1 + \lambda_2 \gamma} \mathbf{I}_n, \dots, \frac{\lambda_N}{1 + \lambda_N \gamma} \mathbf{I}_n \right\}$$

therefore, V_2 can be upper-bounded by

$$\begin{aligned} V_2 &\leq -\alpha \left(\min_{\Delta_x^T \mathbb{1}_{nN} = 0, \Delta_x \neq 0} \mathcal{P} \right) \Delta_x^T(t) \Delta_x(t) \\ &\leq -\frac{\alpha \lambda_2}{\gamma \lambda_2 + 1} \|\Delta_x(t)\|^2 \\ &\leq -\frac{\alpha \lambda_2}{\gamma \lambda_2 + 1} \zeta^2 \end{aligned}$$

Thus, we can recast (5-37) as

$$\dot{V} \leq \left(\mu - \frac{\alpha \lambda_2}{\gamma \lambda_2 + 1} \right) \zeta^2$$

and $\dot{V} < 0$ if condition (5-36) is fulfilled. \square

From condition (5-36) we have that the proportional gain α , is directly proportional to the derivative gain γ . This can be seen in Fig. 5-4, where the slope of the line dividing the blue (synchronization) and red (No synchronization) regions depends on the Lipschitz constant μ and the network structure via λ_2 . Note that, the proportional gain cannot be decreased by

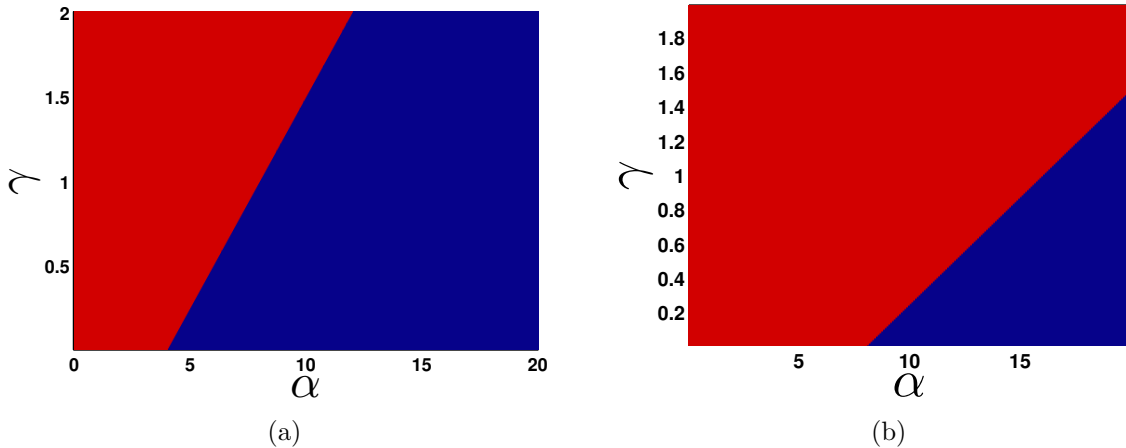


Figure 5-4.: Estimated regions of global synchronization of networks controlled by distributed PD, using (5-36) with $\lambda_2 = 1$ and (a) $\mu = 4$, (b) $\mu = 8$. The blue color, denotes the region where (5-36) is satisfied and red color otherwise.

increasing the derivative one as shown in the local stability analysis early in this Chapter. For example in Fig. 5.1(d) the synchronization regions for the PD case present complex shapes. The estimation obtained using Lyapunov theory is conservative and it provides a linear upper-bound of the synchronization region. We will discuss this fact more in detail in the next Section using Chua's circuits. Moreover, a better approximation of the synchronization region could be obtained by considering different Lyapunov functions to prove that the zero equilibrium of the disagreement dynamics (5-23) is globally asymptotically stable.

5.2.2. Distributed PI control

Here we consider the closed-loop network given in (5-14), then we can write

$$\begin{bmatrix} \dot{\mathbf{x}}_i(t) \\ \dot{\mathbf{z}}_i(t) \end{bmatrix} = \begin{bmatrix} \mathbf{f}(\mathbf{x}_i) \\ \mathbf{x}_i \end{bmatrix} + \begin{bmatrix} -\alpha \sum_{j=1}^N \mathcal{L}_{ij} \boldsymbol{\Gamma} & -\beta \sum_{j=1}^N \mathcal{L}_{ij} \boldsymbol{\Gamma} \\ \mathbb{0}_{n \times n} & \mathbb{0}_{n \times n} \end{bmatrix} \begin{bmatrix} \mathbf{x}_j(t) \\ \mathbf{z}_j(t) \end{bmatrix} \quad (5-40)$$

now, using the disagreement dynamics defined in (5-21) together with

$$\delta \mathbf{z}_i(t) = \mathbf{z}_i(t) - \hat{\mathbf{z}}(t), \hat{\mathbf{z}}(t) = \frac{1}{N} \sum_{k=1}^N \mathbf{z}_k(t), \forall i \in \mathcal{N} \quad (5-41)$$

one has

$$\begin{bmatrix} \dot{\delta \mathbf{x}}_i(t) \\ \dot{\delta \mathbf{z}}_i(t) \end{bmatrix} = \begin{bmatrix} \mathbf{f}(\mathbf{x}_i) - (1/N) \sum_{k=1}^N \mathbf{f}(\mathbf{x}_k)(t) \\ \delta \mathbf{x}_i \end{bmatrix} + \begin{bmatrix} -\alpha \sum_{j=1}^N \mathcal{L}_{ij} \boldsymbol{\Gamma} & -\beta \sum_{j=1}^N \mathcal{L}_{ij} \boldsymbol{\Gamma} \\ \mathbb{0}_{n \times n} & \mathbb{0}_{n \times n} \end{bmatrix} \begin{bmatrix} \delta \mathbf{x}_j(t) \\ \delta \mathbf{z}_j(t) \end{bmatrix} \quad (5-42)$$

thus, considering $\boldsymbol{\Gamma} = \mathbf{I}_n$ and defining the block matrix

$$\boldsymbol{\mathcal{Q}} := \begin{bmatrix} -\alpha \boldsymbol{\mathcal{L}} & -\beta \boldsymbol{\mathcal{L}} \\ \mathbf{I}_N & \mathbb{0}_{N \times N} \end{bmatrix}$$

the network disagreement dynamics can be recast as

$$\begin{bmatrix} \dot{\Delta}_x(t) \\ \dot{\Delta}_z(t) \end{bmatrix} = \begin{bmatrix} \mathbf{F}(\mathbf{x}) - (1/N)(\mathbb{1}_N \mathbb{1}_N^T \otimes \mathbf{I}_n) \mathbf{F}(\mathbf{X}) \\ \mathbb{0}_{(nN \times 1)} \end{bmatrix} + (\boldsymbol{\mathcal{Q}} \otimes \mathbf{I}_n) \begin{bmatrix} \Delta_x(t) \\ \Delta_z(t) \end{bmatrix} \quad (5-43)$$

where $\Delta_z(t) := [\delta \mathbf{z}_1^T(t), \dots, \delta \mathbf{z}_N^T(t)]^T$.

Theorem 5.2.3. *Under distributed PI control, a network of nonlinear units (5-1) satisfying Lipschitz condition with $\boldsymbol{\Gamma} = \mathbf{I}_n$, achieves admissible synchronization if the following condition holds*

$$\alpha > 1 + \mu \frac{1}{\lambda_2} + \frac{\mu^2}{4\beta} \frac{\lambda_N^2}{\lambda_2^3} \quad (5-44)$$

Proof. Following [80], we consider the candidate Lyapunov function

$$V(\Delta_x, \Delta_z) = \frac{1}{2} \begin{bmatrix} \Delta_x^T & \Delta_z^T \end{bmatrix} (\boldsymbol{\mathcal{R}} \otimes \mathbf{I}_n) \begin{bmatrix} \Delta_x \\ \Delta_z \end{bmatrix} \quad (5-45)$$

where,

$$\boldsymbol{\mathcal{R}} = \begin{bmatrix} \mathbf{I}_N & \boldsymbol{\mathcal{L}} \\ \boldsymbol{\mathcal{L}} & \beta \boldsymbol{\mathcal{L}} + \alpha \boldsymbol{\mathcal{L}}^2 \end{bmatrix}$$

We split the proof into two stages. Firstly, we will show that the candidate Lyapunov function $V(\Delta_x, \Delta_z)$ is indeed a positive definite radially unbounded function. Secondly, we provide conditions under which the function \dot{V} is negative definite.

Step 1: To show that $V > 0$, we consider two new states given by $\tilde{\Delta}_x^T := (\mathbf{U}^T \otimes \mathbf{I}_n)\Delta_x^T$ and $\tilde{\Delta}_z^T := (\mathbf{U}^T \otimes \mathbf{I}_n)\Delta_z^T$. For the eigenvector $\mathbf{u}_1 = (1/\sqrt{N})\mathbf{1}_N^T$ corresponding to the null eigenvalue of \mathcal{L} we have that $\tilde{\delta}\mathbf{x}_1(t) := ((1/N)\mathbf{1}_N^T \otimes \mathbf{I}_n)\Delta_x(t) = \mathbf{0}_{n \times 1}$ and $\tilde{\delta}\mathbf{z}_1(t) := ((1/N)\mathbf{1}_N^T \otimes \mathbf{I}_n)\Delta_z(t) = \mathbf{0}_{n \times 1}$. Hence, neglecting those trivial states we can recast the candidate Lyapunov function as

$$V = \frac{1}{2} \left[\begin{array}{cc} \tilde{\Delta}_x^T & \tilde{\Delta}_z^T \end{array} \right] \underbrace{\begin{bmatrix} \mathbf{I}_{N-1} & \bar{\Lambda} \\ \bar{\Lambda} & \beta\bar{\Lambda} + \alpha\bar{\Lambda}^2 \end{bmatrix}}_{\mathbf{A}} \left[\begin{array}{c} \tilde{\Delta}_x^T \\ \tilde{\Delta}_z^T \end{array} \right]$$

where $\tilde{\Delta}_x^T := [\tilde{\delta}\mathbf{x}_2^T(t), \dots, \tilde{\delta}\mathbf{x}_N^T(t)]^T$, $\tilde{\Delta}_z^T := [\tilde{\delta}\mathbf{z}_2^T(t), \dots, \tilde{\delta}\mathbf{z}_N^T(t)]^T$, and $\bar{\Lambda} := \text{diag}\{\lambda_2, \dots, \lambda_N\}$. Hence, from Proposition 2.4.2 we have that $\mathbf{A} \succ 0$ if

$$((\alpha - 1)\lambda_k + \beta\lambda_k) \lambda_k^2 > 0, \quad k = \{2, \dots, N\}$$

From the assumption, we have that the graph is connected so that the eigenvalues λ_k of \mathcal{L} are non-negative quantities; therefore, choosing $\alpha > 1$ one has that $V(\Delta_x, \Delta_z)$ is always a positive definite function.

Step 2: Next, differentiating (5-45) along the trajectories of (5-43) we obtain

$$\dot{V}(\Delta_x, \Delta_z) = V_1(\Delta_x, \Delta_z) + V_2(\Delta_x, \Delta_z)$$

where

$$V_1(\Delta_x, \Delta_z) = \left[\begin{array}{cc} \Delta_x^T & \Delta_z^T \end{array} \right] (\mathcal{R}\mathcal{Q} \otimes \mathbf{I}_n) \left[\begin{array}{c} \Delta_x(t) \\ \Delta_z(t) \end{array} \right] \quad (5-46)$$

$$V_2(\Delta_x, \Delta_z) = \left[\begin{array}{cc} \Delta_x^T & \Delta_z^T \end{array} \right] (\mathcal{R} \otimes \mathbf{I}_n) \left[\begin{array}{c} \mathbf{F}(\mathbf{x}) - (1/N)(\mathbf{1}_N \mathbf{1}_N^T \otimes \mathbf{I}_n)\mathbf{F}(\mathbf{x}) \\ \mathbf{0}_{(nN \times 1)} \end{array} \right] \quad (5-47)$$

Next, we rewrite V_1 as

$$V_1 = \frac{1}{2} \left[\begin{array}{cc} \Delta_x^T & \Delta_z^T \end{array} \right] (\mathcal{R}\mathcal{Q} + \mathcal{Q}^T\mathcal{R} \otimes \mathbf{I}_n) \left[\begin{array}{c} \Delta_x(t) \\ \Delta_z(t) \end{array} \right]$$

Then, it follows that

$$\begin{aligned} \mathcal{R}\mathcal{Q} + \mathcal{Q}^T\mathcal{R} &= \left[\begin{array}{cc} \mathbf{I}_N & \mathcal{L} \\ \mathcal{L} & \beta\mathcal{L} + \alpha\mathcal{L}^2 \end{array} \right] \left[\begin{array}{cc} -\alpha\mathcal{L} & -\beta\mathcal{L} \\ \mathbf{I}_N & \mathbf{0} \end{array} \right] + \left[\begin{array}{cc} -\alpha\mathcal{L} & \mathbf{I}_N \\ -\beta\mathcal{L} & \mathbf{0} \end{array} \right] \left[\begin{array}{cc} \mathbf{I}_N & \mathcal{L} \\ \mathcal{L} & \beta\mathcal{L} + \alpha\mathcal{L}^2 \end{array} \right] \\ &= -2 \left[\begin{array}{cc} (\alpha - 1)\mathcal{L} & \mathbf{0}_{N \times N} \\ \mathbf{0}_{N \times N} & \beta\mathcal{L}^2 \end{array} \right] \end{aligned}$$

Hence, letting $\zeta := \sum_{k=1}^N \|\delta \mathbf{x}_k\|$, and $\xi := \sum_{k=1}^N \|\delta \mathbf{z}_k\|$, we can rewrite V_1 as

$$\begin{aligned} V_1 &= - \left[\begin{array}{cc} \Delta_x^T & \Delta_z^T \end{array} \right] \left[\begin{array}{cc} (\alpha - 1)\mathcal{L} & \emptyset \\ \emptyset & \beta\mathcal{L}^2 \end{array} \right] \otimes \mathbf{I}_n \left[\begin{array}{c} \Delta_x(t) \\ \Delta_z(t) \end{array} \right] \\ &= -(\alpha - 1)\Delta_x^T(\mathcal{L} \otimes \mathbf{I}_n)\Delta_x - \beta\Delta_z^T(\mathcal{L}^2 \otimes \mathbf{I}_n)\Delta_z \\ &\leq -(\alpha - 1)\lambda_2\Delta_x^T\Delta_x - \beta\lambda_2^2\Delta_z^T\Delta_z \\ &\leq -(\alpha - 1)\lambda_2 \|\Delta_x\|^2 - \beta\lambda_2^2 \|\Delta_z\|^2 \\ &\leq -(\alpha - 1)\lambda_2\zeta^2 - \beta\lambda_2^2\xi^2 \end{aligned} \tag{5-48}$$

Moreover, from (5-47) we have that

$$\begin{aligned} V_2 &= \Delta_x^T \mathbf{F}(\mathbf{x}) - \frac{1}{N} \Delta_x^T (\mathbb{1}_N \mathbb{1}_N^T \otimes \mathbf{I}_n) \mathbf{F}(\mathbf{x}) + \Delta_z^T (\mathcal{L} \otimes \mathbf{I}_n) \mathbf{F}(\mathbf{x}) \\ &\quad - \frac{1}{N} \Delta_z^T (\mathcal{L} \otimes \mathbf{I}_n) (\mathbb{1}_N \mathbb{1}_N^T \otimes \mathbf{I}_n) \mathbf{F}(\mathbf{x}) \end{aligned}$$

It follows from (5-28) that

$$\Delta_x^T (\mathbb{1}_N \mathbb{1}_N^T \otimes \mathbf{I}_n) = \Delta_z^T (\mathbb{1}_N \mathbb{1}_N^T \otimes \mathbf{I}_n) = \emptyset_{1 \times nN}$$

and from the fact that $\mathcal{L} \in \Omega$ one has

$$(\mathcal{L} \otimes \mathbf{I}_n) (\mathbb{1}_N \mathbb{1}_N^T \otimes \mathbf{I}_n) = \emptyset_{nN \times nN}$$

hence, $V_2 = \Delta_x^T \mathbf{F}(\mathbf{x}) + \Delta_z^T (\mathcal{L} \otimes \mathbf{I}_n) \mathbf{F}(\mathbf{x})$. From property (5-27) we know that $\Delta_x^T (\mathbb{1}_N \otimes \mathbf{f}(\hat{\mathbf{x}})) = \emptyset_{1 \times nN}$ and $(\mathcal{L} \otimes \mathbf{I}_n) (\mathbb{1}_N \otimes \mathbf{f}(\hat{\mathbf{x}})) = \emptyset_{nN \times nN}$; therefore, V_2 can be recast as

$$\begin{aligned} V_2 &= \Delta_x^T (\mathbf{F}(\mathbf{x}) - (\mathbb{1}_N \otimes \mathbf{f}(\hat{\mathbf{x}}))) + \Delta_z^T (\mathcal{L} \otimes \mathbf{I}_n) (\mathbf{F}(\mathbf{x}) - (\mathbb{1}_N \otimes \mathbf{f}(\hat{\mathbf{x}}))) \\ &\leq \|\Delta_x^T\| \|\mathbf{F}(\mathbf{x}) - (\mathbb{1}_N \otimes \mathbf{f}(\hat{\mathbf{x}}))\| + \|\Delta_z^T\| \|\mathcal{L}\| \|\mathbf{F}(\mathbf{x}) - (\mathbb{1}_N \otimes \mathbf{f}(\hat{\mathbf{x}}))\| \end{aligned} \tag{5-49}$$

Then, using the triangular inequality and the fact that the vector field is assumed to satisfy the Lipschitz condition $\|\mathbf{f}(\mathbf{x}_i) - \mathbf{f}(\hat{\mathbf{x}})\| \leq \mu \|\mathbf{x}_i - \hat{\mathbf{x}}\|$, yields

$$\begin{aligned} \|\mathbf{F}(\mathbf{x}) - (\mathbb{1}_N \otimes \mathbf{f}(\hat{\mathbf{x}}))\| &\leq \sum_{i=1}^N \|\mathbf{f}(\mathbf{x}_i) - \mathbf{f}(\hat{\mathbf{x}})\| \\ &\leq \mu \sum_{i=1}^N \|\mathbf{x}_i - \hat{\mathbf{x}}\| \\ &\leq \mu\zeta \end{aligned} \tag{5-50}$$

From Lemma 2.4.1 we have that $\|\mathcal{L}\| = \max_k \{|\lambda_k(\mathcal{L})|\} = \lambda_N$; hence, $V_2 \leq \mu(\zeta^2 + \lambda_N\zeta\xi)$. Finally, exploiting the bounds for V_1 and V_2 we have that

$$\dot{V} = -[\zeta \ \xi]^T \underbrace{\left[\begin{array}{cc} \lambda_2(\alpha - 1) - \mu & -\mu\lambda_N/2 \\ -\mu\lambda_N/2 & \beta\lambda_2^2 \end{array} \right]}_{\mathbf{S}} [\zeta \ \xi] \tag{5-51}$$

hence, \dot{V} is negative definite if $\mathbf{S} \succ 0$, and using Proposition 2.4.2 we obtain (5-44) and the proof is complete. \square

Unlike the PD case where the synchronization condition depends linearly of the networks structure, for the PI case the synchronization condition (5-44) (Theorem 5.2.3) is a nonlinear function of the parameters β and the networks structure via λ_2 and λ_N . This can be seen in Fig. 5-5, where the line dividing the blue (synchronization) and red (No synchronization) regions was computed for two different network structures Ring and Star as those depicted in Fig. 3.1(c) and Fig. 5.10(a). The estimation obtained using Lyapunov theory is conservative

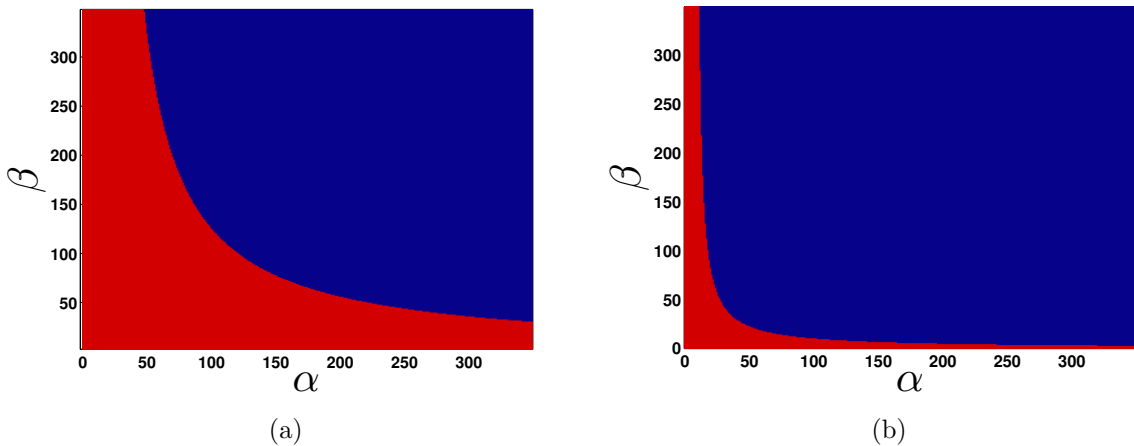


Figure 5-5.: Estimated regions of global synchronization of networks controlled by distributed PI, using (5-44) with $\mu = 4$, for two different network structures and (a) $\lambda_2 = 0.5188$ and $\lambda_N = 5.7105$, (b) $\lambda_2 = 0.382$ and $\lambda_N = 4$. The blue color, denotes the region where (5-44) is satisfied and red color otherwise.

and it provides an upper-bound of the synchronization region obtained in the local stability analysis.

5.3. Performance assessment

In this section we study in detailed the influence of the use of distributed derivative and integral controllers in the overall performance of the network under different scenarios of heterogeneity and disturbances.

5.3.1. Heterogeneity between nodes

Here we investigate the performance of the PD controller when a mismatch in the parameters of each agent is present. To this aim we consider 6 Lorenz chaotic oscillators (2-23) controlled by distributed proportional control. For the sake of simplicity and without loss of generality,

we choose the network topology as a ring graph with unitary link weights as the one depicted in Fig. 5-6. Also we set the parameter $a = 2$ for nodes 1, 4 and 5, and $a = 3$ for all

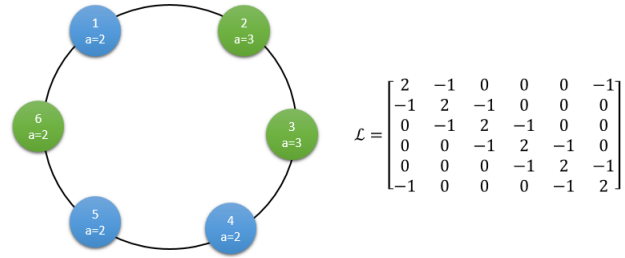


Figure 5-6.: Heterogeneous network of Lorenz systems.

the others. The time response of the disagreement dynamics of the network controlled by distributed proportional control is shown in Fig. 5-7. In fact for heterogeneous node

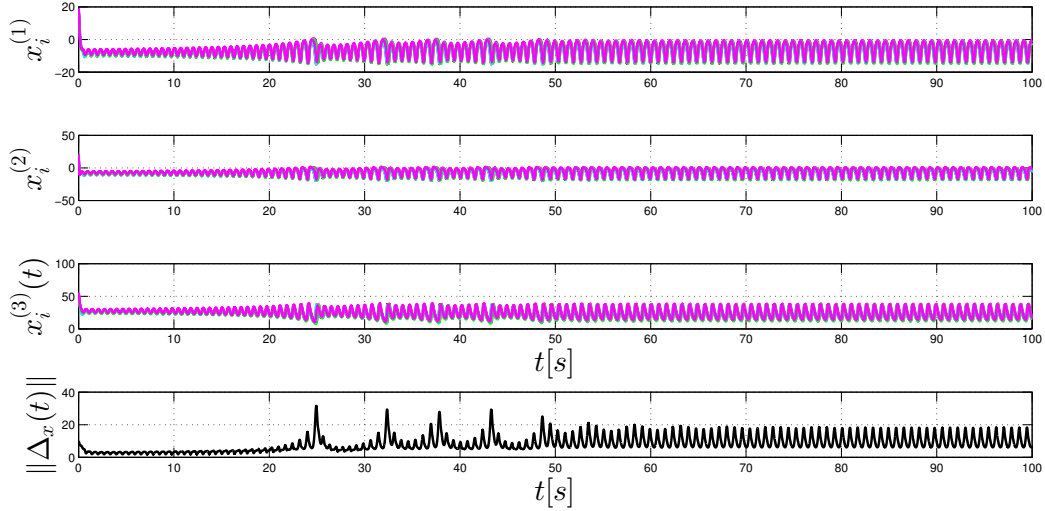


Figure 5-7.: Time response of the closed-loop heterogeneous network of heterogeneous Chaotic Lorenz systems with $\Gamma = \mathbf{I}_n$, controlled by distributed P control with $\alpha = 2$.

dynamics, the proportional controller is not able to provide admissible synchronization, yet bounded synchronization is reached instead. Moreover, comparing the error bounds $\|\Delta_x(t)\|$ on Figs. 5-7, 5-8 we can see that the error bound has been substantially reduced by including a derivative gain as well as the chaotic behaviour is preserved. Therefore, the

derivative action represents an extra degree of freedom for improving the synchronization performance in heterogeneous networks.

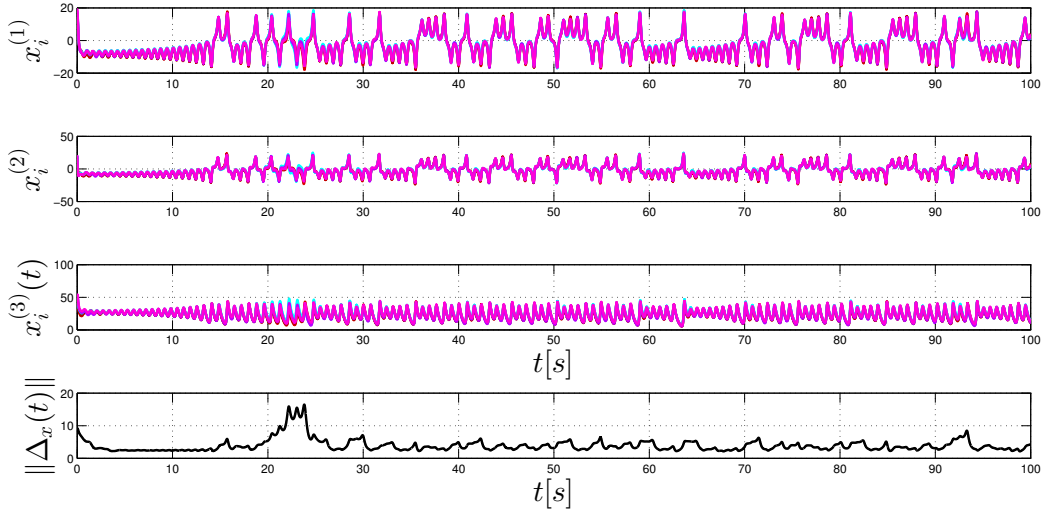


Figure 5-8.: Time response of the closed-loop heterogeneous network of heterogeneous Chaotic Lorenz systems with $\Gamma = \mathbf{I}_n$, controlled by distributed P control with $\alpha = \gamma = 2$.

5.3.2. Constant disturbances

As discussed in Chapters 3 and 4, a distributed integral action is able to reject constant disturbances for networks of linear and heterogeneous node dynamics. Hence, the PI control strategy may be also useful for networks of homogeneous nonlinear systems affected by constant disturbances, possibly nonidentical, acting on each node.

$$\dot{\mathbf{x}}_i(t) = \mathbf{f}(\mathbf{x}_i(t)) + \mathbf{d}_i + \mathbf{u}_i(t) \quad (5-52a)$$

$$\mathbf{y}_i(t) = \boldsymbol{\Gamma} \mathbf{x}_i(t), i \in \mathcal{N} \quad (5-52b)$$

where $\mathbf{d}_i \in \mathbb{R}^{n \times 1}$ represents the constant disturbance. We consider the example introduced in Section 5.3, but for six homogeneous Lorenz chaotic oscillators, with $a = 2$ and connected in a ring configuration. We apply some perturbations to nodes 1, 3 and 4, that is we set $\mathbf{d}_1 = [4, 0, 0]^T$, $\mathbf{d}_3 = [6, 0, 0]^T$ and $\mathbf{d}_4 = [7, 0, 0]^T$. For the sake of comparison, we first deploy just proportional control, by setting $\alpha = 3$, $\beta = \gamma = 0$ in (5-3). The time response of this perturbed network can be seen in Fig. 5-9. The constant disturbances in the nodes render them heterogeneous; hence, just bounded synchronization is attained. To reject those

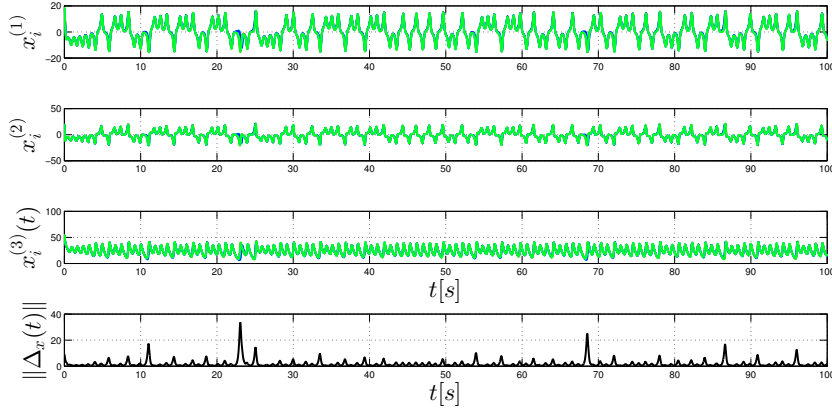


Figure 5-9: Time response of a ring network of six homogeneous Lorenz oscillators with $a = 2$ under constant perturbations acting on nodes 1, 3 and 4. The network is controlled by just distributed proportional control with $\alpha = 3$.

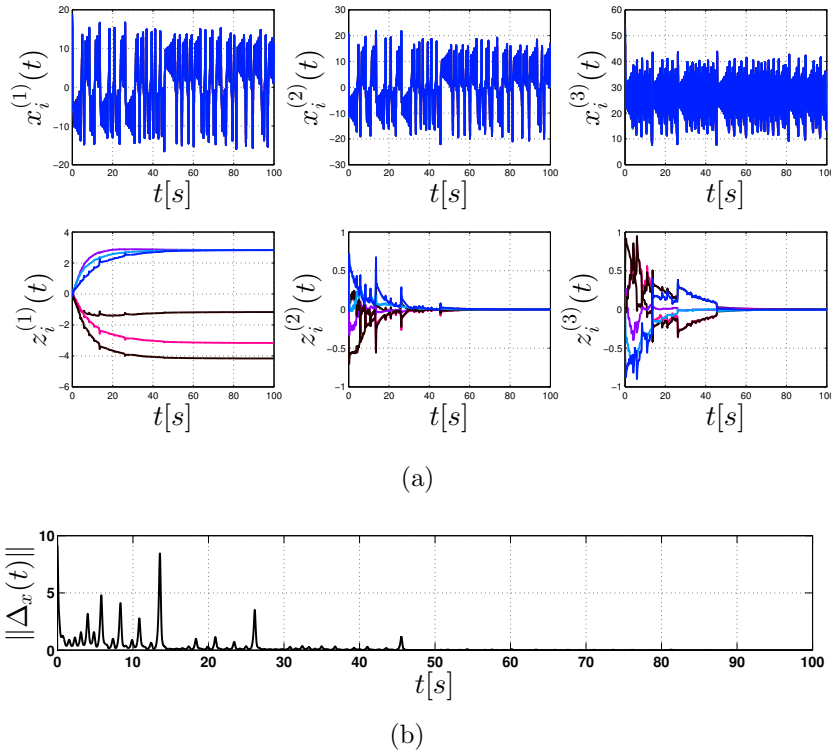


Figure 5-10: (a) Time response of a ring network of six Lorenz oscillators with $a = 2$ and affected by constant perturbations acting in nodes 1, 3 and 4 controlled by distributed proportional and integral actions with $\alpha = 3$ and $\beta = 1$. (b) Evolution of the disagreement dynamics.

heterogeneous constant disturbances, we deploy the integral action by setting $\beta = 1$. The results are shown in Fig. 5-10 where admissible synchronization is achieved.

Note that, despite the presence of constant disturbances affecting some nodes in the network, the controller is able to guarantee perfect agreement among all states of the units. Here, the integral action grows until the heterogeneities of the nodes are compensated, so that all nodes share the same perturbed nonlinear dynamics. This can be seen as a sort of homogenization of the nodes, since the integral action adapts its value such that all perturbed nodes become equal; so then, the proportional action acts and guarantee synchronization.

This, can be compared with the property of the classical PI control, where the proportional action stabilize the system and the integral action eliminates the residual error. We can then conclude that the beneficial properties of the classical PID control are preserved even when the controller is deployed in a distributed fashion.

Moreover, the controllers provide an extra degree of freedom for controlling heterogeneity, disturbances and most importantly, for modifying the synchronization region in the parameter space.

CHAPTER 6

Applications

6.1. Synchronization of power generators

In this section, an application of the multiplex PI-Control strategy introduced in Chapter 3 is presented for synchronizing power generators. In particular we consider N power generators governed by the swing equation [51]

$$\frac{2H_i}{\omega_R} \ddot{\delta}_i = P_i^m(t) - P_i^{net}(t), i \in \mathcal{N} \quad (6-1)$$

where H_i and ω_R are constants representing the inertia and reference frequency for the i -th generator. The quantity $P_i^m(t) := P_i^* - d_i \dot{\delta}_i(t)$ is the mechanical power provided by the i -th generator and it is composed by a constant power injection P_i^* and a damping term $d_i \dot{\delta}_i(t)$, $d_i > 0$ which models power losses. Moreover, $P_i^{net}(t)$ is the power demanded by the network. Note that when (6-1) is at equilibrium state, $P_i^m = P_i^{net}$ the frequency of each generator $\omega_i(t) := \dot{\delta}_i(t)$ remains equal to a common constant for all generators in the grid. For the sake of simplicity, we linearize the swing equation (6-1) around the synchronous state $\omega_1(t) = \dots = \omega_N(t)$, and letting $m_i = 2H_i/\omega_R$, we obtain [1, 51]

$$m_i \dot{\omega}_i(t) = -d_i \omega_i(t) + P_i^* - P_i^{net}(t) + v_i(t) \quad (6-2a)$$

$$\dot{P}_i^{net}(t) = \sum_{j=1, j \neq i}^N E_i E_j |Y_{ij}| (\omega_i - \omega_j), i \in \mathcal{N} \quad (6-2b)$$

where $E_i > 0$ is the nodal voltage, and Y_{ij} is the admittance among buses i and j .

6.1.1. Distributed controller

To achieve synchronization, we propose to use a combination of local and distributed control actions as also done in [2, 34] with the notable difference that we now consider the case of

heterogeneous local state-feedback actions characterized by different gains which are deployed together with the distributed PI strategy proposed in Chapter 3. In particular, we set

$$v_i(t) = \frac{1}{m_i} \left(k_i \omega_i(t) + \alpha \sum_{k=1}^N \mathcal{P}_{ij} \omega_k(t) \right) \quad (6-3)$$

with k_i being a constant representing a local feedback gain for the i -node, $\alpha > 0$ and $\mathcal{P} \in \Omega$ represents the Laplacian matrix of the proportional layer \mathcal{G}_P with link weights w_{ij} .

From a practical viewpoint, the control strategy corresponds to enhance the coupling between the agents in the open-loop network via additional proportional and integral control interconnections. This could be implemented via appropriate digital devices or by a TCP/IP communication protocol with optical fiber links, feeding the control action to the nodes rather than physically establishing a connection [7].

Now, let $g_{ij} := E_i E_j |Y_{ij}|$ be the weights on each edge of the power network in (6-2b) and $\mathcal{I} \in \Omega$ the associated Laplacian matrix describing the equivalent distributed integral action (6-2b). Setting $z(t) = -(1/m_i) P_i^{net}(t)$, the problem becomes that of proving convergence in the heterogeneous network given by

$$\dot{\omega}(t) = (\mathbf{H} - \alpha \mathcal{P}) \omega(t) + \mathbf{z}(t) + \Delta \quad (6-4a)$$

$$\dot{\mathbf{z}}(t) = -\mathbf{M} \mathcal{I} \omega(t) \quad (6-4b)$$

where $\omega(t) := [\omega_1(t), \dots, \omega_N(t)]$, $\mathbf{z}(t) := [z_1(t), \dots, z_N(t)]$ are the stack vectors of frequency and rescaled electrical power respectively, $\mathbf{H} := \text{diag}\{k_1 - d_1/m_1, \dots, k_N - d_N/m_N\}$, $\mathbf{M} := \text{diag}\{1/m_1, \dots, 1/m_N\}$ and the vector $\Delta := \text{diag}\{P_1^*/m_1, \dots, P_N^*/m_N\}$.

Proposition 6.1.1. *The closed-loop power network (6-4) has a unique equilibrium given by $\omega^* := \omega_\infty \mathbf{1}_N$, with $\omega_\infty := -\sum_{i=1}^N P_i^*/\sum_{i=1}^N (m_i k_i - d_i)$ and $\mathbf{z}^* := -(\omega_\infty \mathbf{H} \mathbf{1}_N + \Delta)$*

Proof. As done in the proof of Proposition 3.1.1 by setting the left-hand side of (6-4) to zero one has that $\mathbf{x}^* = a \mathbf{1}_N$, $\forall a \in \mathbb{R}$ and $\mathbf{z}^* = -(a \mathbf{P} \mathbf{1} + \Delta)$. Now letting $\mathbf{v} := [m_1, \dots, m_N]^T$, by the definition of $\mathbf{z}(t)$ one has that $\mathbf{v}^T \mathbf{z}(t) = 0$. Therefore $\mathbf{v}^T \mathbf{z}^* = 0$ and we obtain

$$a = -\frac{\mathbf{v}^T \Delta}{\mathbf{v}^T \mathbf{H} \mathbf{1}_N} = -\frac{\sum_{i=1}^N P_i^*}{\sum_{i=1}^N (m_i k_i - d_i)} =: \omega_\infty \quad (6-5)$$

which completes the proof. \square

Remark 6.1.1. Note that the equilibrium point ω_∞ depends on the average of all generator parameters, as well as on the control gains k_i . Therefore, the values of the control gains, can be exploited for changing the consensus frequency value, despite heterogeneity among generator dynamics.

Corollary 6.1.1. Under the control dynamics (6-3), the power network (6-2) with $m_i = m, m > 0 \forall i \in \mathcal{N}$ asymptotically converges to (6-5) if the following conditions are satisfied

$$\psi_{11} = \sum_{i=1}^N \left(k_i - \frac{d_i}{m} \right) < 0 \quad (6-6a)$$

$$\alpha \lambda_2(P) > \frac{\sum_{i=1}^N \left(k_i - \frac{d_i}{m} \right)^2}{N |\psi_{11}|} + \max_i \left\{ k_i - \frac{d_i}{m} \right\} \quad (6-6b)$$

Proof. Note that (6-4) can be seen as a group of N first order heterogeneous agents controlled by a multiplex PI strategy. Specifically, letting $A_i = k_i - d_i/m$, the dynamics of each node can be written as

$$\begin{aligned} \dot{\omega}_i(t) &= A_i \omega_i(t) + \delta_i - \alpha \sum_{j=1}^N \mathcal{P}_{ij} \omega_j(t) + z_i(t) \\ \dot{z}_i(t) &= -(1/m) \sum_{j=1}^N \mathcal{I}_{ij} \omega_j(t) \end{aligned}$$

Therefore, using Theorem (4.3.1) with $\sigma = 0$, and $\beta = (1/m)$ completes the proof. \square

6.1.2. Simulation

As an illustration, consider the power network shown in Fig. 6.1(a). For the sake of simplicity and without loss of generality we assume that all weights in the power network model (6-4) are unitary, that is $g_{ij} = 1 \forall i, j \in \mathcal{N}$.

Moreover we assume $m = 0.1382$, and four different values of damping, that is $d_i = 0.005$, for $i \in \{1, 4, 7, 8, 11, 14\}$, $d_i = 0.0045$, $i \in \{2, 6, 9, 13, 15\}$, $d_i = 0.0040$, $i \in \{3, 10, 12\}$, while $d_i = 0.006$, $i \in \{5, 16\}$. Furthermore the vector containing the nominal power injections for each node is given by

$$\Delta = (1/m)[100, 200, -300, 100, 90, 80, 50, -100, 200, -100, -155, 100, -500, 200, 125, 10]$$

The aim is to synchronize all generators to a common frequency value, say 60, despite the fact that the network is heterogeneous. We then introduce feedback controllers with appropriate gains at nodes 1, 5, and 10 (self feedback loops indicated in black in Fig. 6.1(a)) in

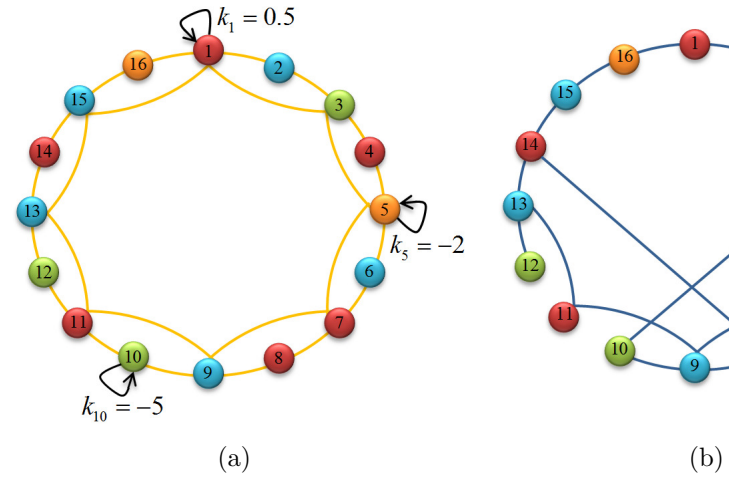


Figure 6-1.: (a) Power network represented by the integral layer, (b) Architecture of the network in the proportional layer.

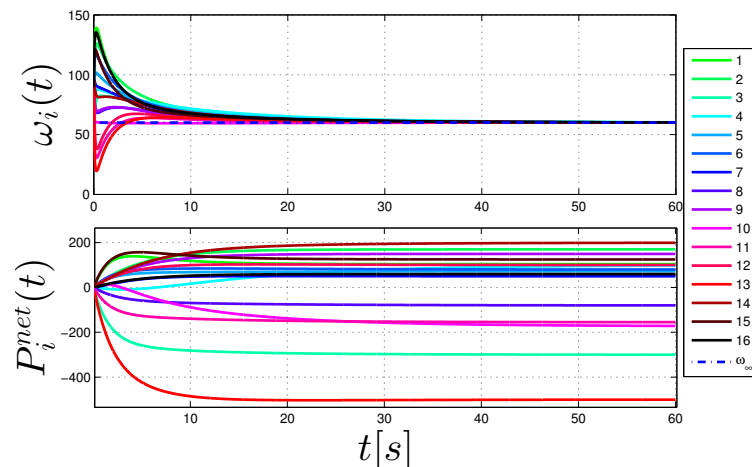


Figure 6-2.: Time response of the controlled power network. The blue dash-dot line represent the convergence value ω_∞ .

order to shift ω_∞ as given by (6-5) to the desired value $\omega_\infty = 60$. To address the stability of such consensus equilibrium, we use Corollary (6.1.1).

Firstly we find that $\psi_{11} := -0.7533$ and condition (6-6a) is fulfilled. Secondly, we have that $\max_i \{k_i - \frac{d_i}{m}\} = 0.4638$ and therefore the power network reaches admissible consensus if $\alpha\lambda_2(\mathcal{P}) > 9.1738$. Hence, choosing the proportional network as in Fig. 6.1(b) where all weights among links are set to $w_{ij} = 5$ yields $\alpha > 6.77$. Setting $\alpha = 7$ we obtain the behaviour depicted in Fig. 6-2 where admissible consensus is obtained to the expected value ω_∞ .

6.2. Electrical Circuits

Consider the case where the agents or units are described by a non-linear circuit as shown in Fig. 6-3. Each circuit is composed of a linear subsystem modeled by a passive impedance, z_{osc} , and a nonlinear voltage-dependent current source, $g(\cdot)$.

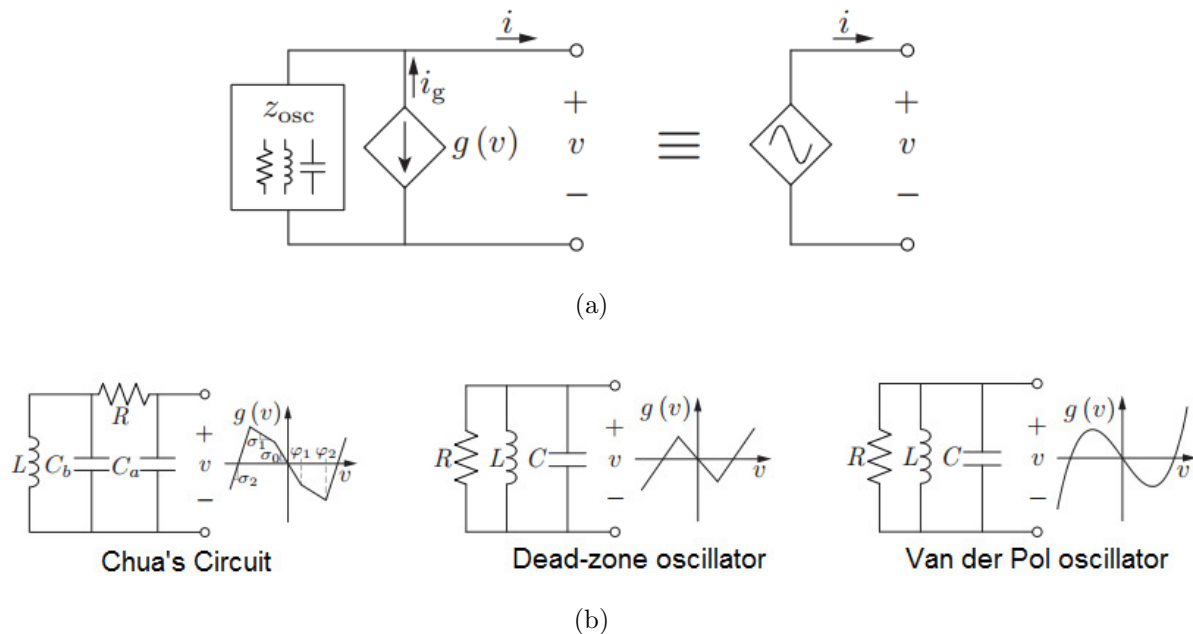


Figure 6-3: (a) Schematic of the nonlinear circuit [24], (b) Different examples of nonlinear circuits.

Suppose the problem is to design an electrical network interconnecting N non-linear circuits for synchronizing all their states. Synchronization in electrical circuits is a problem

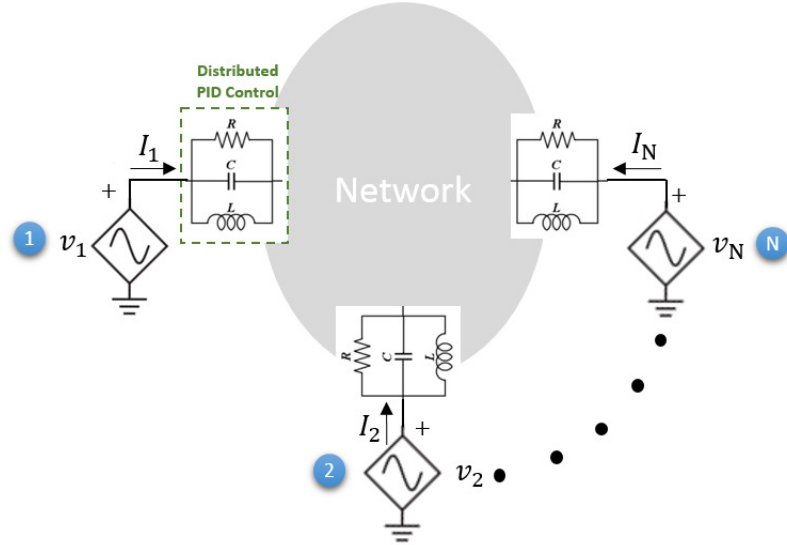


Figure 6-4.: Distributed PID (RLC) network for synchronization in networks of nonlinear circuits.

of notable importance for applications such as AC electrical grid, solid-state circuit oscillators, semiconductor laser arrays, secure communications, and microwave oscillator arrays [24, 31]. We propose the use of distributed PID actions which are equivalent to parallel RLC interconnections (as can be seen in Fig.6-4) for synchronizing nonlinear circuits. Note that the current I_i for all $i = \{1, \dots, N\}$ can be calculated using Kirchoff's laws in each link interconnecting two circuits. Letting R_{ij} , L_{ij} and C_{ij} as the resistance, inductance, and capacitance between circuits i and j then, the current I_i can be recast as

$$I_i(t) = \sum_{j=1}^N \frac{1}{R_{ij}} (v_j(t) - v_i(t)) + \sum_{j=1}^N C_{ij} (\dot{v}_j(t) - \dot{v}_i(t)) + \sum_{j=1}^N \frac{1}{L_{ij}} \int_0^t (v_j(\tau) - v_i(\tau)) d\tau \quad (6-7)$$

Next, assuming $\alpha w_{ij} = 1/R_{ij}$, $\gamma w_{ij} = C_{ij}$, and $\beta w_{ij} = 1/L_{ij}$ where $\alpha, \beta, \gamma, w_{ij}$ are positive constants. Therefore, the electrical network can be represented by a graph $\mathcal{G} = (\mathcal{N}, \mathcal{E})$ where w_{ij} denotes the strength of the a link between nodes i and j . We can rewrite (6-7) as

$$I_i(t) = - \sum_{j=1}^N \mathcal{L}_{ij} \left(\alpha v_j(t) + \beta \int_0^t v_j(\tau) d\tau + \gamma \dot{v}_j(t) \right) \quad (6-8)$$

where \mathcal{L} is the Laplacian Matrix associated to the graph \mathcal{G} . Note that equation (6-8) is the same as the PID strategy introduced in (5-3). Therefore, the synchronization analysis derived in Chapter 5 can be used for analyzing this networks of electrical circuits. As a representative example we consider the problem of synchronizing N Chua's circuits controlled by distributed PID

6.2.1. Chua's Circuit

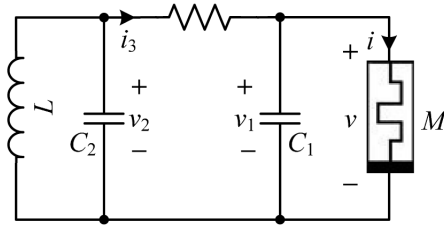


Figure 6-5.: Schematic diagram of Chua's circuit.

The adimensional equation of Chua's circuit of Fig. 6-5 is given by [80]

$$\begin{bmatrix} \dot{x}_1(t) \\ \dot{x}_2(t) \\ \dot{x}_3(t) \end{bmatrix} = \underbrace{\begin{bmatrix} -a & a & 0 \\ 1 & -1 & 1 \\ 0 & -b & 0 \end{bmatrix} \begin{bmatrix} x_1(t) \\ x_2(t) \\ x_3(t) \end{bmatrix}}_{\mathbf{f}(x_1, x_2, x_3)} + \begin{bmatrix} -ah(x_1) \\ 0 \\ 0 \end{bmatrix} \quad (6-9)$$

where

$$h(x_1) = cx_1 + \frac{d_1 - d_2}{2} (|x_1(t) + 1| - |x_1(t) - 1|)$$

with $x_1(t)$, $x_2(t)$ and $x_3(t)$ being the rescaled states of v_1 , v_2 and i_3 and a, b, c, d_1, d_2 being the rescaled circuit parameters in Fig. 6-5. Then, without loss of generality, setting $a = 10$, $b = 18$, $c = -3/4$, $d_1 = -4/3$ and $d_2 = -3/4$, the electrical circuit exhibit chaotic behaviour as can be seen in Fig. 6-6. Then, letting $v = x_1$ in (6-8) and $\mathbf{x} = [x_1, x_2, x_3]$, we have that the closed-loop network reads

$$\dot{\mathbf{x}}_i(t) = \mathbf{f}(\mathbf{x}_i(t)) - \sum_{j=1}^N \mathcal{L}_{ij} \Gamma \left(\alpha \mathbf{x}_j(t) + \beta \int_0^t \mathbf{x}_j(\tau) d\tau + \gamma \dot{\mathbf{x}}_j(t) \right) \quad (6-10)$$

with $\Gamma = \text{diag}\{1, 0, 0\}$. Nevertheless, different types of couplings can also be considered varying the structure of matrix Γ as we shall discuss later. Next, we present local and global synchronization analysis of the closed-loop network (6-10).

6.2.2. Synchronization in networks of Chua's Circuit

Here, we exploit the local synchronization analysis of Section 5.1, as well as the global Theorems for PD and PI founded in Section 5.2.

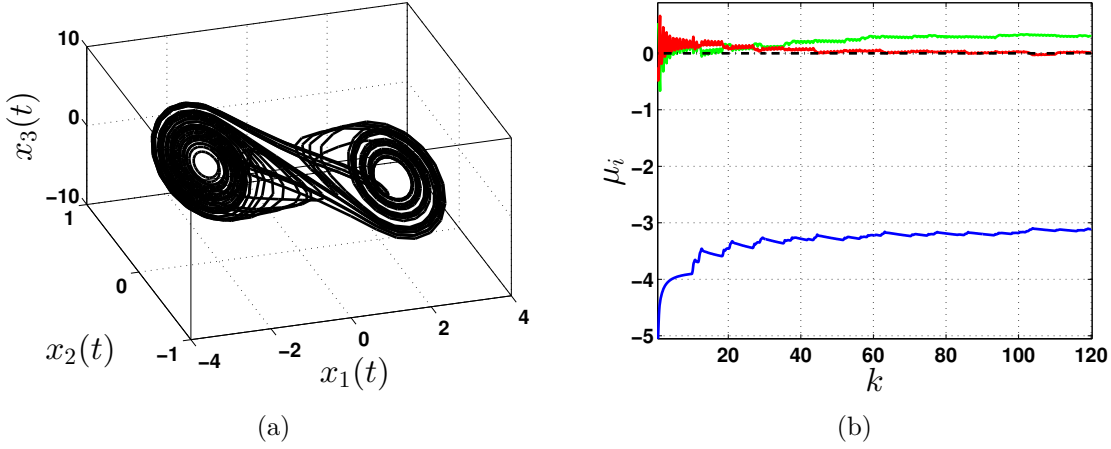


Figure 6-6.: Chaotic Lorenz attractors with their respective Lyapunov exponents μ_p . k represents the step-number of the L.E. algorithm

6.2.2.1. Local admissible synchronization of Chua's Circuit

Using the analysis developed in Chapter 5, we then make use of the MSF approach for PD and PI. Hence, we solve the variational equations (5-13) and (5-20) and following a similar derivation as in example 10, we obtain the diagrams depicted in Fig. 6-7.

Next, we consider an electrical network of ten Chaotic Chua's Circuits with $\Gamma = \text{diag}\{1, 0, 0\}$, where its structure is described by the graphs depicted in Fig. 2.5(a). Accordingly to the diagram on Fig. 6.7(b), if we choose the point $\tilde{\alpha} = 3$ and $\tilde{\gamma} = 0.15$ we have that the MSF function is positive and no synchronization is expected. Therefore, we have that $\alpha = \tilde{\alpha}/\lambda_2 = 12.8755$ and $\gamma = \tilde{\gamma}/\lambda_2 = 0.6438$. The time response of the network is shown in Fig. 6.8(a). Moreover, increasing the value of the derivative gain to $\tilde{\gamma} = 0.45$ we have that $\gamma = 1.9313$ and the network achieves synchronization as expected (Fig. 6.8(b)).

6.2.2.2. Global admissible synchronization of Chua's Circuit

First, we prove that the vector-field $\mathbf{f}(\cdot)$ of the Chua's circuit is Lipschitz. Hence, substituting the parameter values in the circuit model we have that the vector-field of (6-9) can be recast as

$$\mathbf{f}(\mathbf{x}) = \begin{bmatrix} -\frac{7}{4}x_1 + x_2 + g(x_1) \\ x_1 - x_2 + x_3 \\ -18x_2 \end{bmatrix}, g(x_1) = -\frac{7}{24}(|(x_1+1)| - |x_1-1|) \quad (6-11)$$

Then let \mathbf{x} , and \mathbf{y} be two generic vectors in \mathbb{R}^3 one has

$$\mathbf{f}(\mathbf{x}) - \mathbf{f}(\mathbf{y}) = \mathbf{A}(\mathbf{x} - \mathbf{y}) + \mathbf{v}(\mathbf{x}) - \mathbf{v}(\mathbf{y})$$

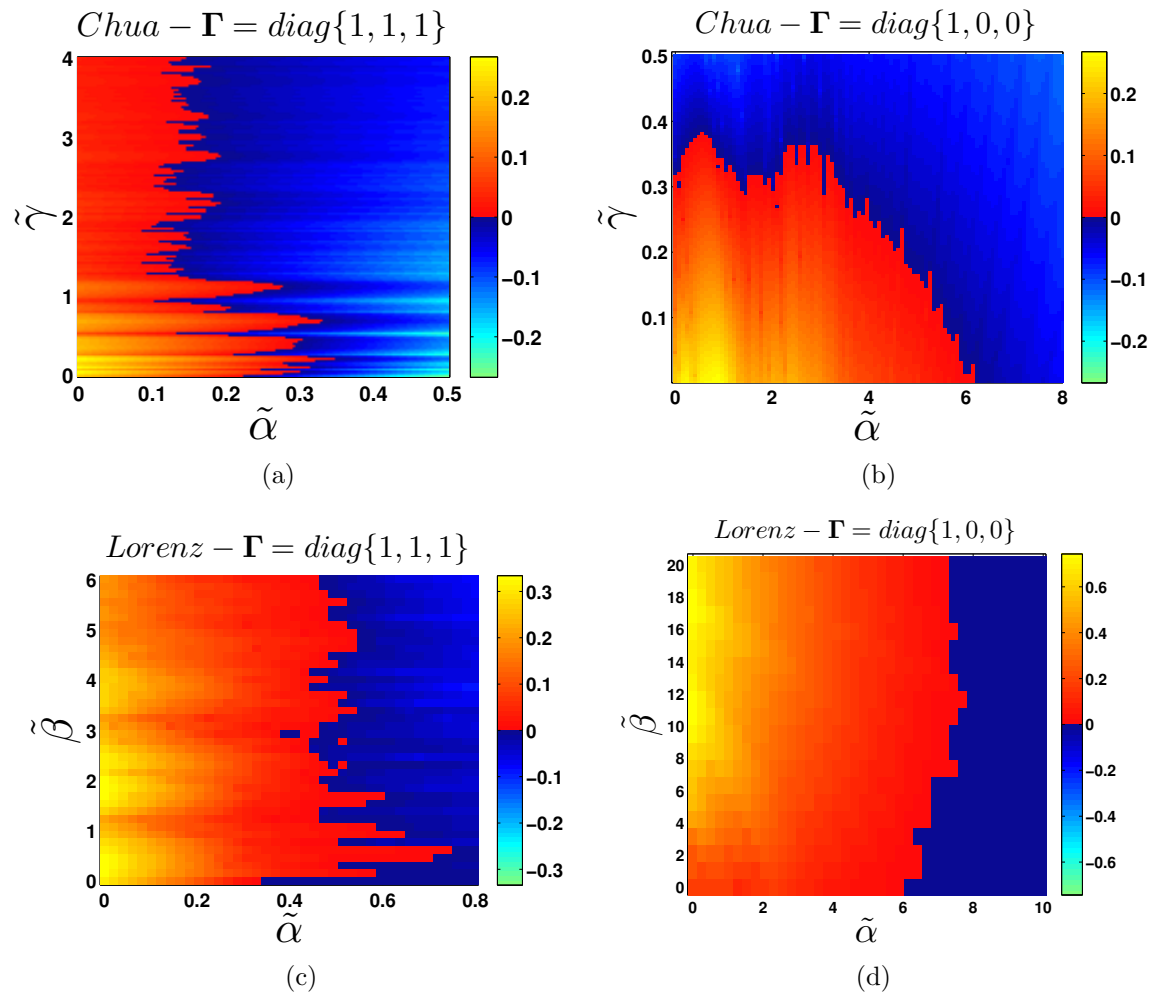


Figure 6-7: Two dimensional representation of the master stability function for Chaotic Chua. For each point in the plane corresponds the value of the MSF evaluated at that point, which is represented with different colors. The red-scale colors denote positive values of the MSF, while negative values are represented by the blue-scale. (a)-(b) $\Psi(\tilde{\alpha}, \tilde{\gamma})$ function computed for distributed PD control, (c)-(d) $\Psi(\tilde{\alpha}, \tilde{\beta})$ function computed for PI control.

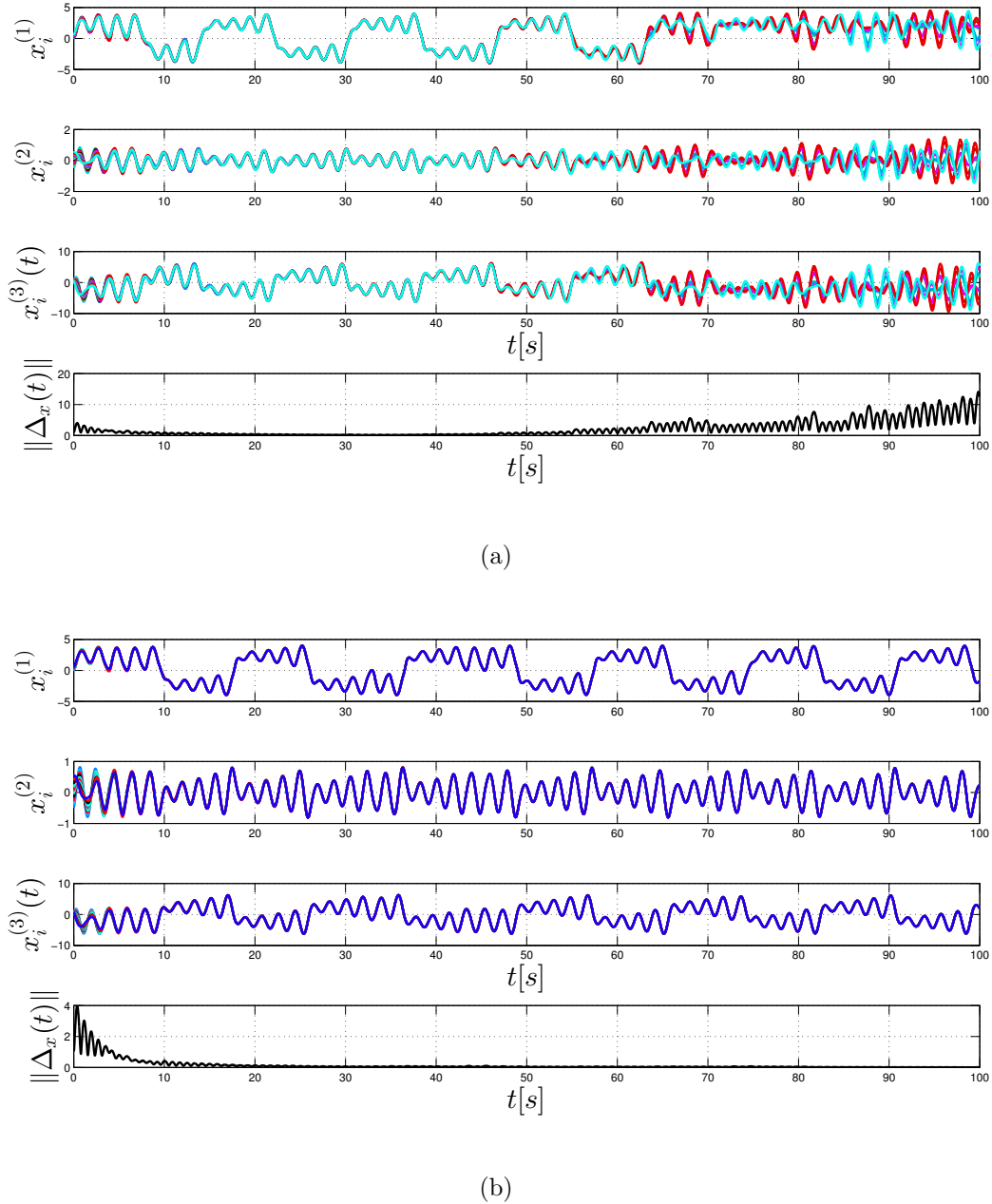


Figure 6-8.: Time response of a network of ten chaotic Chua's circuit controlled by distributed PD control with $\alpha = 12.8755$ and (a) $\gamma = 0.6438$ (b) $\gamma = 1.9313$

where

$$\mathbf{A} := \begin{bmatrix} -7/4 & 1 & 0 \\ 1 & -1 & 1 \\ 0 & -18 & 0 \end{bmatrix}$$

It follows from Lemma 1 in [37] that $\|\mathbf{g}(\mathbf{x}) - \mathbf{g}(\mathbf{y})\| \leq (7/12) \|\mathbf{x} - \mathbf{y}\|$; therefore

$$\|\mathbf{f}(\mathbf{x}) - \mathbf{f}(\mathbf{y})\| \leq (\|\mathbf{A}\| + (7/12)) \|\mathbf{x} - \mathbf{y}\|$$

and by Definition 5.2.1 we have that the Lipschitz constant of (6-11) is $\mu = 18.7784$. Next, we assume that the coupling matrix $\mathbf{\Gamma} = \mathbf{I}_3$, which means that the circuits are coupled by the three states variables. This can be implemented by adding an extra RL or RC link between the v_2 terminal of each circuit and also including a current source to the inductor of each Chua's circuit, which also depend on PI or PD type coupling; nevertheless, the circuit implementation of this coupling goes beyond the scope of this work, and this is a simple idea of how it could be designed. Next, consider a group of 10 Chua's circuits coupled in a star topology (See Fig. 5.10(a)) where $\lambda_2 = 1$ and $\lambda_N = 10$. The using Theorem 5.2.2 for the PD case and Theorem 5.2.3 for the PI we can plot the global synchronization regions as depicted in Fig. 6-9. The estimation of the synchronization region using the results for

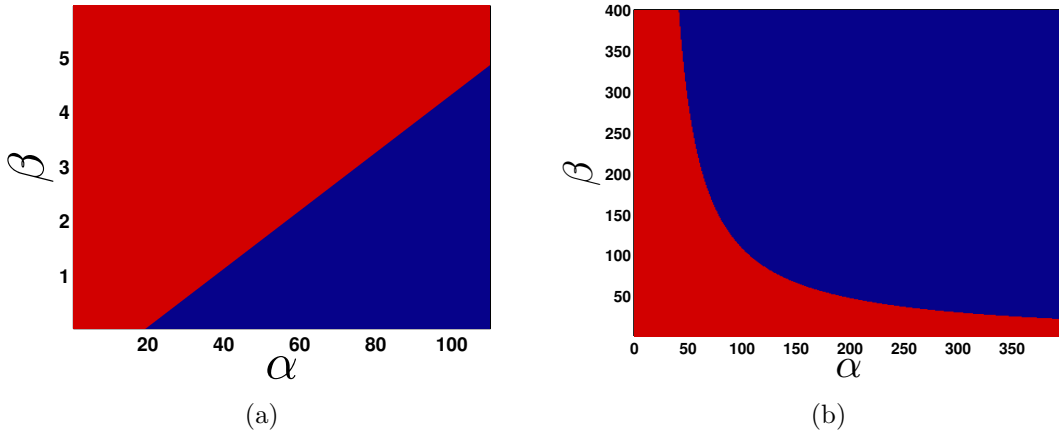


Figure 6-9: Estimated regions of global synchronization of a network of Chua's circuits controlled by distributed (a) PD and (PI). The blue color, denotes the region where (5-36) is satisfied and red color otherwise.

the global approach are conservative and can be improved by considering different Lyapunov functions. By comparing global and local synchronization results (see Fig. 6-7) we note a large difference between them. However, the global results obtained from Theorems 5.2.2 and 5.2.3 are more general, since the network will synchronize no matter the initial condition.

6.2.2.3. Heterogeneity between nodes

Here we investigate the performance of the PD controller when a mismatch in the parameters of the Chua's circuit is present. Thus, consider a 6 nodes ring network with unitary link weights, and let the parameter $b = 18$ for nodes 2, 3 and 5, and $b = 15$ otherwise. The time

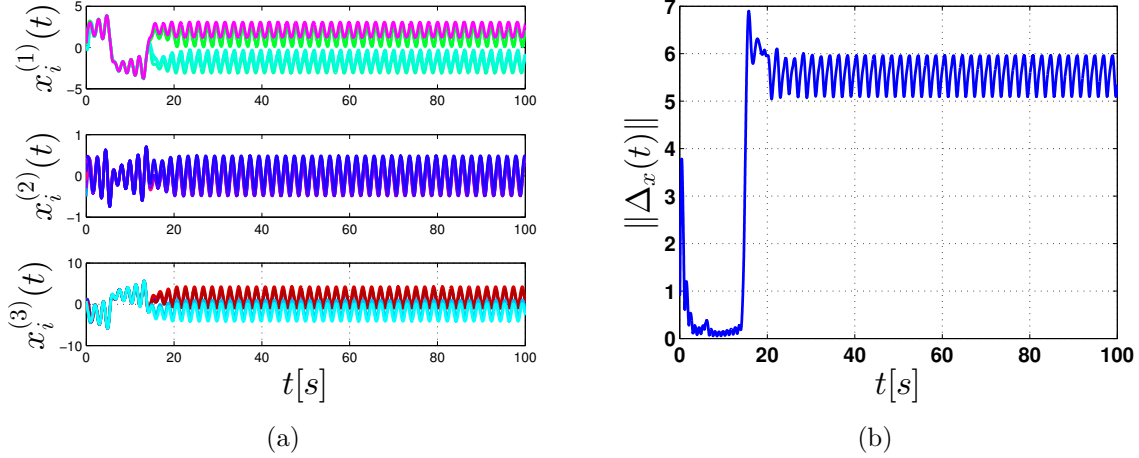


Figure 6-10.: Time response of the closed-loop heterogeneous network of Chua's circuits controlled by distributed P with $\Gamma = \mathbf{I}_n$.

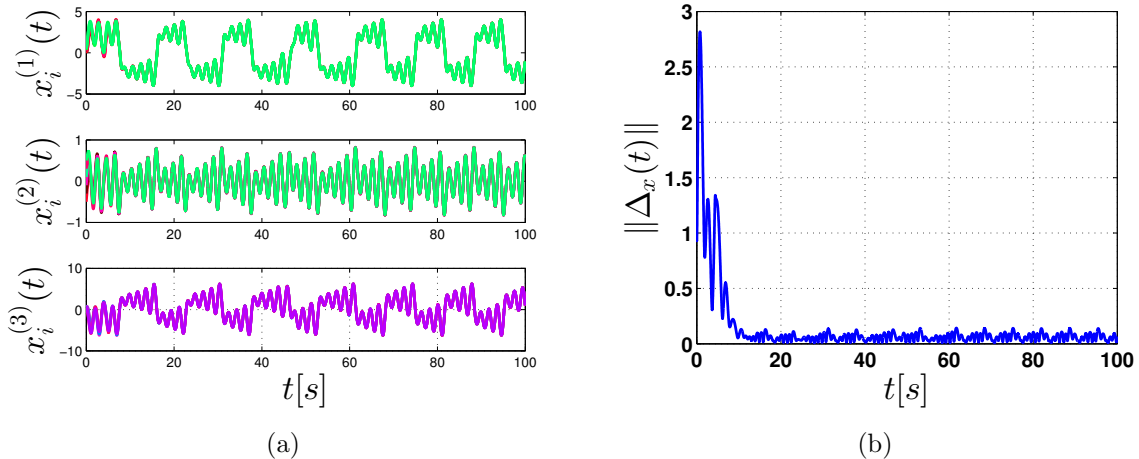


Figure 6-11.: Time response of the closed-loop heterogeneous network of Chua's circuits controlled by distributed PD with $\Gamma = \mathbf{I}_n$.

response of the network controlled by just distributed proportional control with $\alpha = 1$ is shown in Fig. 6-10. In fact for heterogeneous node dynamics, this controller is not able to

provide admissible synchronization, but bounded synchronization instead. The error bound can be substantially decreased by increasing the proportional gain; nevertheless, the control effort will also increase and this represent an strong limitation from a practical point of view. Moreover, considering proportional and derivative actions by setting $\alpha = \gamma = 1$ we obtain the time response of Fig. 6-11 where the error bound has been significantly decreased. Therefore, the derivative action represents an extra degree of freedom for improving the performance of synchronization in heterogeneous networks.

CHAPTER 7

Conclusions

We discussed several distribute PID strategies to control networks of linear or nonlinear agents so as to achieve consensus or synchronization.

In Chapter 3, we have investigated the use of a distributed PID protocol to achieve consensus in homogeneous and heterogeneous multi-agent networks. Convergence of the strategy in both cases was obtained by using appropriate state transformations, linear algebra and Lyapunov functions. Explicit expressions for the consensus values were obtained together with analytical estimates of the upper bound for all integral actions. Also, where possible, estimates of the rate of convergence where obtained as functions of the gains of the distributed control actions and the network structure. It was found that the network architecture, the nodal dynamics and the control gains all contribute to determine the stability and performance of the closed-loop network.

In Chapter 4 a novel approach for controlling networks of heterogeneous nodes with generic n -dimensional linear dynamics in the presence of constant disturbances was proposed. In particular, we discussed the use of different control layers deploying proportional and integral actions across the network. Each layer has its own structure which allows to deploy a combination of P, I and PI couplings among nodes to achieve consensus. We proved convergence of the strategy and derived conditions to select the control gains as a function of the open loop and control network structures and the node dynamics. We illustrated the effectiveness of the proposed strategy via numerical simulations on a set of representative examples.

Also, an extension of the distribute PID controller to the case of networks of homogeneous nonlinear units was presented in Chapter 5. Both local and global stability analysis were developed using the MSF approach and Lyapunov theory. It was revealed that the derivative and integral actions both contribute to enhance the synchronization region; as well as, they

can be properly used for decreasing the residual error when the nodes are heterogeneous and also the integral action rejects constant disturbances.

In both cases of linear and nonlinear node dynamics, we observe that the most important properties the classical PID are preserved even if the controller is deployed in a distributed fashion.

7.1. Future Work

Several open problems are left for further study.

- First and foremost the effect of varying the structure of the network control layers on the multiplex strategy should be studied in more detail as preliminary results show the performance of the network evolution towards consensus can be affected by such variations.
- Also, it remains to be investigated if the additional degrees of freedom represented by the gains of the distributed P and I actions can be exploited to improve the performance of the closed-loop network, possibly in an optimal manner.
- We wish to emphasize that more sophisticated approaches can be developed by considering other linear or nonlinear control actions rather than the simpler proportional and integral actions considered in this work. For example, robustifying the distributed action could be designed by considering an extra network control layer of variable structure controllers. Also, designing adaptive strategies where the gains α , β and γ are time-varying functions.
- An interesting extension of the distributed PID control may be consider the strategy for undirected networks and possible time-varying structures.

APPENDIX A

Matrix Calculations

A.1. Computation of Ψ matrix

We know that $\Psi = \mathbf{U}^{-1} \tilde{\mathcal{L}}^{-1} \mathbf{P} \mathbf{U}$, and

$$\begin{bmatrix} \psi_{11} & \Psi_{12} \\ \Psi_{12} & \Psi_{22} \end{bmatrix} = \mathbf{U}^{-1} \tilde{\mathcal{L}}^{-1} \begin{bmatrix} 1 & \mathbb{0}_{1 \times (N-1)} \\ \mathbb{0}_{(N-1) \times 1} & \hat{\mathbf{P}} \end{bmatrix} \mathbf{U}$$

Next, we simplify the expression of each block in the matrix. Specifically, from (3-9) we have that $\mathbf{R}_{12} = r_{11} \mathbb{1}_{N-1}^T$ and the first block can be expressed as

$$\begin{aligned} \psi_{11} &= r_{11} \left(\hat{l}_{11} \rho_1 + \hat{\mathcal{L}}_{12} \bar{\mathbf{P}} \mathbb{1}_{N-1} \right) + \mathbf{R}_{12} \left(\hat{\mathcal{L}}_{21} \rho_1 + \hat{\mathcal{L}}_{22} \hat{\mathbf{P}} \mathbb{1}_{N-1} \right) \\ &= r_{11} \hat{l}_{11} \rho_1 + r_{11} \mathbb{1}_{N-1}^T \hat{\mathcal{L}}_{21} \rho_1 + r_{11} \hat{\mathcal{L}}_{12} \hat{\mathbf{P}} \mathbb{1}_{N-1} + \mathbf{R}_{12} \hat{\mathcal{L}}_{22} \hat{\mathbf{P}} \mathbb{1}_{N-1} \end{aligned}$$

From (3-36) one has $\mathbb{1}_{N-1}^T \hat{\mathcal{L}}_{21} = 1 - \hat{l}_{11}$, where $\hat{\mathcal{L}}_{12} = \hat{\mathcal{L}}_{21}^T$. Thus, using (3-37) yields

$$\begin{aligned} \psi_{11} &= r_{11} \rho_1 + r_{11} \hat{\mathcal{L}}_{12} \hat{\mathbf{P}} \mathbb{1}_{N-1} + r_{11} \mathbb{1}_{N-1}^T \hat{\mathcal{L}}_{22} \hat{\mathbf{P}} \mathbb{1}_{N-1} \\ &= r_{11} \rho_1 + r_{11} \hat{\mathcal{L}}_{12} \bar{\mathbf{P}} \mathbb{1}_{N-1} + r_{11} (\mathbb{1}_{N-1}^T - \hat{\mathcal{L}}_{12}) \hat{\mathbf{P}} \mathbb{1}_{N-1} \\ &= r_{11} \rho_1 + r_{11} \mathbb{1}_{N-1}^T \hat{\mathbf{P}} \mathbb{1}_{N-1} \\ &= (1/N) \sum_{k=1}^N \rho_k \end{aligned}$$

We move next to the second block given by

$$\Psi_{12} = N r_{11} (\hat{l}_{11} \rho_1 \mathbf{R}_{21}^T + \hat{\mathcal{L}}_{12} \hat{\mathbf{P}} \mathbf{R}_{22}^T) + N \mathbf{R}_{12} (\rho_1 \hat{\mathcal{L}}_{21} \mathbf{R}_{21}^T + \hat{\mathcal{L}}_{22} \hat{\mathbf{P}} \mathbf{R}_{22}^T)$$

from (3-9) we have that $\mathbf{R}_{12} = r_{11} \mathbb{1}_{N-1}^T$. Some algebraic manipulation yields

$$(1/N) \Psi_{12} = r_{11} \rho_1 \hat{l}_{11} \mathbf{R}_{21}^T + \rho_1 r_{11} \mathbb{1}_{N-1}^T \hat{\mathcal{L}}_{21} \mathbf{R}_{21}^T + r_{11} \hat{\mathcal{L}}_{12} \hat{\mathbf{P}} \mathbf{R}_{22}^T + \mathbf{R}_{12} \hat{\mathcal{L}}_{22} \hat{\mathbf{P}} \mathbf{R}_{22}^T$$

Using (3-36) the right-hand side of this expression can be rewritten so as to get

$$\begin{aligned}\frac{1}{N} \Psi_{12} &= r_{11} \rho_1 \hat{l}_{11} \mathbf{R}_{21}^T + \rho_1 r_{11} (1 - \hat{l}_{11}) \mathbf{R}_{21}^T + r_{11} \widehat{\mathcal{L}}_{12} \widehat{\mathbf{P}} \mathbf{R}_{22}^T + \mathbf{R}_{12} \widehat{\mathcal{L}}_{22} \widehat{\mathbf{P}} \mathbf{R}_{22}^T \\ \frac{1}{N} \Psi_{12} &= r_{11} \rho_1 \mathbf{R}_{21}^T + r_{11} \widehat{\mathcal{L}}_{12} \widehat{\mathbf{P}} \mathbf{R}_{22}^T + r_{11} \mathbb{1}_{N-1}^T \widehat{\mathcal{L}}_{22} \widehat{\mathbf{P}} \mathbf{R}_{22}^T \\ \frac{1}{N} \Psi_{12} &= r_{11} \rho_1 \mathbf{R}_{21}^T + r_{11} \widehat{\mathcal{L}}_{12} \widehat{\mathbf{P}} \mathbf{R}_{22}^T + r_{11} (\mathbb{1}_{N-1}^T - \widehat{\mathcal{L}}_{12}) \widehat{\mathbf{P}} \mathbf{R}_{22}^T \\ \frac{1}{N} \Psi_{12} &= r_{11} \rho_1 \mathbf{R}_{21}^T + \mathbf{R}_{12} \widehat{\mathbf{P}} \mathbf{R}_{22}^T\end{aligned}$$

Finally, adding and subtracting $\rho_1 \mathbf{R}_{12} \mathbf{R}_{22}^T$ and applying property (3-13) yields

$$\begin{aligned}(1/N) \Psi_{12} &= -\rho_1 \mathbf{R}_{12} \mathbf{R}_{22}^T + \mathbf{R}_{12} \widehat{\mathbf{P}} \mathbf{R}_{22}^T \\ (1/N) \Psi_{12} &= \mathbf{R}_{12} \left(\widehat{\mathbf{P}} - \rho_1 \mathbf{I}_{N-1} \right) \mathbf{R}_{22}^T \\ (1/N) \Psi_{12} &= r_{11} \mathbb{1}_{N-1}^T \left(\widehat{\mathbf{P}} - \rho_1 \mathbf{I}_{N-1} \right) \mathbf{R}_{22}^T \\ \Psi_{12} &= [\rho_2 - \rho_1, \dots, \rho_N - \rho_1] \mathbf{R}_{22}^T = \bar{\rho} \mathbf{R}_{22}^T\end{aligned}$$

The third block of the matrix has an expression given by

$$\Psi_{21} = \mathbf{R}_{21} \hat{l}_{11} \rho_1 + \mathbf{R}_{22} \widehat{\mathcal{L}}_{21} \rho_1 + \mathbf{R}_{21} \widehat{\mathcal{L}}_{12} \widehat{\mathbf{P}} \mathbb{1}_{N-1} + \mathbf{R}_{22} \widehat{\mathcal{L}}_{22} \widehat{\mathbf{P}} \mathbb{1}_{N-1}$$

Using (3-11) we get

$$\begin{aligned}\Psi_{21} &= -\mathbf{R}_{22} \mathbb{1}_{N-1} \hat{l}_{11} \rho_1 + \mathbf{R}_{22} \widehat{\mathcal{L}}_{21} \rho_1 + \mathbf{R}_{22} \widehat{\mathcal{L}}_{22} \bar{\mathbf{P}} \mathbb{1}_{N-1} - \mathbf{R}_{22} \mathbb{1}_{N-1} \widehat{\mathcal{L}}_{12} \widehat{\mathbf{P}} \mathbb{1}_{N-1} \\ \Psi_{21} &= \mathbf{R}_{22} ((\widehat{\mathcal{L}}_{22} - \mathbb{1}_{N-1} \widehat{\mathcal{L}}_{12}) \bar{\mathbf{P}} \mathbb{1}_{N-1} + \rho_1 (\widehat{\mathcal{L}}_{21} - \mathbb{1}_{N-1} \hat{l}_{11}))\end{aligned}$$

Then, using (3-39), one finally has $\Psi_{21} = \mathbf{R}_{22} (\widehat{\mathcal{L}}_{22} - \mathbb{1}_{N-1} \widehat{\mathcal{L}}_{12}) (\bar{\mathbf{P}} - \rho_1 \mathbf{I}_{N-1}) \mathbb{1}_{N-1}$ and (3-52) is then obtained. Finally, the last block of Ψ matrix is expressed as

$$(1/N) \Psi_{22} = \mathbf{R}_{21} \hat{l}_{11} \rho_1 \mathbf{R}_{21}^T + \mathbf{R}_{22} \rho_1 \widehat{\mathcal{L}}_{21} \mathbf{R}_{21}^T + \mathbf{R}_{22} \widehat{\mathcal{L}}_{22} \bar{\mathbf{P}} \mathbf{R}_{22}^T + \mathbf{R}_{21} \widehat{\mathcal{L}}_{12} \widehat{\mathbf{P}} \mathbf{R}_{22}^T$$

Using (3-11) and (3-36) one gets

$$\begin{aligned}(1/N) \Psi_{22} &= \rho_1 \mathbf{R}_{22} (\widehat{\mathcal{L}}_{21} - \hat{l}_{11} \mathbb{1}_{N-1}) \mathbf{R}_{21}^T + \mathbf{R}_{22} (\widehat{\mathcal{L}}_{22} - \mathbb{1}_{N-1} \widehat{\mathcal{L}}_{21}) \bar{\mathbf{P}} \mathbf{R}_{22}^T \\ &= \mathbf{R}_{22} (\widehat{\mathcal{L}}_{22} - \mathbb{1}_{N-1} \widehat{\mathcal{L}}_{12}) \widehat{\mathbf{P}} \mathbf{R}_{22}^T - \rho_1 \mathbf{R}_{22} (\widehat{\mathcal{L}}_{21} - \hat{l}_{11} \mathbb{1}_{N-1}) \mathbb{1}_{N-1}^T \mathbf{R}_{22}^T\end{aligned}$$

then, applying (3-39) one has

$$(1/N) \Psi_{22} = \mathbf{R}_{22} (\widehat{\mathcal{L}}_{22} - \mathbb{1}_{N-1} \widehat{\mathcal{L}}_{12}) \widehat{\mathbf{P}} \mathbf{R}_{22}^T + \rho_1 \mathbf{R}_{22} (\widehat{\mathcal{L}}_{22} - \mathbb{1}_{N-1} \widehat{\mathcal{L}}_{12}) \mathbb{1}_{N-1}^T \mathbf{R}_{22}^T$$

and we obtain (3-22)

A.2. Derivation of Ψ for generic node dynamics

Using the block decomposition of \mathbf{R} as done in the proof of 4-17, we have

$$\begin{aligned}\Psi &= \begin{bmatrix} r_{11}\mathbf{I}_n & (\mathbf{R}_{12} \otimes \mathbf{I}_n) \\ (\mathbf{R}_{21} \otimes \mathbf{I}_n) & (\mathbf{R}_{22} \otimes \mathbf{I}_n) \end{bmatrix} \begin{bmatrix} \mathbf{A}_1 & \mathbb{O}_{(n \times n(N-1))} \\ \mathbb{O}_{(n(N-1) \times n)} & \bar{\mathbf{A}} \end{bmatrix} \\ &\cdot \begin{bmatrix} \mathbf{I}_n & N(\mathbf{R}_{21}^T \otimes \mathbf{I}_n) \\ (\mathbb{1}_{N-1} \otimes \mathbf{I}_n) & N(\mathbf{R}_{22}^T \otimes \mathbf{I}_n) \end{bmatrix}\end{aligned}$$

Then, by matrix multiplication one gets

$$\Psi = \begin{bmatrix} \Psi_{11} & \Psi_{12} \\ \Psi_{21} & \Psi_{22} \end{bmatrix}$$

where

$$\Psi_{11} := r_{11}\mathbf{A}_1 + (\mathbf{R}_{12} \otimes \mathbf{I}_n)\bar{\mathbf{A}}(\mathbb{1}_{N-1} \otimes \mathbf{I}_n)$$

$$\Psi_{12} := N(r_{11}\mathbf{A}_1(\mathbf{R}_{21}^T \otimes \mathbf{I}_n) + (\mathbf{R}_{12}^T \otimes \mathbf{I}_n)\bar{\mathbf{A}}(\mathbf{R}_{22}^T \otimes \mathbf{I}_n))$$

$$\Psi_{21} := (\mathbf{R}_{21} \otimes \mathbf{I}_n)\mathbf{A}_1 + (\mathbf{R}_{22} \otimes \mathbf{I}_n)\bar{\mathbf{A}}(\mathbb{1}_{N-1} \otimes \mathbf{I}_n)$$

$$\Psi_{22} := N(\mathbf{R}_{21} \otimes \mathbf{I}_n)\mathbf{A}_1(\mathbf{R}_{21}^T \otimes \mathbf{I}_n) + N(\mathbf{R}_{22} \otimes \mathbf{I}_n)\bar{\mathbf{A}}(\mathbf{R}_{22}^T \otimes \mathbf{I}_n)$$

Now, by some algebraic manipulations we can simplify each block of Ψ . Then, by definition $r_{11} = 1/N$ and $\mathbf{R}_{12} = (1/N)\mathbb{1}_{N-1}^T$ and

$$\Psi_{11} = (1/N)(\mathbf{A}_1 + (\mathbb{1}_{N-1}^T \otimes \mathbf{I}_n)\bar{\mathbf{A}}(\mathbb{1}_{N-1} \otimes \mathbf{I}_n))$$

which is clearly (4-24). For the second block we can add and subtract $N\mathbf{A}(\mathbf{R}_{12}\mathbf{R}_{22}^T \otimes \mathbf{I}_n)$ where $\mathbf{R}_{12} = (1/N)\mathbb{1}_{N-1}^T$. Hence, using (3-14) one has

$$\Psi_{12} = \underbrace{((\mathbb{1}_{N-1}^T \otimes \mathbf{I}_n)\bar{\mathbf{A}} - \mathbf{A}(\mathbb{1}_{N-1}^T \otimes \mathbf{I}_n))}_{\mathbf{P}_1}(\mathbf{R}_{22}^T \otimes \mathbf{I}_n)$$

note that the matrix \mathbf{P}_1 can be recast as $\mathbf{P}_1 = [\mathbf{A}_2 \ \mathbf{A}_3 \ \cdots \ \mathbf{A}_{N-1}] - [\mathbf{A}_1 \ \mathbf{A}_1 \ \cdots \ \mathbf{A}_1] = [\mathbf{A}_2 - \mathbf{A}_1 \cdots \mathbf{A}_N - \mathbf{A}_1]$ and then (4-25) is obtained. Then, following a similar procedure as done before but for Ψ_{21} adding and subtracting $(\mathbf{R}_{22}\mathbb{1}_{N-1}^T \otimes \mathbf{I}_n)\mathbf{A}_1$, and using property (3-12) we obtain

$$\Psi_{21} = (\mathbf{R}_{22} \otimes \mathbf{I}_n) \underbrace{(\bar{\mathbf{A}}(\mathbb{1}_{N-1} \otimes \mathbf{I}_n) - (\mathbb{1}_{N-1} \otimes \mathbf{I}_n)\mathbf{A}_1)}_{\mathbf{P}_2}$$

in this case \mathbf{P}_2 can be rewritten as

$$\mathbf{P}_2 = [\mathbf{A}_2 - \mathbf{A}_1^T, \dots, \mathbf{A}_N - \mathbf{A}_1^T]^T$$

Finally, from properties (3-12) and (3-14) we can express $(\mathbf{R}_{21}^T \otimes \mathbf{I}_n) = -(1/r_{11})(\mathbf{R}_{12}\mathbf{R}_{22}^T \otimes \mathbf{I}_n)$ and $(\mathbf{R}_{21} \otimes \mathbf{I}_n) = -(\mathbf{R}_{22}\mathbf{1}_{N-1} \otimes \mathbf{I}_n)$ and the last block reads

$$\Psi_{22} := (\mathbf{R}_{22} \otimes \mathbf{I}_n)\tilde{\mathbf{A}}_1(\mathbf{R}_{22}^T \otimes \mathbf{I}_n) + N(\mathbf{R}_{22} \otimes \mathbf{I}_n)\bar{\mathbf{A}}(\mathbf{R}_{22}^T \otimes \mathbf{I}_n)$$

where $\tilde{\mathbf{A}}_1 := (\mathbf{1}_{N-1} \otimes \mathbf{I}_n)\mathbf{A}_1(\mathbf{1}_{N-1}^T \otimes \mathbf{I}_n)$. Note that $\tilde{\mathbf{A}}_1$ can be also written as $\tilde{\mathbf{A}}_1 = (\mathbf{1}_{N-1}\mathbf{1}_{N-1}^T \otimes \mathbf{A}_1)$ and by grouping common terms we obtain (3-22).

APPENDIX B

Lyapunov Exponents

Lyapunov exponents provide a quantitative measure of the divergence or convergence of nearby trajectories for a dynamical system. Consider the system

$$\dot{\mathbf{x}} = \mathbf{f}(\mathbf{x}(t)) \quad (\text{B-1})$$

Given some initial condition \mathbf{x}_o , consider a nearby point $\mathbf{x}_o + \boldsymbol{\delta}_o$, where the initial separation or perturbation $\boldsymbol{\delta}_o$ is arbitrary small as shown in Figure B-1. Then, after a time T their images under the flow are given by $\mathbf{f}_T(\mathbf{x}_o)$ and $\mathbf{f}_T(\mathbf{x}_o + \boldsymbol{\delta}_o)$ respectively. Hence, the perturbation

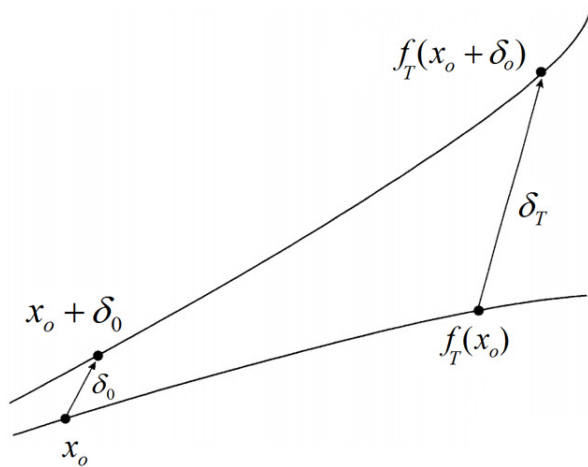


Figure B-1.: Divergence of two solutions for nearby initial conditions

at time T is given by

$$\boldsymbol{\delta}_T = \mathbf{f}_T(\mathbf{x}_o + \boldsymbol{\delta}_o) - \mathbf{f}_T(\mathbf{x}_o)$$

If $\|\delta_T\| \approx e^{\mu T} \|\delta_0\|$, then μ is the exponential rate of divergence or convergence of two trajectories and more formally can be defined by

$$\mu = \lim_{T \rightarrow \infty} \frac{1}{T} \ln \frac{\|\delta_T\|}{\|\delta_0\|} \quad (\text{B-2})$$

where $\|\delta_T\|$ denotes the length of the vector δ_T . Note that for $\mu > 0$ we have exponential divergence of nearby trajectories. Then under some assumptions on the vector-field, μ represents the largest Lyapunov exponent if the limit (B-2) exist. Then, several generalizations to compute the complete spectrum are available in literature; however, we introduce just one based on Gram-Schmidt orthonormalization, which provides a good approximation of the Lyapunov exponents and it is easy to implement.

B.1. Estimating the Lyapunov exponents

A simple estimation of the Lyapunov exponents for a continues time dynamical system is introduced in [69]. Specifically, we have to integrate the system

$$\dot{\mathbf{x}}(t) = \mathbf{f}(\mathbf{x}(t)), \quad \mathbf{x}(0) = \mathbf{x}_0 \quad (\text{B-3a})$$

$$\dot{\mathbf{M}}(t) = D\mathbf{f}(\mathbf{x})\mathbf{M}(t), \quad \mathbf{M}(0) = \mathbf{I}_n \quad (\text{B-3b})$$

where $\mathbf{M}(t) = [\mathbf{u}_1(t), \dots, \mathbf{u}_n(t)]$ with $\mathbf{u}_p(t) \in \mathbb{R}^n$ for $p = \{1, \dots, n\}$ then,

$$\mu_p = \lim_{k \rightarrow \infty} \frac{1}{kT} \sum_{j=1}^k \ln \|\mathbf{w}_i^j\| \quad (\text{B-4})$$

where T is the step size of the integration method, k is the number of iterations, and the superscript j denotes the j -th sample of the vector \mathbf{w}_i . Furthermore, the vectors \mathbf{w}_i are computed using the Gram-Schmidt orthonormalization of the set \mathbf{u}_p as

$$\mathbf{w}_1 = \mathbf{u}_1, \quad \mathbf{v}_1 = \frac{\mathbf{w}_1}{\|\mathbf{w}_1\|} \quad (\text{B-5a})$$

$$\mathbf{w}_2 = \mathbf{u}_2 - (\mathbf{u}_2^T \mathbf{v}_1) \mathbf{v}_1, \quad \mathbf{v}_2 = \frac{\mathbf{w}_2}{\|\mathbf{w}_2\|}, \dots \quad (\text{B-5b})$$

$$\mathbf{w}_p = \mathbf{u}_p - \sum_{i=1}^{p-1} (\mathbf{u}_p^T \mathbf{v}_i) \mathbf{v}_i, \quad \mathbf{v}_p = \frac{\mathbf{w}_p}{\|\mathbf{w}_p\|} \quad (\text{B-5c})$$

Bibliography

- [1] M. Andreasson, D.V. Dimarogonas, H. Sandberg, and K.H. Johansson. Distributed control of networked dynamical systems: Static feedback, integral action and consensus. *IEEE Transactions on Automatic Control*, 59(7):1750–1764, July 2014.
- [2] M. Andreasson, M. Sandberg, D. V. Dimarogonas, and K. H.. Johansson. Distributed integral action: Stability analysis and frequency control of power systems. In *Proceedings of IEEE Conference on Decision and Control, Maui, Hawaii, USA*, pages 2077 – 2083, 2012.
- [3] G. Antonelli. Interconnected dynamic systems: An overview on distributed control. *IEEE Control Systems Magazine*, 33(1):76 –88, 2013.
- [4] Karl J. Astrom and T. Hagglund. *PID Controllers - Theory, Design, and Tuning*. International Society for Measurement and Control, 1995.
- [5] Lászlo Barabási. *Network Science, Interactive book, current version online*. barabasi-lab.neu.edu/networksciencebook/downlPDF.html, 2014.
- [6] Dennis S. Bernstein. *Matrix Mathematics:Theory, Facts, and Formulas (Second Edition)*. Princeton University Press, 2009.
- [7] A. Bidram, F.L. Lewis, and A. Davoudi. Distributed control systems for small-scale power networks: Using multiagent cooperative control theory. *IEEE Control Systems Magazine*, 34(6):56–77, Dec 2014.
- [8] S. Boccaletti, G. Bianconi, R. Criado, C.I. del Genio, J. Gómez-Garde nes, M. Romance, I. Sendi na Nadal, Z. Wang, and M. Zanin. The structure and dynamics of multilayer networks. *Physics Reports*, 544:1 – 122, 2014.

- [9] S. Boccaletti, V. Latora, Y. Moreno, M. Chavez, and D.-U. Hwang. Complex networks: Structure and dynamics. *Physics Reports*, 424(4-5):175 – 308, 2006.
- [10] Stephen Boyd, Laurent El Ghaoui, E. Feron, and V. Balakrishnan. *Linear Matrix Inequalities in System and Control Theory*, volume 15. Society for Industrial and Applied Mathematics (SIAM), 1994.
- [11] D. Burbano and M. di Bernardo. Consensus and synchronization of complex networks via proportional-integral coupling. *IEEE International Symposium on Circuits and Systems (ISCAS)*, pages 1796–1799, June 2014.
- [12] D. Burbano and M. di Bernardo. Distributed PID control for consensus of homogeneous and heterogeneous networks. *IEEE Transactions on Control of Network Systems*, 2014.
- [13] D. Burbano and M. di Bernardo. Multilayer pi control for consensus in heterogeneous multi-agent networks. *Submitted to Conference on Decision and Control*, 2015.
- [14] D. Burbano and M. di Bernardo. Multiplex pi-control for consensus in networks of heterogeneous linear agents. *Submitted to Automatica*, 2015.
- [15] Yongcan Cao, Wenwu Yu, Wei Ren, and Guanrong Chen. An overview of recent progress in the study of distributed multi-agent coordination. *IEEE Transactions on Industrial Informatics*, 9(1):427–438, 2013.
- [16] R. Carli, E. D’Elia, and S. Zampieri. A PI controller based on asymmetric gossip communications for clocks synchronization in wireless sensors networks. In *Proceedings of 50th IEEE Conference on Decision and Control and European Control Conference (CDC-ECC)*, pages 7512–7517, 2011.
- [17] Ruggero. Carli, Alessandro. Chiuso, Luca. Schenato, and Sandro. Zampieri. A PI consensus controller for networked clocks synchronization. In *17th IFAC World Congress*, volume 17, pages 10289–10294, 2008.
- [18] Guanrong Chen. Problems and challenges in control theory under complex dynamical network environments. *Acta Automatica Sinica*, 39(4):312 – 321, 2013.
- [19] Anna Chmiel, Peter Klimek, and Stefan Thurner. Spreading of diseases through comorbidity networks across life and gender. *New Journal of Physics*, 16:1–14, 2014.
- [20] Sean P. Cornelius, William L. Kath, and Adilson E. Motter. Realistic control of network dynamics. *Nature Communications*, 4(1942), 2013.

- [21] Manlio De Domenico, Albert Solé-Ribalta, Emanuele Cozzo, Mikko Kivelä, Yamir Moreno, Mason A. Porter, Sergio Gómez, and Alex Arenas. Mathematical formulation of multilayer networks. *Phys. Rev. X*, 3:041022, 2013.
- [22] P. DeLellis, M.D. Bernardo, T.E. Gorochowski, and G. Russo. Synchronization and control of complex networks via contraction, adaptation and evolution. *IEEE Circuits and Systems Magazine*, 10(3):64–82, 2010.
- [23] P. DeLellis, M. diBernardo, F. Garofalo, and Maurizio Porfiri. Evolution of complex networks via edge snapping. *IEEE Transactions on Circuits and Systems I: Regular Papers*, 57(8):2132–2143, 2010.
- [24] S.V. Dhople, B.B Johnson, Dörfler, and A. F. Hamadeh. Synchronization of nonlinear circuits in dynamic electrical networks with general topologies. *eprint arXiv:1310.4550*, pages 1–13, 2013.
- [25] M. di Bernardo, A. Salvi, and S. Santini. Distributed consensus strategy for platooning of vehicles in the presence of time-varying heterogeneous communication delays. *IEEE Transactions on Intelligent Transportation Systems*, PP(99):1,11, 2014.
- [26] Ian Dobson. Complex networks: Synchrony and your morning coffee. *Nature Physics*, 9:133–134, 2013.
- [27] F. Döfler and F. Bullo. Synchronization and transient stability in power networks and nonuniform kuramoto oscillators. *SIAM Journal on Control and Optimization*, 50(3):1616–1642, 2012.
- [28] F. Döfler and F. Bullo. Synchronization and transient stability in power networks and nonuniform kuramoto oscillators. *SIAM Journal on Control and Optimization*, 50(3):1616–1642, 2012.
- [29] F. Döfler and F. Bullo. Synchronization in complex networks of phase oscillators: A survey. *Automatica*, 50(6):1539 – 1564, 2014.
- [30] F. Döfler, M. Chertkov, and F. Bullo. Synchronization in complex oscillator networks and smart grids. *Proceedings of the National Academy of Sciences*, 110(3):2005–2010, 2013.
- [31] F. Döfler, S.V. Dhople, B.B. Johnson, and A. Hamadeh. Synchronization of nonlinear circuits in dynamic electrical networks. In *Proceedings of the European Control Conference (ECC)*, pages 552–557, June 2014.

- [32] J.A. Fax and R.M. Murray. Information flow and cooperative control of vehicle formations. *IEEE Transactions on Automatic Control*, 49(9):1465 – 1476, 2004.
- [33] A.L. Fradkov, G. Grigoriev, and A. Selivanov. Decentralized adaptive controller for synchronization of dynamical networks with delays and bounded disturbances. In *Proceedings of 50th IEEE Conference on Decision and Control and European Control Conference (CDC-ECC)*, pages 1110–1115, 2011.
- [34] R.A. Freeman, Peng Yang, and K.M. Lynch. Stability and convergence properties of dynamic average consensus estimators. In *Proceedings of 45th IEEE Conference on Decision and Control*, pages 338 –343, 2006.
- [35] David J. Hill and Guanrong Chen. Power systems as dynamic networks. In *Proceedings of International Symposium on Circuits and Systems ISCAS*, pages 722–725, 2006.
- [36] Petter Holme, Beom Jun Kim, Chang No Yoon, and Seung Kee Han. Attack vulnerability of complex networks. *Phys. Rev. E*, 65:056109, May 2002.
- [37] Wang Jun-Wei, Ma Qing-Hua, and Zeng Li. A novel mixed-synchronization phenomenon in coupled chua’s circuits via non-fragile linear control. *Chinese Physics B*, 20:080506–1–080506–7, 2011.
- [38] Wang. Jun-Wei, Ma. Qing-Hua, and Li. Zeng. A novel mixed-synchronization phe-nomenon in coupled chua’s circuits via non-fragile linear control. *Chinese Physics B*, 20:080506, 2011.
- [39] F. Kenji and H. Yuko. On convergence rate of distributed consensus for homogeneous graphs. *Proceedings of the 18th IFAC World Congress*, 18:10032–10037, 2011.
- [40] Hongkeun Kim, Hyungbo Shim, and Jin Heon Seo. Output consensus of heterogeneous uncertain linear multi-agent systems. *IEEE Transactions on Automatic Control*, 56(1):200–206, 2011.
- [41] Jaeyong Kim, Jongwook Yang, Jungsu Kim, and Hyungbo Shim. Practical consensus for heterogeneous linear time-varying multi-agent systems. In *Proceedings of 12th International Conference on Control, Automation and Systems (ICCAS)*, pages 23 –28, 2012.
- [42] Mikko Kivela, Alex Arenas, Marc Barthelemy, James P. Gleeson, Yamir Moreno, and Mason A. Porter. Multilayer networks. *Journal of Complex Networks*, 2(3):203–271, 2014.

- [43] Peter Klimek, Alexandra Kautzky-Willer, Anna Chmie, Irmgard Schiller-Fruhwirth, and Stefan Thurner. Quantifying age- and gender-related diabetes comorbidity risks using nation-wide big claims data. *eprint arXiv:1310.7505*, 2013.
- [44] Zhi Li and Guanrong Chen. Global synchronization and asymptotic stability of complex dynamical networks. *IEEE Transactions on Circuits and Systems II: Express Briefs*, 53(1):28–33, Jan 2006.
- [45] Yang-Yu Liu and Jean-Jacques Slotine. Controllability of complex networks. *Nature*, 473:167–173, 2011.
- [46] Rodolfo R. Llinás. The contribution of santiago ramon y cajal to functional neuroscience. *Nature Reviews Neuroscience*, 4:77–80, 2003.
- [47] Wenlian Lu and Tianping Chen. New approach to synchronization analysis of linearly coupled ordinary differential systems. *Physica D: Nonlinear Phenomena*, 213(2):214 – 230, 2006.
- [48] Wenlian Lu and Tianping Chen. New approach to synchronization analysis of linearly coupled ordinary differential systems. *Physica D: Nonlinear Phenomena*, 213(2):214 – 230, 2006.
- [49] Sandro Meloni and Jesús Gómez-Gardeñes. Local empathy provides global minimization of congestion in communication networks. *Phys. Rev. E*, 82:056105, Nov 2010.
- [50] Adilson E. Motter and Ying-Cheng Lai. Cascade-based attacks on complex networks. *Phys. Rev. E*, 66:065102, Dec 2002.
- [51] Adilson E. Motter, Seth A. Myers, arian Anghel, and Takashi Nishikawa. Spontaneous synchrony in power-grid networks. *Nature Physics*, 9:191–197, 2013.
- [52] G. J L Naus, R.P.A. Vugts, J. Ploeg, M. J G Van de Molengraft, and M. Steinbuch. String-stable CACC design and experimental validation: A frequency-domain approach. *IEEE Transactions on Vehicular Technology*, 59(9):4268–4279, 2010.
- [53] M. E. J. Newman. The structure and function of complex networks. *SIAM Review*, 45(2):167–256, 2003.
- [54] R. Olfati-Saber, J.A. Fax, and R.M. Murray. Consensus and cooperation in networked multi-agent systems. *Proceedings of the IEEE*, 95(1):215 –233, 2007.

- [55] R. Olfati-Saber and R.M. Murray. Graph rigidity and distributed formation stabilization of multi-vehicle systems. In *Proceedings of the 41st IEEE Conference on Decision and Control*, volume 3, pages 2965–2971, 2002.
- [56] R. Olfati-Saber and R.M. Murray. Consensus problems in networks of agents with switching topology and time-delays. *IEEE Transactions on Automatic Control*, 49(9):1520 – 1533, 2004.
- [57] Louis M. Pecora and Thomas L. Carroll. Master stability functions for synchronized coupled systems. *Phys. Rev. Lett.*, 80:2109–2112, Mar 1998.
- [58] Arkady Pikovsky, Michael Rosenblum, and Jurgen Kurths. *Synchronization: A universal concept in nonlinear sciences*. Cambridge University Press, 2001.
- [59] Håvard Fjær Grip, Tao Yang, Ali Saberi, and Anton A. Stoorvogel. Output synchronization for heterogeneous networks of non-introspective agents. *Automatica*, 48(10):2444 – 2453, 2012.
- [60] W. Ren and Y. Cao. *Distributed Coordination of Multi-agent Networks*. Springer-Verlag, 2011.
- [61] Wei Ren. Formation keeping and attitude alignment for multiple spacecraft through local interactions. *Journal of Guidance, Control, and Dynamics*, 30:633–638, 2007.
- [62] Wei. Ren and Ella. Atkins. Second-order consensus protocols in multiple vehicle systems with local interactions. In *AIAA Guidance, Navigation, and Control Conference and Exhibit, San Francisco, California*, 2005.
- [63] Wei Ren and Randal W. Beard. *Distributed Consensus in Multi-vehicle Cooperative Control: Theory and Applications*. Springer-Verlag, 1st edition, 2007.
- [64] Wei Ren, R.W. Beard, and E.M. Atkins. Information consensus in multivehicle cooperative control. *IEEE Control Systems Magazine*, 27(2):71–82, 2007.
- [65] Wei Ren, Kevin L. Moore, and Yangquan Chen. High-order and model reference consensus algorithms in cooperative control of multivehicle systems. *Dynamic Systems, Measurement, and Control*, 129:678–688, 2007.
- [66] Wei Ren, Kevin L. Moore, and Yangquan Chen. High-order and model reference consensus algorithms in cooperative control of multivehicle systems. *Journal of Dynamic Systems, Measurement, and Control*, 129(5):678–688, 2007.

- [67] Horn A. Roger and Johnson R. Charles. *Matrix Analysis*. Cambridge Univ. Press, 1987.
- [68] R.O. Saber and R.M. Murray. Consensus protocols for networks of dynamic agents. In *Proceedings of the American Control Conference*, volume 2, pages 951 – 956, 2003.
- [69] M. Sandri. Numerical calculation of Lyapunov exponents. *The Mathematica Journal*, 6:78 – 84, 1996.
- [70] Alain Sarlette, Jing Dai, Yannick Phulpin, and Damien Ernst. Cooperative frequency control with a multi-terminal high-voltage DC network. *Automatica*, 48(12):3128 – 3134, 2012.
- [71] G. Stephan, A. Daducci, A. Lemkadem, R. Meuli, J.P. Thiran, and P. Hagmann. The connectome viewer toolkit: an open source framework to manage, analyze and visualize connectomes. *Frontiers in Neuroinformatics*, 5(3), 2011.
- [72] Steven Strogatz. Exploring complex networks. *Nature*, 410:268–276, 2001.
- [73] J. Sun, E. M. Bollt, and T. Nishikawa. Master stability functions for coupled nearly identical dynamical systems. *EPL (Europhysics Letters)*, 85(6):60011, 2009.
- [74] Y. Susuki, I. Mezic, and T. Hikihara. Global swing instability in the new england power grid model. In *American Control Conference (ACC)*, pages 3446–3451, 2009.
- [75] Yang Tang, Feng Qian, Huijun Gao, and Jurgen Kurths. Synchronization in complex networks and its applications: A survey of recent advances and challenges. *Annual Reviews in Control*, 38(2):184 – 198, 2014.
- [76] Yinhe Wang, Yongqing Fan, Qingyun Wang, and Yun Zhang. Stabilization and synchronization of complex dynamical networks with different dynamics of nodes via decentralized controllers. *IEEE Transactions on Circuits and Systems I: Regular Papers*, 59(8):1786–1795, 2012.
- [77] Zhenhua Wang, Juanjuan Xu, and Huanshui Zhang. Consensusability of multi-agent systems with time-varying communication delay. *Systems & Control Letters*, 65:37 – 42, 2014.
- [78] Peter Wieland, Rodolphe Sepulchre, and Frank Allögwer. An internal model principle is necessary and sufficient for linear output synchronization. *Automatica*, 47(5):1068 – 1074, 2011.

- [79] George F. Young, Luca Scardovi, Andrea Cavagna, Irene Giardina, and Naomi E. Leonard. Starling flock networks manage uncertainty in consensus at low cost. *PLoS Comput Biol*, 9(1):e1002894, 2013.
- [80] Wenwu Yu, Guanrong Chen, Ming Cao, and J. Kurths. Second-order consensus for multiagent systems with directed topologies and nonlinear dynamics. *IEEE Transactions on Man, and Cybernetics, Part B: Cybernetics*, 40(3):881–891, June 2010.
- [81] Jun Zhao, D.J. Hill, and Tao Liu. Synchronization of dynamical networks with non-identical nodes: Criteria and control. *IEEE Transactions on Circuits and Systems I: Regular Papers*,, 58(3):584–594, 2011.
- [82] Wei-Song Zhong, Guo-Ping Liu, and C. Thomas. Global bounded consensus of multiagent systems with nonidentical nodes and time delays. *IEEE Transactions on Systems, Man, and Cybernetics, Part B: Cybernetics*,, 42(5):1480–1488, 2012.
- [83] Jiandong Zhu. On consensus speed of multi-agent systems with double-integrator dynamics. *Linear Algebra and its Applications*, 434(1):294 – 306, 2011.